

Aus dem Institut für Medizintechnologie  
der Universität Heidelberg und der Hochschule Mannheim  
Center for Mass Spectrometry and Optical Spectroscopy (CeMOS)  
(Leiter: Prof. Dr. rer. nat. Carsten Hopf)

Development of an Automated MALDI Mass Spectrometry Assay for  
direct Analysis of Cellular Drug Uptake via the Organic Anion  
Transporting Polypeptide OATP2B1

Inauguraldissertation  
zur Erlangung des Doctor scientiarum humanarum (Dr. sc. hum)  
der  
Medizinischen Fakultät Mannheim  
der Ruprecht-Karls-Universität  
zu  
Heidelberg

vorgelegt von  
Melissa Simone Unger

aus  
Kitzingen  
2020

Dekan: Prof. Dr. med. Sergij Goerd  
Referent: Prof. Dr. rer. nat. Carsten Hopf

# TABLE OF CONTENTS

<b>ABBREVIATIONS .....</b>	<b>1</b>
<b>1 INTRODUCTION .....</b>	<b>3</b>
1.1 TRANSPORT PROCESSES ACROSS THE CELL MEMBRANE .....	3
1.1.1 TRANSPORTERS MEDIATING UPTAKE AND EFFLUX IN CELLS.....	4
1.1.2 DRUG TRANSPORTER HISTORY .....	5
1.1.3 SLC TRANSPORTERS AND THEIR LINK TO HUMAN DISEASE .....	7
1.1.4 DRUG APPROVAL – INFLUENCE OF DRUG-DRUG INTERACTIONS .....	8
1.1.5 OATP2B1 AS AN EMERGING DDI-RELEVANT DRUG TRANSPORTER .....	9
1.2 ASSAY TECHNOLOGIES IN PHARMACEUTICAL RESEARCH AND DEVELOPMENT.....	11
1.3 MASS SPECTROMETRY ASSAY TECHNOLOGIES.....	15
1.3.1 HISTORICAL BACKGROUND OF MALDI MASS SPECTROMETRY .....	17
1.3.2 BASICS OF MALDI MASS SPECTROMETRY.....	18
1.3.3 EMERGENCE OF MALDI MASS SPECTROMETRY WHOLE CELL ASSAYS .....	20
1.3.4 SAMPLE PREPARATION FOR SMALL MOLECULE MALDI MASS SPECTROMETRY .....	21
<b>2 AIMS.....</b>	<b>24</b>
<b>3 MATERIALS AND METHODS.....</b>	<b>25</b>
3.1 MATERIALS .....	25
3.1.1 GENERAL CHEMICALS .....	25
3.1.2 CHEMICALS FOR CELL CULTURE .....	25
3.1.3 COMPOUNDS FOR CELL CULTURE TREATMENT .....	26
3.1.4 CHEMICALS FOR MATRIX PREPARATION .....	26
3.1.5 CONSUMABLES .....	27
3.1.6 EQUIPMENTS AND INSTRUMENTS .....	27
3.1.7 HUMAN CELL LINES.....	29
3.1.8 BUFFERS FOR WESTERN BLOT .....	29
3.1.9 SOFTWARE FOR DATA ACQUISITION .....	29

3.1.10	SOFTWARE FOR DATA ANALYSIS, VISUALISATION AND CHEMICAL DRAWING .....	30
<b>3.2</b>	<b>METHODS .....</b>	<b>30</b>
3.2.1	WESTERN BLOT.....	30
3.2.2	CULTIVATION OF HUMAN CELL LINES.....	31
3.2.3	FLUORESCENCE-BASED ASSAY.....	34
3.2.4	MALDI MASS SPECTROMETRY WHOLE CELL MEASUREMENTS .....	36
3.2.5	VIABILITY TEST: CELLTITER-GLO .....	39
3.2.6	DATA ANALYSIS USING COMMERCIAL SOFTWARE.....	40
<b>4</b>	<b>RESULTS .....</b>	<b>41</b>
4.1	WESTERN BLOT CONFIRMING THE OVEREXPRESSION OF OATP2B1	42
4.2	FLUORESCENCE-BASED ASSAY .....	43
4.2.1	DEVELOPMENT OF A FLUORESCENCE-BASED ASSAY FOR THE UPTAKE OF DIBROMOFLUORESCEIN THROUGH OATP2B1 .....	43
4.2.2	SCREEN OF 294 DRUGS IDENTIFIES MANY INHIBITORS THAT ARE LIKELY TO CAUSE DRUG-DRUG INTERACTIONS.....	48
4.2.3	AUTOFLUORESCENCE AND QUENCHING EFFECT TEST .....	54
4.3	MALDI MASS SPECTROMETRY UPTAKE ASSAY .....	56
4.3.1	DEVELOPMENT OF A WHOLE-CELL MALDI MASS SPECTROMETRY UPTAKE METHOD .....	57
4.3.2	AUTOMATION OF THE METHOD LEADS TO POSSIBLE HIGH-THROUGHPUT SCREENING .....	74
4.3.3	CHECK OF THE REPRODUCIBILITY THROUGH CONCENTRATION-/TIME-DEPENDENCE AND pIC <sub>50</sub> DETERMINATION.....	80
4.3.4	MALDI MASS SPECTROMETRY-BASED SCREENING OF INHIBITORS OF DRUG UPTAKE.....	83
4.3.5	SEARCH FOR SUBSTRATES OF OATP2B1 DURING SCREEN .....	94
<b>5</b>	<b>DISCUSSION.....</b>	<b>99</b>
5.1	FLUORESCENCE-BASED ASSAYS AND THEIR POSSIBLE DISADVANTAGES IN SCREENING .....	99
5.2	DEVELOPMENT OF FIRST LABEL-FREE UPTAKE ASSAY USING MALDI MASS SPECTROMETRY .....	102

5.3	MALDI MASS SPECTROMETRY SCREENING OF INHIBITORS AS AN EMERGING METHOD FOR DRUG-DRUG INTERACTION TESTING .....	106
5.4	COMPARISON OF BOTH ASSAY TYPES REVEALS DIFFERENCES .....	110
5.5	CONCLUSION .....	112
<b>6</b>	<b>SUMMARY .....</b>	<b>114</b>
<b>7</b>	<b>REFERENCES .....</b>	<b>116</b>
<b>8</b>	<b>CURRICULUM VITAE .....</b>	<b>137</b>
<b>9</b>	<b>ACKNOWLEDGEMENT .....</b>	<b>138</b>

**ABBREVIATIONS**

ABC	ATP-binding cassette
ACN	Acetonitrile
ADMET	Absorption, distribution, metabolism, excretion and toxicity
ATP	Adenosine triphosphate
AU	Arbitrary unit
AUC	Area under the curve
CETSA	Cellular thermal shift assay
CV	Coefficient of variation
Da	Dalton
DBF	4',5'-Dibromofluorescein
DD	Dried Droplet
ddH <sub>2</sub> O	Double-distilled water
DDI	Drug-Drug Interaction
DHAP	2',5'-dihydroxyacetophenone
DHB	2',5'-dihydroxybenzoic acid
DMEM	Dulbecco's modified Eagle Medium
DMSO	Dimethylsulfoxide
FCS	Fetal calf serum
FDA	Food and Drug Administration
FDI	Food-Drug Interaction
FRET	Förster resonance energy transfer
HPLC	High performance liquid chromatography

HTS	High-throughput screening
IC <sub>50</sub>	Half maximal inhibitory concentration
<i>m/z</i>	Mass-to-charge ratio
MALDI	Matrix assisted laser desorption/ionisation
MS	Mass spectrometry
MTP	MALDI target plate
OAT	Organic Anion Transporter
OATP2B1	Organic Anion Transporting Polypeptide 2B1
PBS	Phosphate buffered saline
PEN/STREP	Penicillin-streptomycin
Ph-CCA-NH <sub>2</sub>	4-Phenyl- $\alpha$ -cyanocinnamic acid amide
pIC <sub>50</sub>	Negative decadic logarithm of IC <sub>50</sub>
rpm	Revolutions per minute
S/N	Signal to noise
SLC	Solute Carrier
TFA	Trifluoroacetic acid
TOF	Time of flight
uHTS	Ultra High-throughput screening
WC	Whole Cell

## 1 INTRODUCTION

### 1.1 TRANSPORT PROCESSES ACROSS THE CELL MEMBRANE

Cells as living organisms have to be in constant exchange with their environment to keep up their normal function. Without the uptake of important nutrients, the unlimited capacity of a cell cannot be granted. Substances need to cross the lipid bilayer of a cell, which is keeping it in its shape and delimiting it from other cells ensuring a specific cellular environment<sup>1</sup>. The easiest way to pass this membrane is by passive diffusion, which is the primary route for gases and water. The eased diffusion includes transport through channels and carriers, like ion channels or glucose carriers. The active transport is dependent on adenosine triphosphate (ATP). Primary active transport directly uses ATP to energise for instance a  $\text{Na}^+/\text{K}^+$ -ATPase whereas secondary active transport uses an electrochemical gradient built up by a primary active transporter<sup>2</sup>. For example, the activity of  $\text{Na}^+/\text{K}^+$ -ATPase leads to an accumulation of  $\text{Na}^+$  in the extracellular space, which can be used to co-transport glucose into the cytosol by a secondary active transporter (**Figure 1**). Besides the two mentioned active transport processes, there is also a tertiary active transport, which uses a concentration gradient built up by a secondary active transporter. Alongside the “conventional” transport ways, molecules can also be transported into the cells by invagination of the cell membrane. This process is called endocytosis and includes four mechanisms named clathrin-mediated, caveolae, phagocytosis and pinocytosis<sup>3, 4</sup>. This transport process results in a taken-up particle enclosed by a vesicle. For the export via this transport route, particles are enclosed by a vesicle and transported outside of the cell through exocytosis.



## Introduction

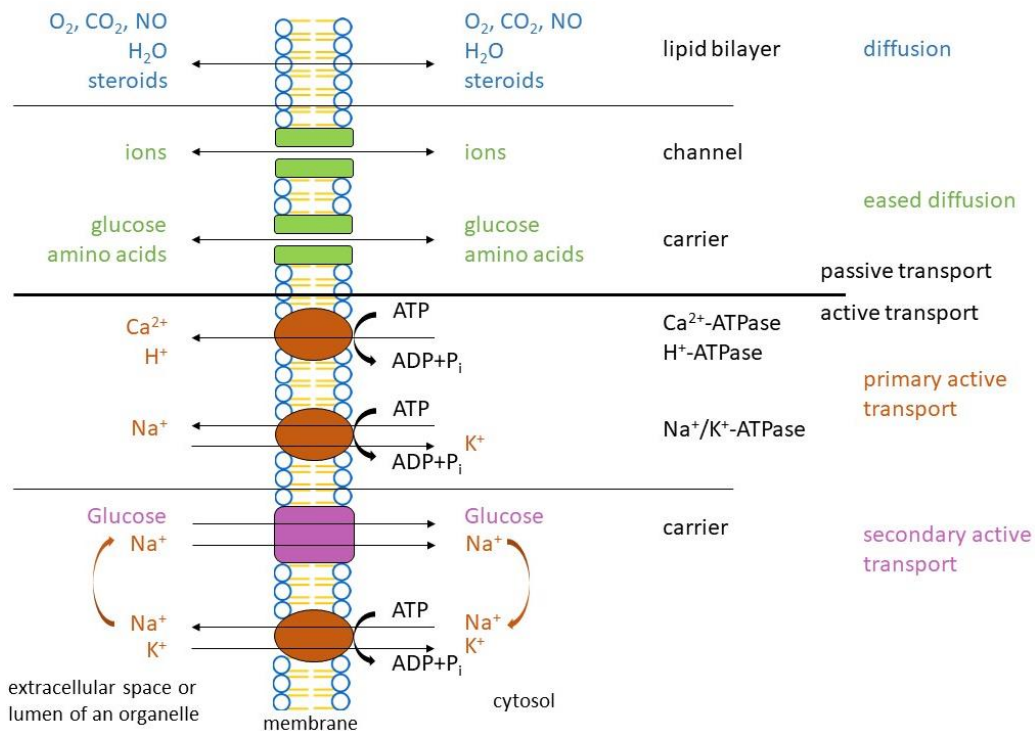


**Figure 1: Different ways of transport across the cell membrane:** Passive and active transport in a cell including diffusion, eased diffusion, primary and secondary active transport. (Figure adapted from Rassow *et al.*)<sup>5</sup>

### 1.1.1 TRANSPORTERS MEDIATING UPTAKE AND EFFLUX IN CELLS

The size, charge and polarity of a molecule affects the way it is transported<sup>6</sup>. Diffusion is only possible for small and lipophilic compounds that follow their concentration gradient. As soon as the molecule to be transported is hydrophilic, larger or has to be transported against the concentration gradient, the help of transport proteins comprising solute carriers (SLC), adenosine triphosphate (ATP)-binding cassette (ABC) transporters, channels, carriers and ATP-driven pumps, is needed. Both import and export of compounds is managed by transporters with the ABC transporters being almost exclusively responsible for export from cells and the SLC transporters for import of substances into the cells<sup>7</sup>. SLC transporters comprise more than 400 members<sup>8, 9</sup> organised into 65 families<sup>10</sup>. They are integral membrane proteins and are localised on the cell surface and in organellar membranes, depending on the type of SLC transporter. According to their substrate selectivity, they are grouped in families<sup>11</sup>. There are transporters mediating the uptake of organic anions (Organic

anion transporter(OAT)) and organic cations (Organic cation transporter (OCT)), which are besides the organic anion transporting polypeptide (OATP) family two of the best known and investigated SLC families.

Before transporter proteins that act as uptake routes for drugs, were identified, it was believed that passive transport across the biological membrane constitutes the main uptake route of drugs<sup>12</sup>. The route of drug uptake of biological compounds into cells is still controversial. While Kell *et al.* postulate the drug transport as being carrier-mediated only<sup>13</sup>, many other laboratories insist on the coexistence of both passive and carrier-mediated drug uptake<sup>12</sup>. Kell argues with most studies being conducted with non-transfected cells that are used as a control for passive transport. It has to be noted that the non-transfected cells of course also contain a variety of transporters and thus in their opinion cannot be used as control for passive transport<sup>13</sup>. Nonetheless, there is a common agreement on transport proteins accounting for drug uptake into cells. Like the just described controversy, it also took a while for transport proteins as such catching the attention of scientists.

### 1.1.2 DRUG TRANSPORTER HISTORY

In the 1940s, probenecid was discovered as a compound that affects the half-life of penicillin due to interference with renal clearance<sup>14</sup>. This can be seen as the first notice of drug-transporter interaction, as Pascale *et al.*, described the effect of probenecid on the organic anion transporters located in the kidney leading to the reduced clearance activity<sup>15</sup>. In the 1950s, pathologists discovered the Dubin-Johnson syndrome leading to a discolouration of the liver due to an increase of bilirubin in the serum<sup>16</sup>. This syndrome later could be explained by the mutation in an organic anion transporter gene<sup>17</sup> giving a hint about the importance of transporter research. In 1976, Juliano and Ling first depicted P-glycoprotein (P-gp)<sup>18</sup>, a primary active efflux ABC-transporter<sup>19</sup>, which got more attention, as it could subsequently be connected to multidrug resistance of tumour cell lines against anticancer agents<sup>20</sup>. As P-gp overexpression ranks as a major cause for the treatment failure of chemotherapeutics in cancer<sup>21, 22</sup>, research focused on finding inhibitors that could help to keep the chemotherapeutic drug inside the cancer cell. Amongst others, verapamil and cyclosporine A were found as inhibitors of P-gp<sup>23, 24</sup> in the years after. In 1998, the transporter research field

gained even more interest by the identification of another important ABC transporter: the breast cancer resistance protein (BCRP)<sup>25</sup>, which plays an important role in the cytostatic drug resistance of cancer cells, making it a big topic of cancer research<sup>26</sup>.

BCRP transporters that turned out to be involved in multidrug resistance and the already seen links to human diseases like Dubin-Johnson syndrome and cancer led to the recognition of the research field, which resulted in the first International Transporter Consortium (ITC) White Paper in 2010<sup>7</sup>. To date, there were three ITC workshops followed by several white papers published in prestigious journals<sup>7, 27, 28</sup>. On the basis of the white papers published by the ITC, the Food and drug administration (FDA) concluded on publishing guidances for industry, which are intended to help drug developers plan and evaluate studies to determine the drug-drug-interaction (DDI) potential of an investigational drug product. Additionally, the FDA has recommended to monitor several transport proteins in the process of drug approval such as for example a guidance for P-gp and OATP1B1/1B3. The latter two should be investigated if the hepatic/biliary elimination is a significant clearance pathway for the investigational drug and the drug is likely to be taken up into the liver. Those directives are adapted periodically and help to manage adverse events. **Figure 2** illustrates the timeline of drug transporter history with the highlights that ended up in the formation of the ITC.

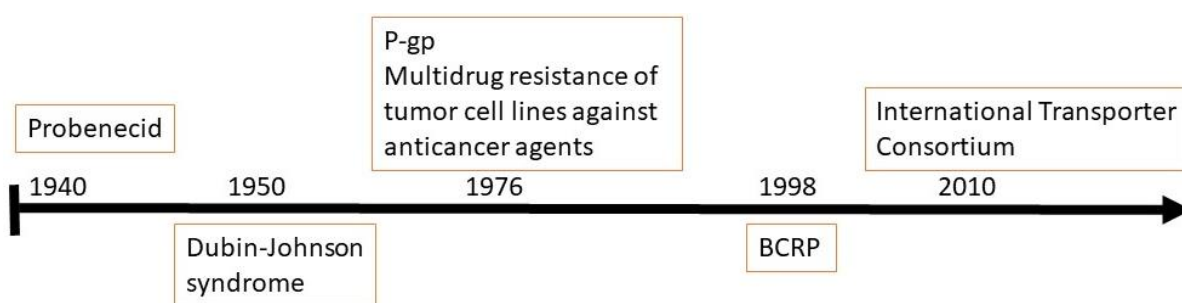


**Figure 2: Timeline drug transporter history:** Time line showing the most important events in drug transporter history from the discovery of probenecid and its effects on penicillin due to clearance issues to the publication of the first ITC white paper in 2010.

### 1.1.3 SLC TRANSPORTERS AND THEIR LINK TO HUMAN DISEASE

As the history of transporter research already showed, the need to investigate transport proteins is high. Speaking of the SLC transporters, more than 80 out of the more than 400 known SLCs are linked to human diseases<sup>29</sup>. Therefore, the already mentioned Dubin-Johnson syndrome is not the only disease linked to a malfunction, mutation or genetic variant of an SLC gene. Besides little known diseases as Barter and Gitelman syndrome, which are caused by a mutation in SLC12<sup>30</sup>, SLCs are also connected to diseases that have occupied science for several years like amyotrophic lateral sclerosis, Parkinson's disease, Alzheimer's disease, epilepsy, schizophrenia or autism. Those neurological disorders seem to be influenced by the dysfunction of SLC1/SLC6 transporters<sup>29, 31-33</sup>. With metabolic diseases like diabetes<sup>34, 35</sup>, gout<sup>36, 37</sup> and cardiovascular diseases like elevated blood pressure<sup>38, 39</sup> the list gets even longer.

Surprisingly, SLC transporters also have a connection to cancer. They do not only play a role in the uptake of many cancer therapeutics, but there is also evidence of a change in the expression patterns of SLC transporters in cancer cells<sup>40</sup>. Cancer cells of course have a higher need for nutrition and energy than healthy cells. Those degenerated cells seem to help themselves with the upregulation of some SLC transporters<sup>41, 42</sup>. Overexpression of those uptake transporters might be an advantage for the cancer cells because of possible increase in uptake of hormones and nutrients. For the special case of Organic anion transporting polypeptide 2B1 (OATP2B1), belonging to the SLC family, it has been noted that in estrogen-receptor (ER)-positive breast cancer, the increase in uptake of hormones (estrogen) through OATP2B1 led to an increase of the survival of breast cancer cells<sup>43</sup>.

The upregulated SLC transporters in cancer cells could have not only supportive, but also restricting effects for the cancer development, as SLC transporters also are known to interact with anticancer agents<sup>41, 44</sup>. An increased uptake of anticancer compounds by targeting SLC transporters could help improve the efficacy of chemotherapy<sup>45</sup>. Also, a future application could be to design drugs that can only specifically be taken up by SLC transporters expressed in the cancer cells leading to a possible cell-type specific drug delivery<sup>42</sup>.

Due to their involvement in cancer and many more human diseases, SLC transporters represent an emerging drug target. Unfortunately, to date, there are only 12 drugs on

the market, which target a SLC gene product<sup>46</sup>. As the several entanglements with human diseases showed, the goal should be to focus on SLC transporters as drug targets in the coming years due to the possibility of improving the bioavailability of certain drugs by designing them to use the transporters as their specific route of uptake<sup>47</sup>.

### 1.1.4 DRUG APPROVAL – INFLUENCE OF DRUG-DRUG INTERACTIONS

Another fact that makes the SLC transporters worth investigating is the broad specificity of the protein class. They are involved in the uptake and further transport of nucleotides, amino acids, fatty acids, inorganic ions, sugars, neurotransmitters and drug molecules<sup>8</sup>. This abundance of different molecules makes up a big number of available molecules in a cellular environment. With the quantity of substances influenced by the transport proteins comes a critical effect that should not be underestimated. Drug-drug interaction (DDI) is a generic term for two or more pharmaceutical drugs or molecules that both interact with the transport protein and affect each other when administered concomitantly. This manifests itself by a change in the drug levels after concomitant application compared to the drugs administered alone<sup>7</sup>. Due to transport proteins intervening in the absorption, distribution, metabolism and excretion (ADME) of drugs, an alteration in ADME by transporters can lead to drug-drug interactions<sup>48</sup>. In detail, an inhibition of the transporter by one substance can lead to the other substrate not being transported anymore leading to the drug not getting to its target. Another possible consequence is that through the blocking of the transporter by a drug, another drug cannot be taken up into a metabolising organ anymore and the drug accumulates in the blood, which can lead to a toxic enrichment of the drug in the blood or other organs<sup>49</sup>.

The group of Dawson *et al.* found that cholestasis, leading in the end to drug-induced liver injury, results from the inhibition of the bile salt export pump (BSEP). This transport protein is a key player in the further transport of bile salts from the liver and through inhibition can provoke an accumulation of the bile salts in liver triggering cholestasis<sup>50</sup>. Another severe example of drug-drug interaction happened in the 1990s and led to a sudden death of patients administered with terfenadine and ketoconazole concomitantly<sup>51</sup>. Not only DDI are a reason for an increased need for investigation of

transporters, but also interactions with food, referred to as food-drug interactions (FDI). Especially OATPs are known for interactions with juices<sup>52</sup>. An investigation of OATP2B1 showed a decrease in the area under the curve (AUC) of the plasma concentration of fexofenadine by 86 % and aliskiren by 63 % with a concomitant administration with apple juice. Also grapefruit juice had an effect on the AUC of fexofenadine (decrease 52 %), aliskiren (decrease 61 %) and celiprolol (decrease 84 %)<sup>53</sup>.

As DDIs are also known to be involved in adverse events<sup>54-56</sup>, and the population is getting older, which makes DDIs more likely due to people being on several medications simultaneously, it is important to investigate the DDI potential of a drug during its approval. What makes the investigation of the DDI potential even more important is the fact that half of the drugs withdrawn from the market in the 2000s were due to important drug interactions<sup>57</sup>. Drug development and approval are a very cost-intensive issue and even facing a “reproducibility crisis” with the enormous rise in research and development costs per drug in the last 60 years<sup>58</sup>. Therefore, the detailed investigation of the efficacy, potency, ADME, toxicity, mechanism of action and side effects of the pharmaceutical compounds is an essential component in ensuring the prerequisites and increasing the chances for clinical trials and drug approval<sup>59, 60</sup>.

As the members of the SLC family gained attention due to their known involvement in ADME processes<sup>61</sup>, they are included routinely in the drug development process and proposals for emerging clinical transporters are updated by the ITC as the responsible regulatory authority<sup>8</sup>. This together with guidances published by the FDA helped researchers to gain a better understanding of the drug interactions in the last years<sup>54</sup>. Nonetheless, a complete picture of the transport proteins and processes is still not available yet and an analysis showed that the SLC transporters are relative to their meaning in health and drug approval understudied<sup>9</sup>.

### 1.1.5 OATP2B1 AS AN EMERGING DDI-RELEVANT DRUG TRANSPORTER

An SLC transporter with emerging clinical importance is the organic anion exchanger<sup>62</sup> OATP2B1. It was first described as clinically important in the ITC whitepaper from 2010<sup>7</sup> and still has to be described further because of lack of information on the drug-

drug interaction likelihood. Even though OATP2B1 is less known and studied than OATP1B1 and OATP1B3, which are liver-specific, it is expressed in multiple organs, predominantly in liver<sup>63, 64</sup>, but also at the blood-brain barrier<sup>65</sup>, at the ciliary epithelium<sup>66, 67</sup>, in the intestine<sup>68</sup>, in skeletal muscle<sup>69</sup> and in the placenta<sup>70</sup> (**Figure 3**) and should therefore be treated as equally relevant<sup>71</sup>. The main drug uptake site is believed to be in the intestine<sup>72</sup> and through its high abundance in liver and intestine, it is an important drug uptake transporter for many compounds, which increases the probability of DDI and FDI<sup>71</sup>.

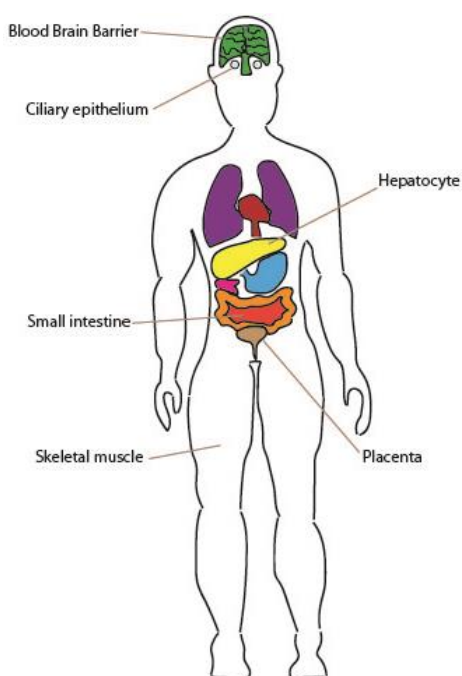


**Figure 3: Expression of OATP2B1 in the human body:** OATP2B1 is expressed ubiquitously throughout the body<sup>73</sup>. Figure adapted from Hagenbuch *et al*<sup>74</sup>.

There are some known events of DDI and FDI associated with OATP2B1. Fruit juices are the best studied DDI mechanisms for OATP2B1<sup>75</sup> and as described in 1.1.4 can lead to a decrease in the plasma concentration of 86 % of a drug. Until now, the only DDI occurrence with OATP2B1 is an inhibition of OATP2B1 by ronacaleret, which results in a decrease in the exposure of rosuvastatin. As statins are frequently administered to older people, this represents a high risk for DDI, as older people tend to be co-medicated with other drugs<sup>76</sup>. Also, a decreased statin disposition by the

inhibition of transporters, which mediate the disposition, can result in the development of a statin-related myopathy<sup>76</sup>, which can be a life-restricting disease.

But not only because of the DDIs, OATP2B1 is an interesting research object, it is also involved in human cancer. It has been identified in multiple tumour cell lines, where the abundance of the protein increased with tumour grade<sup>65, 77</sup>. Furthermore, overexpression has been found in various tumours<sup>45</sup>. As described already in 1.1.3, this overexpression of transport proteins in tumour cells could help the cancerous cell to facilitate its uptake of nutrients and hormones. Estrone-3-Sulfate (E3S) is a hormone that is also related with cancer and is a substrate for OATP2B1<sup>73</sup>, which makes this hypothesis conceivable<sup>43</sup>. Targeted inhibition of OATP2B1 could be a strategy to reduce the growth of the tumours in which the transport protein is overexpressed<sup>78</sup>.

Finally, OATP2B1 is also an interesting research object, because it seems to have multiple binding sites that also differ in their pH sensitivity. Thus, substrate and inhibitor differences could likely evolve<sup>68, 72, 79</sup>. This finding has not yet been fully clarified and together with the other aspects leads to a high interest in OATP2B1 research.

## 1.2 ASSAY TECHNOLOGIES IN PHARMACEUTICAL RESEARCH AND DEVELOPMENT

Pharmaceutical research and development relies on a wide range of assay technologies. Various fluorescence techniques are among the technologies. The term fluorescence was first introduced back in 1852 by George Stokes, The basis of fluorescence is the electronic and vibrational excitation of a system by a higher-energy (lower wavelength) photon and emission of a photon at a higher wavelength (**Figure 4**).



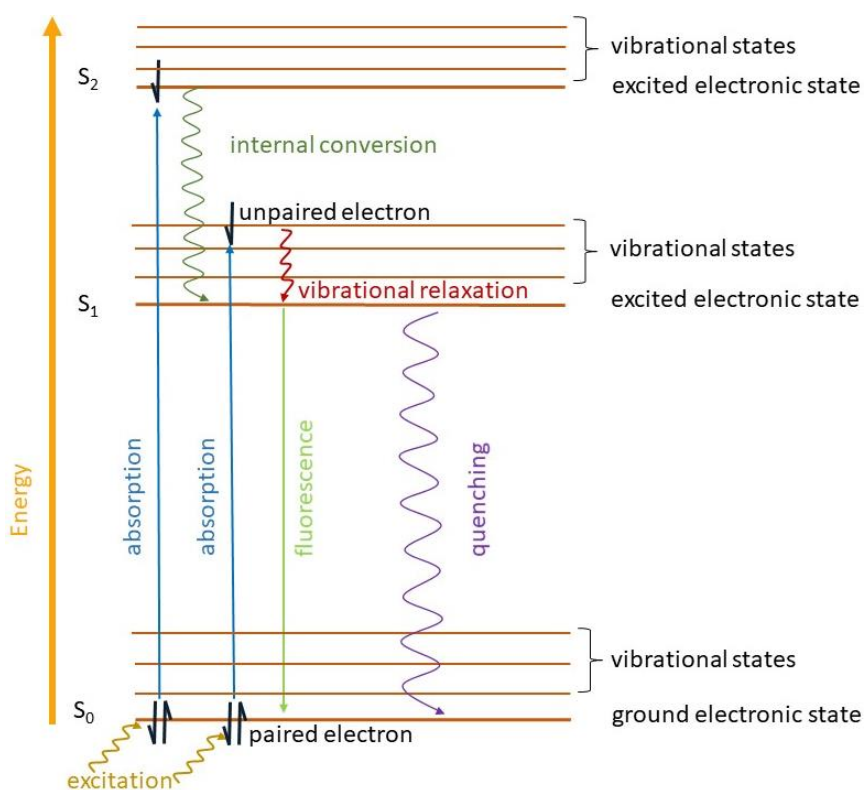


**Figure 4: Basis of fluorescence:** Jablonski diagram: A paired electron in the singlet ground state ( $S_0$ ) absorbs a photon. One electron of the pair gets excited electronically to the first excited singlet electronic states ( $S_1$ ) or higher. In this example, also a vibrational excitation is shown, where the electron is excited to a vibrational state of  $S_1$ . An unpaired electron is a very unstable form of an electron, thus leading to the need to fall back on the ground state. This can happen by internal conversion, which leads to a change in the electronic state due to a transformation of the excitation energy to heat. Here, the internal conversion is shown from the second excited singlet state ( $S_2$ ) to  $S_1$ . Also, vibrational relaxation can occur followed by emission of a photon, called fluorescence or quenching, which leads to a reduction of the fluorescence intensity due to various effects.

A fluorescence intensity measurement is usually conducted with a microplate reader consisting of a light source, filters or monochromators for excitation and emission and a detector for the measurement of the emitted light, which usually is a photomultiplier tube. Several other methods are also based on the fluorescence effect. A fluorophore is a fluorescent chemical compound and if excited with polarised light, most of them also emit polarised light, which is the basis for fluorescence polarisation (FP). For the measurement of FP, the probe is excited with linear polarised light generated by a polarisator. A second polarisator analyses the emitted light. In pharmaceutical

research, FP is used as a basic readout<sup>80</sup>, but can also be coupled with an immunoassay to detect antibodies or antigens in samples<sup>81</sup>. Förster resonance energy transfer (FRET) is another fluorescence-based technique used in pharmaceutical research. The physical process, which was discovered 1948 by Theodor Förster is a radiation-free energy transfer process between two dyes possessing a spectral overlap and being in proximity to another. The energy is transferred from a donor to an acceptor and can be measured indirectly by analysis of the decrease of radiation intensity of the donor or emission of the acceptor using a fluorescence microscope or a fluorometer. FRET is a common technique in pharmaceutical research<sup>82</sup> and is also applied as time-resolved fluorescence (TR) FRET<sup>83, 84</sup> through the use of fluorophores with a long lifespan, defining the time the molecule stays in an excited state before the emission of a photon. FRET and TR-FRET are suitable techniques for drug discovery as they cover the analysis of protein-protein interactions<sup>85</sup>. Fluorescence-lifetime imaging microscopy (FLIM) includes, as the name already suggests, a measurement of the lifetime of a fluorophore and not the intensity and is frequently used for pharmacological questions<sup>86, 87</sup>. Comparable to FRET, there is a technique with the same principle, transferring bioluminescence energy from a donor to an acceptor. Due to the same methodological principle, it is called bioluminescence resonance energy transfer (BRET)<sup>88</sup>. For most BRET reactions, the enzyme Rluc is used with its acceptor coelenterazin<sup>89</sup>. Luminescence measurements are most of the time conducted with luciferase and its acceptor luciferin<sup>90</sup> and also find application in drug uptake studies<sup>91</sup>. Also biochemical methods are an important tool in pharmaceutical research. The cellular thermal shift assay (CETSA) is used for the analysis of protein interactions. It depends on the change in thermostability of the protein folding when adding a binding partner and can also be applied in a screen<sup>92</sup>.

For the implementation of the research on the emerging transport protein OATP2B1 and others, there are currently several methods used. Important here is to distinguish between methods used in search for new substrates and methods used for inhibitor screening. Most of the research is conducted either radio-labelled or fluorescence-labelled<sup>48</sup>. A radioisotope assay can serve both needs and therefore is a suitable method for the investigation and characterisation of transport proteins<sup>48, 93</sup>. For the uptake assays, possible substrates are labelled usually either with tritium or <sup>14</sup>C-carbon. After treatment of the cells with the substrate and stopping of the reaction,

cells are lysed and the radioactivity analysed using a scintillation counter (**Figure 5**). This measurement device for the determination of the intensity of ionised radiation consists of a scintillator, a photomultiplier tube and a counter. A high energy photon reaches the scintillator and through the ionised radiation several low energy photons are produced. When a photon reaches the photocathode, it will emit a primary electron. The focusing electrode directs the electrostatically accelerated electron towards the first dynode in the photomultiplier tube. The electron gets multiplied and the resulting secondary electrons are multiplied at every dynode. This process leads to an enrichment of signal and a measurable and countable energy, which reaches the anode in the end.

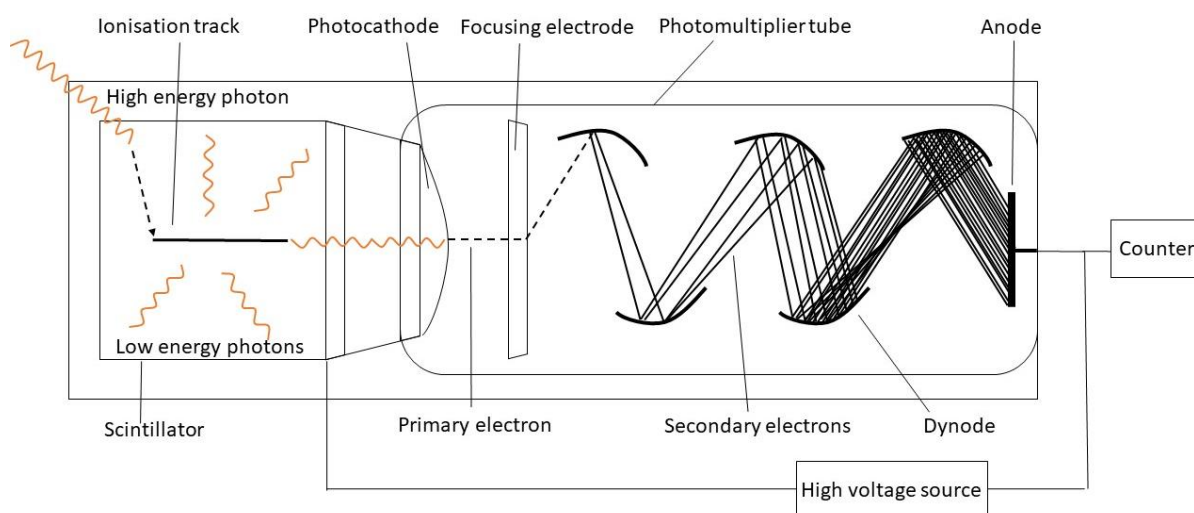


**Figure 5: Scintillation counter:** The measurement device for ionised radiation in radioactive assays consists of scintillator, photomultiplier tube and counter.

Even though radioactive assays are very simple and sensitive in detection and the required labelling does not falsify the outcome because of the same chemical identity, the big problem with the technique is on the one hand the waste management, but also of course on the other hand the exposure of the working personnel<sup>94</sup>.

An alternative for the investigation of transporters are fluorescent methods. They too need a labelling of the substrate, but are also very sensitive<sup>95</sup>, low in cost, automatable and therefore applicable in high-throughput screening (HTS)<sup>96</sup>. Nevertheless, there are several negative aspects about the method, like a short lifespan of the fluorophore,

a susceptibility in regard to pH changes and the influence of false-positives and – negative hits<sup>97</sup>. False assumptions can result out of autofluorescence of the investigated compound itself<sup>93</sup>. If it is fluorescent at the investigated wavelength, there will be a detection of light, even though the compound could have led to an inhibition of the uptake of the fluorescent substrate. False assumptions can also result out of quenching effects<sup>93</sup>. In this case, properties of the investigated compound lead to a decrease of the emission of the fluorescent substrate and would therefore be identified as inhibitor, even if an inhibition did not take place. Additionally, a clear negative aspect about fluorescence-based methods is that a fluorescent label is needed. This reduces the possibilities of measurements and also affects the outcome. Summed up, a fluorescence-based method often picks up artefacts and therefore a preferably label-free counter screening confirming the hits is advised<sup>98</sup>.

### 1.3 MASS SPECTROMETRY ASSAY TECHNOLOGIES

A possible counter screening for a fluorescence-based method can be mass spectrometry (MS), as it may be less prone to false-negatives and -positives. The basic principle of mass spectrometry is to generate ions and to separate those ions in vacuum according to their mass-to-charge ratio ( $m/z$ ). The technology is used in multiple application areas like sequencing of peptides<sup>99</sup>, analysis of whole cells<sup>100</sup> and structure elucidation of unknown and known compounds<sup>101, 102</sup>. All of the mass spectrometers have a similar basic structure: they consist of a sample inlet, ion source, mass analyser and a detector (**Figure 6**). Different types of mass analysers are illustrated in **Figure 6**. Among them are besides time of flight (TOF) also quadrupole (QUAD) and triple quad, ion traps, where orbitrap is a special form, sector field and fourier-transform ion cyclotron resonance (FT-ICR)<sup>103</sup>. They all have the same goal: to separate ions to gather more information about them.

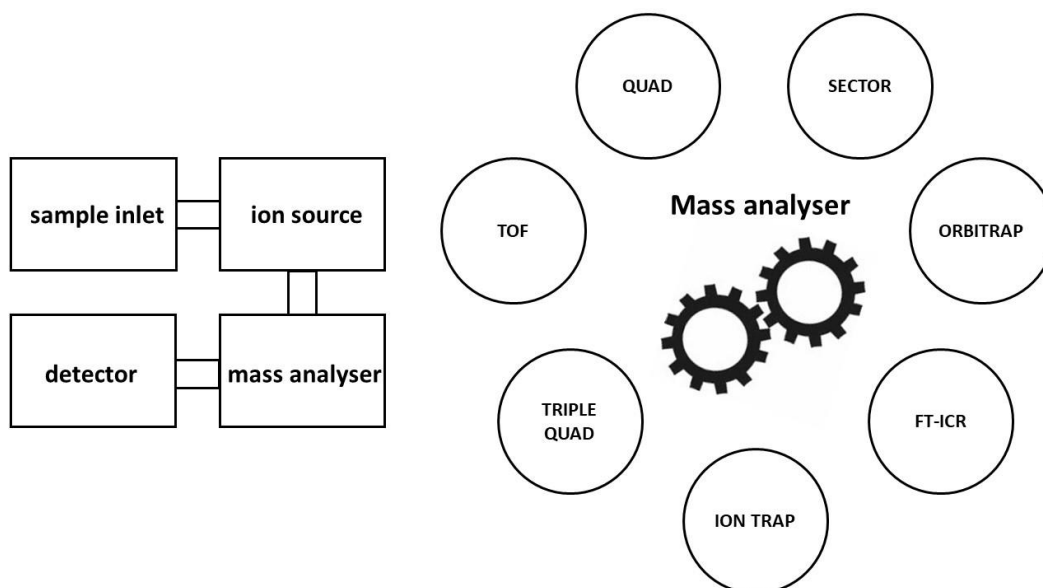


**Figure 6: Components of a mass spectrometer/ Different types of mass analysers:** A mass spectrometer typically consists of 4 components: sample inlet, ion source, mass analyser and mass detector. Various types of mass analysers are illustrated on the right.

MS assays have been used in pharmaceutical and pharmacological research for decades. In the 2000s, accelerator mass spectrometry (AMS) became a popular method for the quantification of isotopes in humans with the possibility to conduct ADME studies<sup>104</sup>. Due to the immense cost, there are only about 80 laboratories worldwide equipped with that technique. A far more used mass spectrometric technique is secondary ion mass spectrometry (SIMS). This method, which uses primary ions to produce secondary ions that are then analysed, is capable of a high depth analysis and the possibility to create 3D images of the probes, which are especially relevant in terms of drug distribution<sup>105</sup>. Due to its high spatial resolution, it also made single-cell imaging possible<sup>106</sup>. Common in pharmaceutical research is also the liquid chromatography (LC)-MS-based approach, which can be for example used for proteomics<sup>107</sup>. Also metabolomic studies showed to be helpful in the identification of transporter substrates<sup>48</sup>. In an untargeted approach, the analysis of the serum and urine of OAT1 knockout mice and wildtype with LC-MS identified substrates of the transport protein<sup>108</sup>. Gordon *et al.* developed a method, dependent on LC-MS, which is capable of directly measuring the intracellular compound concentration in whole cells<sup>109</sup>. The methodological background for this is the usage of a RapidFire high-

throughput MS system together with a triple quadrupole mass spectrometer. Through electrospray-ionisation (ESI) an ion is produced, which is isolated in the first quadrupole and excited in the second. The third quadrupole determines the products of the isolated ion. A clear disadvantage of the method is its limited HTS capacity. This puts another method in the focus of pharmaceutical mass spectrometric analyses. Matrix assisted laser desorption/ionisation (MALDI) MS is a method, which in the last years gained acceptance as a suitable technology for pharmaceutical research and drug development<sup>110</sup>. Not only in imaging<sup>111, 112</sup>, but also in biotyping<sup>113, 114</sup> it has found its place as a commonly used technique for pharmaceutical and pharmacological questions.

### 1.3.1 HISTORICAL BACKGROUND OF MALDI MASS SPECTROMETRY

The very first experiments for the investigation of mass separation were done by Thomson, who also demonstrated the existence of the electron<sup>115</sup>. The first mass spectrometer with the property to measure charged atoms was also built by him<sup>116</sup>. The first time of flight (TOF)-analyser was constructed in 1946 by Stephens<sup>117</sup>. The principle of this analyser is the dispersion of ions along a field-free drift distance. With the theoretically simultaneous formation of ions, this leads to those being separated by their  $m/z$  according to their longer or shorter drift time. The determination of the  $m/z$  value is dependent on the flight time ( $T_f$ ). Ions with the charge  $q$  result in taking up energy through the exposure with the voltage  $U$ .

$$E = U * q$$

Due to the energy being then present as kinetic energy, the relation  $E = \frac{1}{2}mv^2$  is valid and leads to the proportionality of the flight time with the mass-to-charge ratio  $m/z$ .

$$(T_f)^2 \sim m/z$$

A pulsed ionisation leads to a simultaneous start of flight time of the ions. The lower the mass of the ions, the faster they will reach the detector. In most cases, a secondary electron multiplier (SEM), which has the same functionality as the photomultiplier tube in 1.2, acts as a detector and registers the time of arrival of the ions at the end of the drift distance.

The technique got more and more attention in the 1980s<sup>118</sup>. That success of the technique was mainly due to the development of Matrix-assisted laser desorption/ionisation (MALDI)<sup>119</sup> as a pulsed ionisation technique, which is ideal to be coupled with a TOF<sup>120-122</sup>. The two fit perfectly together because both are dependent on pulsed ionisation and MALDI as a soft ionisation technique required a mass analyser capable of analysis of molecules with a high mass up to  $10^5$  u<sup>120</sup>.

### 1.3.2 BASICS OF MALDI MASS SPECTROMETRY

MALDI requires matrices, which are small organic crystalline molecules that, due to their chromophores, absorb energy at the employed laser wavelength. A matrix functions as a proton donator or acceptor, which ionises the analyte. The process is predicated on the co-crystallisation of matrix and analyte. The analyte gets incorporated into the matrix crystals during matrix crystallisation. By shooting with a pulsed ultraviolet (UV) laser beam onto the matrix-analyte mixture (nowadays often applied: frequency-tripled Nd:YAG laser), the analyte molecules desorb and get ionised. The gas phase protonation model consists of two steps. First, a photoionisation of the matrix is taking place through the irradiation of the laser. Secondly, the charge is transferred to the neutral analyte molecules<sup>123</sup>. The lucky survivor model postulates the generation of singly charged molecular ions<sup>123, 124</sup>. In case of multiply charged ions, the neutralisation of the matrix-analyte cluster is done quicker than for singly charged ions, which are the lucky survivors in that case. This makes MALDI MS a technique, for which data is easy to interpret, because of the low occurrence of highly charged molecular ions and a relatively easy isotopic pattern.

MALDI MS, which is due to its soft ionisation a suitable method especially for large molecules like proteins or even polymers<sup>125</sup>, is dependent on the matrix, which is used for the ionisation. The basic principle is the desorption and ionisation through a laser beam, followed by the guiding of the molecular ions through an electric field generator into the mass analyser like a TOF (**Figure 7**). MALDI can also be coupled to a Fourier transform ion cyclotron resonance (FT-ICR) analyser<sup>126</sup> or other mass analysers to get an even higher resolving power. Once the molecular ions arrived at the TOF analyser, they are separated due to their mass-to-charge ratio. There are two possibilities for the application of a detector. The linear detector is located directly in the row after the

flight tube. Bigger molecules, like proteins for example, are typically measured with the linear detector. Usage of the reflector detector is additionally associated with the use of electrodes in front of the linear detector, where an electrical field is applied that leads to the deceleration of the ions followed by an acceleration into the opposing direction in a U-shaped manner. Two ions with the same mass but different kinetic energies result in leaving the ion mirror at the same time, which acts as a flight time correction and thus improves the resolution while using the reflector mode for measurements<sup>127</sup>.

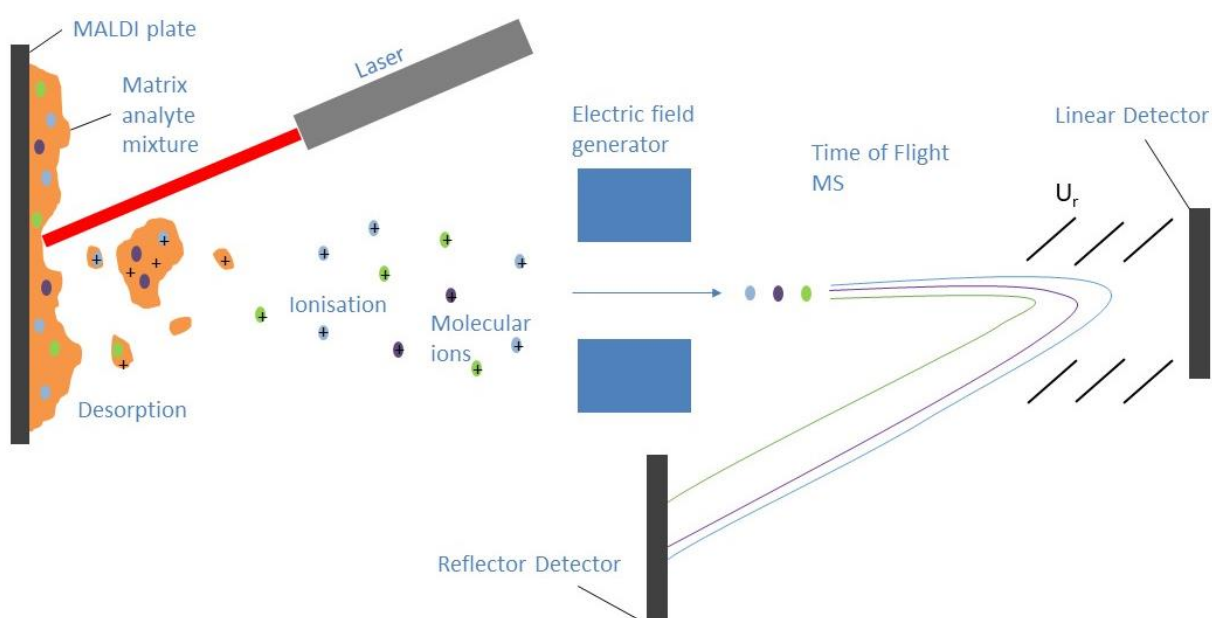


**Figure 7: Principle of MALDI-TOF-MS:** Desorption and ionisation of the matrix-analyte mixture through a laser beam, time of flight mass analyser leads to separation of molecular ions due to their mass. Linear measurement with linear detector, reflector measurement with use of voltage to reflect the ions, measurement via reflector detector.

The usage of an FT-ICR clearly improves the resolution compared to linear and reflector mode what comes along with an extension of the time needed for the measurement. The ICR setup includes a strong magnetic field, in which the ions are kept on circular trajectories with a frequency based on the respective  $m/z$ . After an impulse of excitation, an alternating electric field is used to generate the cyclotron resonance. The change in cyclotron radius can be measured by a detector. The



Fourier transformation of the signal leads to a mass spectrum out of the obtained frequency spectrum<sup>128, 129</sup>.

### 1.3.3 EMERGENCE OF MALDI MASS SPECTROMETRY WHOLE CELL ASSAYS

Generally, cell-based assays are a widely applied system, due to the ease in multiplexing, automation and predictability<sup>130</sup>. Concomitantly, MALDI MS emerged as a suitable technique for whole cell (WC) analysis in the last years due to its applicability to a wide range of masses, its ease of measurement and possibility of application to human diseases<sup>131</sup>. Whole cell means that the method does not include fractionation or extraction steps and thus creates an overview of the cell profile while maintaining easy handling steps. Already in 1975, there was evidence for the possibility to analyse bacteria with MS<sup>132</sup>. Beyond the first MALDI MS WC measurements, pathogens have been identified and classified due to cell-type specific mass spectral fingerprints<sup>133</sup>. By the fact that MALDI is a soft ionisation technique, also the analysis of protein fingerprints helped in identifying and classifying bacteria<sup>134</sup>. The application of MALDI MS in clinical microbiology started 20 years ago<sup>135, 136</sup>, and it is now seen as the gold-standard method for microbial identification<sup>137</sup>. The possibility of the characterisation of a cell line by its fingerprint was first showed several years later<sup>138</sup>. The Hopf lab was one of the first to develop a WC-based MALDI MS biotyping method outside microbiology<sup>139</sup>. Other studies relied on the analysis of primary cells<sup>140</sup> or purified blood cells<sup>141</sup>. Even though the origins of the method lay in the identification of microbial cells and to this day, the method is still mostly applied in this area of research, much progress has been made for mammalian cell lines. Dong *et al.* were able to identify protein patterns corresponding with viability or apoptosis of mammalian cells, which can be seen as the first pharmacological study representing another step further for WC MS<sup>113</sup>. Apart from that, also the application to more complex systems like mixtures of cell lines got possible. Petukhova *et al.* were able to detect cancer cells in a mixed cell population, which enabled the usage of more complex biological systems<sup>142</sup>. With reporting IC<sub>50</sub> values of histone deacetylase inhibitors, the first quantitative WC-MALDI MS study was published<sup>143</sup>. Apart from the protein-based assays used for pharmacodynamics characterisations<sup>114</sup>, Weigt *et al.* also established

WC-based assays for the identification of lipid marker molecules<sup>144</sup> and fatty acid synthase inhibitors<sup>145</sup>.

Starting in 2011, the first approaches to HTS were made as Gurard-Levin *et al.* designed a method capable for HTS, which is dependent on self-assembled monolayers (SAMs), measured with MALDI-TOF-MS<sup>146</sup> and therefore called SAMDI. A few years later, the method once again demonstrated the feasibility of high throughput studies with MALDI MS, as Wagle *et al.* used SAMDI as a screening tool for lysine demethylases<sup>147</sup>. In 2014, Ritorto *et al.* succeeded in developing the first high-throughput screen, which is not dependent on the chemically modified target surfaces anymore<sup>148</sup>. Several studies followed, which included MALDI MS as a HTS technology<sup>149-151</sup>. The first study not designed as proof-of-concept, but as a screen for inhibitors in a diverse compound set was conducted by Simon *et al.*<sup>152</sup>. This development shows that the automation and HTS-suitability of an assay gained more and more attention in the last years. As Beeman *et al.* and Haslam *et al.*<sup>150, 153</sup> predict, MALDI MS as a HTS application will become increasingly important for drug discovery in the upcoming years and should therefore be given more attention.

Also for drug uptake into cells, MALDI MS showed to be a suitable method. Burlina *et al.* and Aussedat *et al.* analysed drug uptake via streptavidin-coated magnetic beads<sup>154, 155</sup>. Another drug uptake method relied on the analysis of the cell lysate<sup>156</sup>. Also a transwell model has been built up, which analyses the uptake of peptides indirectly and resembles the conditions in the blood brain barrier<sup>157</sup>. These methods gave a first hint about the applicability of MALDI MS for the analysis of drug uptake, but still, to date, there are no label-free WC MALDI MS methods known that investigate the transporter-mediated uptake of small molecules into the cells directly.

### 1.3.4 SAMPLE PREPARATION FOR SMALL MOLECULE MALDI MASS SPECTROMETRY

MALDI MS biotyping, which this work focuses on, is in its workflow dependent on the analyte investigated. For cell-based methods, the workflow contains several critical steps: Seeding out the cells in plates, incubation with the compound of interest, harvesting of the cells including washing, then freezing of the cells followed by

resuspension in solvent and spotting on a target plate. Finally, the plates are measured and the data is evaluated.

For the analysis of compounds, there are several matrices possibly suited, like 2,5 dihydroxybenzoic acid (DHB)<sup>158</sup>, sDHB<sup>159</sup>, 2,5 Dihydroxyacetophenone (DHAP)<sup>160</sup>, 9-aminoacridine (9AA)<sup>161</sup> and 4-Phenyl- $\alpha$ -cyanocinnamic acid amide (Ph-CCA-NH<sub>2</sub>)<sup>162</sup> (**Figure 8,A**). The uneven distribution of the analyte throughout the sample spot is a common burden for MALDI. This heterogeneity results from various processes that affect the sample preparation, like the decision for matrix, application, solvent, drying technique and various others. It can result in the formation of some crystals, where no analyte is incorporated<sup>163</sup> and others with an incorporation of much analyte. Those are referred to as “sweet spots” (**Figure 8,B**), where the best MALDI MS performance is achieved<sup>164, 165</sup>. This inhomogeneity complicates an automated measurement and production of reproducible results. Suitable techniques to compensate the heterogeneity are the usage of a random walk on the spot during measurement to address stochastically, the optimisation of matrix application to a homogeneous layer and the inclusion of internal standards with the same ionisation properties<sup>166, 167</sup>.

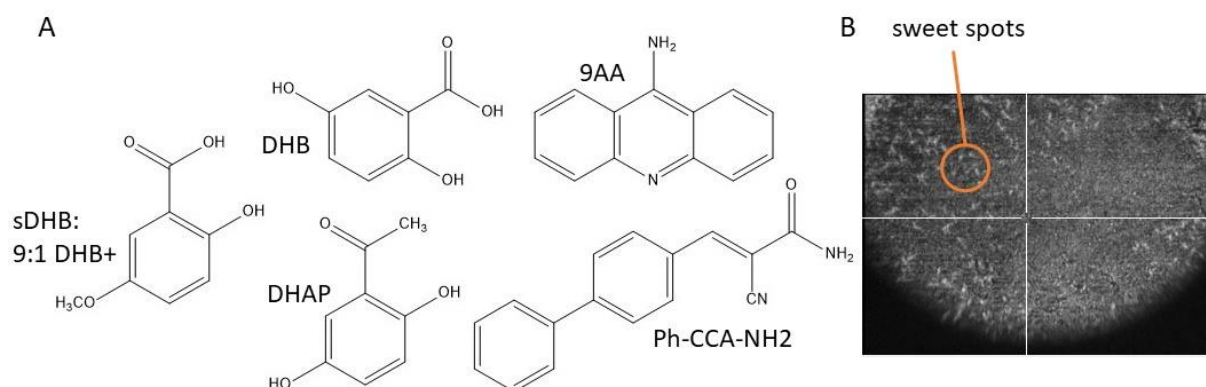


**Figure 8: Chemical structures of MALDI matrices and “sweet spots”:** (A) Chemical structures of matrices sDHB (9:1 mixture of DHB and 2-hydroxy-5-methoxybenzoic acid), DHB, DHAP, 9AA and Ph-CCA-NH<sub>2</sub>. (B) Picture of crystallised matrix that forms “sweet spots”, which are complicated to be measured automatically.

Also, the different application techniques of matrix influence the crystallisation. Dried droplet, which is still among the most used application types, is a manual or automated

application of the matrix-analyte mixture. An application technique referred to as “sandwich” includes coating of the MALDI target plate (MTP) with matrix first and a dried droplet application on top, so that the analyte is encompassed by two layers of matrix<sup>138</sup>. PrimaDrop is conducted by application of the analyte first and letting it dry before applying matrix on top of the dried spot by pipetting<sup>168</sup>. A method that is dependent on the use of another device is the sprayed method. Here, the analyte gets applied to the MTP first and the matrix gets sprayed on top by a matrix sprayer<sup>169</sup> (**Figure 9**). In addition to this, some matrices can't be applied in different application techniques with special solvents, so the method development is a crucial step, where a high focus should be put on evaluating the best matrix and solvent and application for the analyte of interest. Especially also in the context of method automation, some matrix application ways are superior to others.

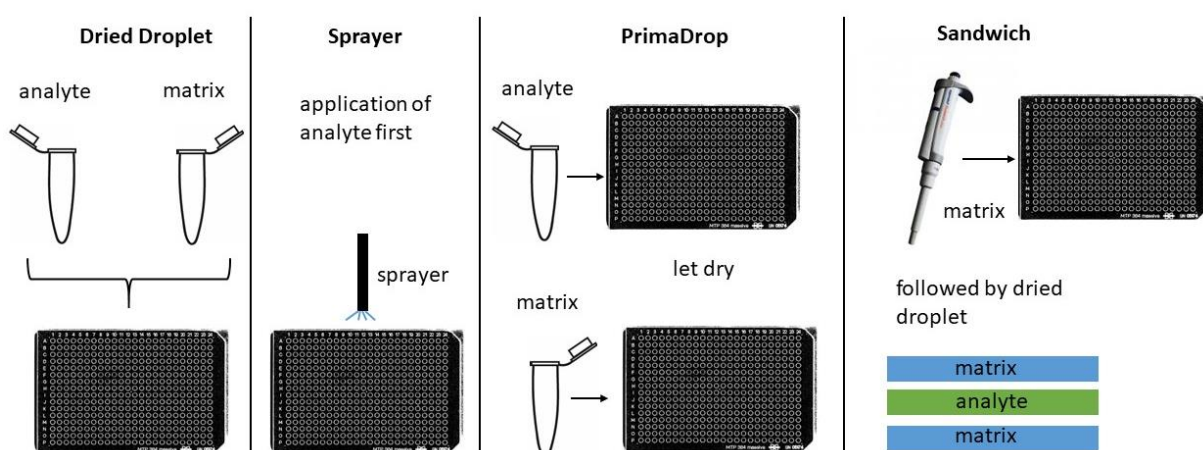


**Figure 9: Different application ways for matrix: dried droplet, sprayer, PrimaDrop and sandwich application.**

## 2 AIMS

In the last years, research on cellular influx has strengthened the common opinion of transport proteins being the major determinants of drug uptake into a cell. With transporter experts reporting to the FDA, it is assumed that more drug approval regulations will have to focus on transport processes. This has been done by radioactive and fluorescent assays the last years. However, new assay technologies need to be developed and tested, in order to achieve less danger and fewer photonic interferences, respectively. MALDI MS represents a method that is label-free, sensitive and automatable. As MALDI MS assays got more and more attention in pharmacology in the last years, it was the method of choice to characterise the cellular transport process of SLC transport proteins. The development of a fast and robust MALDI MS assay for the detection of possible DDI could lead to completely new tools on the way to drug approval.

Therefore, the thesis focused on the following three objectives:

- Using the transport process of the SLC transporter OATP2B1 as an example, development of a MALDI MS workflow that enables sensitive and reproducible measurement of an OATP2B1 substrate in whole cells.
- Incorporation of the developed MALDI MS workflow into pharmacologically relevant assays and assay automation.
- Screening of 300 marketed drugs and discovery of OATP2B1 inhibitors (and possible DDI) by MALDI MS and comparison of screening results with a fluorescence-based reference assay.

### 3 MATERIALS AND METHODS

#### 3.1 MATERIALS

##### 3.1.1 GENERAL CHEMICALS

<b>Chemical</b>	<b>Company (Headquarter)</b>	<b>Catalogue number</b>
Acetone	VWR International (Darmstadt, GER)	1.00012
Acetonitrile	VWR International (Darmstadt, GER)	1.00030
Ethanol absolute	VWR International (Darmstadt, GER)	20825
Milli-Q-water	Prepared in-house	
Peptide Calibration Standard II	Bruker Daltonics (Bremen, GER)	8222570

##### 3.1.2 CHEMICALS FOR CELL CULTURE

<b>Chemical</b>	<b>Company (Headquarter)</b>	<b>Catalogue number</b>
Ammonium formate	VWR International (Darmstadt, GER)	AA14157-30
DMEM	GE Healthcare (Solingen, GER)	HYCLSH30022.FS
DMSO	VWR International (Darmstadt, GER)	A3672
FCS	Life Technologies (Darmstadt, GER)	10270
G418	Sigma Aldrich (Munich, GER)	G8168
HBSS	Sigma Aldrich (Munich, GER)	H9269
PBS	Sigma Aldrich (Munich, GER)	P3744
PEN/STREP	Life Technologies (Darmstadt, GER)	15140122
Poly-L-Lysine	Sigma Aldrich (Munich, GER)	P8920
Trypan blue	Sigma Aldrich (Munich, GER)	T8154
Trypsin/EDTA	Corning (Wiesbaden, Germany)	25-053-CI

## 3.1.3 COMPOUNDS FOR CELL CULTURE TREATMENT

Compound	Company (Headquarter)	Catalogue number
294 compound library <sup>170</sup>	GSK Compound management (Stevenage, UK); Tocris (Bristol, UK), Selleckchem (Houston, USA), Cayman (Ann Arbor, USA)	
Dibromofluoresceine <sup>170</sup> (DBF)	Sigma-Aldrich (St. Louis, USA)	216720
Erlotinib <sup>171</sup>	LC Laboratories (Woburn, USA)	E-4007
Estrone-3-Sulfate (E3S) <sup>73</sup>	Sigma-Aldrich (Steinheim, GER)	E-9145

All commercially sourced inhibitors were  $\geq 99$  % pure, all internally sourced inhibitors had  $\geq 95$  % purity, except raloxifene and novobiocin (94 %), tipranavir (91 %), cetirizine (90 %), diacerein (88 %) and P-3004 Unergol (87 %).

## 3.1.4 CHEMICALS FOR MATRIX PREPARATION

Chemical	Company (Headquarter)	Catalogue number
D <sub>4</sub> -E3S	Toronto Research Chemicals (Toronto, CAN)	E889071
DHAP (2,5-Dihydroxy-acetophenone)	Bruker Daltonics (Bremen, GER)	8231829
DHB (2,5-Dihydroxybenzoic acid)	Bruker Daltonics (Bremen, GER)	8201346
Ph-CCA-NH <sub>2</sub> (4-Phenyl- $\alpha$ -cyanocinnamic acid amide) <sup>162</sup>	SiChem (Bremen, GER)	SC-1400
sDHB	Bruker Daltonics (Bremen, GER)	8702557
Trifluoroacetic acid	Merck (Darmstadt, GER)	1082620025

## 3.1.5 CONSUMABLES

<b>Consumable</b>	<b>Company (Headquarter)</b>	<b>Catalogue number</b>
Cell culture dishes	VWR International (Darmstadt, GER)	734-2322
Cell culture plates with 6 / 24 / 96 wells	Greiner bio-one (Solingen, GER)	M8562 / M8812 / M0812
Centrifuge tubes 0.5 / 1.5 / 2 mL	Eppendorf (Hamburg, GER)	0030121023 / 0030120086 / 0030120094
Centrifuge Tubes 15 / 50 mL	VWR International (Darmstadt, GER)	525-0150 / 525-0155
CyBio® RoboTipTray 96/60 µL	Analytik Jena (Jena, GER)	OL3810-25-441
Low-lint wipers; Kimwipes	Kimberly-Clark( Dallas, USA)	Z188956
MALDI 384 ground steel target	Bruker Daltonics (Bremen, GER)	8280784
Neubauer Improver	VWR International (Darmstadt, GER)	631-0696
Nitrile examination gloves	VWR International (Darmstadt, GER)	112-4513
Pipet tips 10 / 200 / 1000 µL	VWR International (Darmstadt, GER)	613-0576 / 613-0579 / 613-0582
Serological pipettes 10 / 25 mL	VWR International (Darmstadt, GER)	612-3700DE / 612-3698DE

## 3.1.6 EQUIPMENTS AND INSTRUMENTS

<b>Equipment/Instrument</b>	<b>Model, Company (Headquarter)</b>
Balances	Analytical Balance Sartorius Research R200D, Sartorius (Göttingen, GER)
Cell Culture Incubator	Heracell 150, Thermo Fisher Scientific (Schwerte, GER)



## Materials and methods

<b>Equipment/Instrument</b>	<b>Model, Company (Headquarter)</b>
Centrifuges	Heraeus Fresco 21, Thermo Fisher Scientific (Schwerte, GER)  SIGMA 6K15, Sigma Laborzentrifugen GmbH (Osterode, GER)
Clean Bench	AireGard ES NU-140 Vertical Laminar Airflow Workstation, Nuaire (Caerphilly, UK)
Envision Plate Reader	Perkin Elmer (Waltham, USA)
Fluorescence microscope	Olympus (Shinjuku, Japan)
Mass spectrometer	rapifleX MALDI-TOF MS, Bruker Daltonics (Bremen, GER)  ultrafleXtreme MALDI-TOF/TOF MS, Bruker Daltonics (Bremen, GER)
Matrix spray device	SunCollect Sprayer, SunChrom (Friedrichsdorf, GER)  HTX M5 Sprayer, HTX Technologies (Chapel Hill, North Carolina, USA)
Microscope	Invert light microscops AE 31, Motic (Wetzlar, GER)
Pipettes 10/ 100/ 1000 $\mu$ L	Eppendorf Research plus, Eppendorf (Hamburg, GER)
Pipetting Platform	CyBio FeliX, Head R 96/60 $\mu$ L, Analytik Jena (Jena, GER)  Integra ViaFlo, 96 well head, 300 $\mu$ L tip tray Integra Biosciences (Zizers, CH)
Sonic bath	VWR International (Darmstadt, GER)
Trans-Blot Turbo	Biorad (Hercules, USA)
Vacuum aspirator	Vacunsafe, Integra Biosciences (Zizers, CH)
Water purification system	EMD Millipore™ Milli-Q™ Reference Ultrapure Water Purification System, Thermo Fisher Scientific (Schwerte, GER)

### 3.1.7 HUMAN CELL LINES

Cell line	Provider
HEK293-OATP2B1 <sup>172</sup>	Anne Nies, Matthias Schwab
HEK293-vector control	Anne Nies, Matthias Schwab

### 3.1.8 BUFFERS FOR WESTERN BLOT

Specification	Composition
10xTransfer buffer for semi-dry transfer	58.1g Trizma base, 29.3g Glycine, add distilled H <sub>2</sub> O to a total volume of 1 L
20 % Tween solution	100 g Tween 20, add distilled H <sub>2</sub> O to a total volume of 500 mL
1 M DTT	Dissolve 7.7g DTT in 50 mL distilled H <sub>2</sub> O, filter solution through 0.22 µm
1x Running buffer	20 mL 50X MOPS buffer; add distilled H <sub>2</sub> O to a total volume of 1 L
1x Transfer buffer	100 mL 10xtransfer buffer, 1.875 mL 20 % SDS w/v, 100 ml EtOH, add distilled H <sub>2</sub> O to a total volume of 1L
Washing buffer	5 mL 20 % Tween 20, add PBS to a total volume of 1 L PBS
2x SDS/DTT sample buffer	250 µL 4xNuPAGE sample buffer, 25 µL DTT 1M, 225 µL distilled H <sub>2</sub> O

### 3.1.9 SOFTWARE FOR DATA ACQUISITION

Name	Instrument	Company (Headquarter)
flexControl 4.0	rapifleX MALDI-TOF	Bruker (Bremen, GER)
MPP 2.2	rapifleX MALDI-TOF	Bruker (Bremen, GER)

### 3.1.10 SOFTWARE FOR DATA ANALYSIS, VISUALISATION AND CHEMICAL DRAWING

<b>Software</b>	<b>Company (Headquarter)</b>
Adobe Illustrator CS5	Adobe (California, USA)
ChemDraw 19	Perkin Elmer (Waltham, USA)
ClinPro Tools 3.0	Bruker (Bremen, GER)
flexAnalysis 4.0	Bruker (Bremen, GER)
Microsoft Powerpoint	Microsoft (Redmond, USA)
Prism 5	GraphPad Software (California, USA)

## 3.2 METHODS

### 3.2.1 WESTERN BLOT

For verification of the overexpression of OATP2B1, a western blot was done. A cell pellet was harvested from 1/6 of a petri dish for both OATP2B1 and vector control. SDS lysis was done to break up the cells: the frozen cell pellets were resuspended with one cell pellet volume of pre-heated lysis buffer (200  $\mu$ L 20 % SDS, 50  $\mu$ L Tris-HCl pH 7.4 and 750  $\mu$ L ddH<sub>2</sub>O water). Samples were heated for 3 min at 95 °C in a Thermomixer, shaking at 700 rpm. Samples were cooled to room temperature before briefly centrifuging (10 s, 10000g). The 24x benzoylase stock was diluted 1:24 in the samples, incubated 30 min at 37 °C and 850 rpm and vortexed 1-2 times in between. To complete the digestion, fresh benzoylase was added: the 24x benzoylase stock was diluted 1:48 in the samples, incubated for another 45 min at 37 °C and 850 rpm and vortexed 1-2 times in between.

Next, a BCA assay was conducted to determine the protein concentration. A BCA assay kit (VWR) was used according to instructions by vendor. Samples were measured using the Envision Plate Reader. After protein concentration determination, samples were mixed 1:1 with 2xSDS/DTT buffer and incubated for 7 min at 95 °C for denaturation of proteins. Cells were then centrifuged at 13200 rpm for 5 min in a table top centrifuge before loading to remove precipitated material. A NuPAGE 4-12 % Bis-Tris Gel was positioned in an electrophoresis chamber filled up with running buffer.

Anti-oxidant was added and 4  $\mu$ L molecular weight marker was loaded into one well. The samples were diluted to 10  $\mu$ g protein per well (prepared in SDS/DTT sample buffer) and loaded into the wells. 80 V was applied until the samples have fully migrated into the gel, then the voltage was increased to 160 V. Samples were migrated until the dye front reached the bottom of the gel.

For the transfer of the samples from the gel onto the membrane, the nitrocellulose membrane was rehydrated shortly in 20 % EtOH. Blot papers, membrane and gel were equilibrated in 1x transfer buffer. A sandwich was formed out of blotting paper, membrane, gel and on top again blotting paper. The transfer was performed with a Trans-Blot Turbo (Biorad) for 10 min. After transfer, the membrane got blocked for 1 h at room temperature in odyssey blocking buffer. It got incubated over night at 4 °C with the primary antibody IRDye680RD Goat anti-rabbit (Leicor) diluted in OBB, 0.2 % Tween 20. On the following day, the membrane got washed 4 times 5 min with washing buffer and further incubated 1 h at room temperature with the secondary antibody anti-OATP2B1 (IKP Stuttgart) diluted in OBB (1:200), 0.2 % Tween 20, 0.02 % SDS. The membrane got washed 4 times 5 min with washing buffer and the membrane finally rinsed with PBS once. An odyssey infrared imager (Leicor) was used to scan the membrane.

### 3.2.2 CULTIVATION OF HUMAN CELL LINES

#### 3.2.2.1 CULTIVATION OF HEK293 CELLS

HEK293 cells overexpressing OATP2B1 or vector control were generated and cultured as described by Nies *et al.*<sup>172</sup> at 37 °C, 5 % CO<sub>2</sub> and 95 % humidity in supplemented DMEM. Cells were grown to 70 % confluency in cell culture plates. For splitting, a cell culture plate was washed with 5 mL PBS prior to incubation with 3 mL trypsin buffer for 5 min. Cells were resuspended in 7 mL fresh medium and split into a new maintaining plate. A maintaining plate was seeded at 10-30 % confluency.

<b>Supplements added to DMEM for OATP2B1/vector control cultivation</b>	
10 %	FCS
5 %	PEN/STREP
8 mL/500 mL	G418

### 3.2.2.2 POLY-L-LYSINE COATING OF THE PLATES

Because of adherence reasons, the 24- and 96-well plates that contained the cells during a treatment had to be coated with poly-L-lysine. For that reason, every well of those plates was incubated with 0.01 % poly-L-lysine for one hour. After removal of the solution, the wells got washed with sterile water once. Then they were let dry for about one hour before they were stored at 4 °C closed with parafilm prior to use.

### 3.2.2.3 CELL SAMPLE PREPARATION FOR FLUORESCENCE MEASUREMENT

48 h prior to the fluorescence-based assay, trypsinised, adherent culture cells were counted in a CASY counter and also the viability of the cells was determined in that step. For preparation of the treatment, the cells were resuspended at  $0.5 \cdot 10^6$  cells per mL. 50  $\mu$ L of cell suspension was added to each well of a coated black-well 96-well plate. 24 h before the assay, the cells were incubated with 5 mM sodium butyrate to increase the OATP2B1 expression.

### 3.2.2.4 CELL HARVEST FOR MALDI MASS SPECTROMETRY MEASUREMENT

Trypsinised, adherent culture cells were counted in a Neubauer counting chamber. While doing so, also the viability was checked with trypan blue. Cells were aliquoted to  $10^6$  cells per Eppendorf cup and centrifuged at 2000 rpm at 4 °C on a benchtop centrifuge. Supernatants were removed using a vacuum aspirator. The cell pellets were snap-frozen and stored at -80 °C until further use.

### 3.2.2.5 CELL PELLET GENERATION FOR MALDI MASS SPECTROMETRY METHOD DEVELOPMENT

For treatment of the cells during method development, they were resuspended at  $0.25 \times 10^6$  cells per mL in cell culture medium. 1 mL of the cell suspension was added to each well of a coated 24-well plate. On the second day, the cells got treated with 5 mM sodium butyrate dissolved in PBS. On the assay day, the cells got preincubated with the standard inhibitor erlotinib<sup>171</sup> (4  $\mu$ M) or vehicle (dimethylsulfoxide (DMSO)) for 10 min before addition of either dibromofluorescein (DBF)<sup>173</sup> or estrone-3-sulfate ((E3S)<sup>73</sup>, varying concentrations from 3 nM to 100  $\mu$ M) for varying time points from 20 sec to 30 min. To stop the uptake, the supernatant was removed by a vacuum aspirator and the cells got washed once with ice cold PBS. After removal of PBS, the cells got trypsinised and were further portioned in Eppendorf cups. Those were spun down with a benchtop centrifuge at 2000 rpm and 4 °C for 5 min. The supernatant was removed, the cells were snap-frozen and stored at -80 °C until further use. The optimal screening conditions (2 min, 10  $\mu$ M) were verified by the use of the standard inhibitor erlotinib. In case of a “spiked-in” experiment, an untreated cell pellet was used and the compound of interest was spiked in at different concentrations.

### 3.2.2.6 CELL PELLET GENERATION FOR MALDI MASS SPECTROMETRY AUTOMATED SCREENING

One day prior to drug treatment, OATP2B1 and vector control cells were resuspended at  $0.5 \times 10^6$  cells per mL in culture medium. 200  $\mu$ L of the suspension was added to each well of a coated 96-well plate. Directly after seeding out the cells, they were incubated with 5 mM sodium butyrate dissolved in PBS. On the day of the assay, one hour before the treatment, the medium was changed to the same amount of serum-free medium in each well, also containing G418 and P/S like the normal growth medium. All of the 294 test compounds were dissolved in DMSO in a separate “inhibition-compound-plate”. Every plate contained erlotinib (4  $\mu$ M final concentration) as a positive control and DMSO as a negative control. The CyBio FeliX pipetting platform was used to transfer 1  $\mu$ L of the test compounds to the cell culture plate. For that purpose, the 96-well 60  $\mu$ L tip tray of the pipetting platform was used to draw 1  $\mu$ L from the “inhibition-compound plate” and release that amount to the 96-well plate

containing the cells. A complete blow out of the sample was conducted including blowing out of air into the cells, which led to an improvement in the mixing. A separate “substrate-plate” was prepared with E3S exhibited in every well. After the preincubation with test compound, which was being conducted for 10 min at 37 °C, the substrate was added to each well with the same CyBio FeliX method as described above. After an incubation time of 2 min, the supernatant was removed by a vacuum aspirator and washed once with ice cold PBS. After removal of PBS, the 96-well plate got snap-frozen and was stored at -80 °C until further use.

### 3.2.3 FLUORESCENCE-BASED ASSAY

#### 3.2.3.1 FLUORESCENCE SUBSTRATE ASSAY

All steps of the cell treatment, if not stated otherwise, were conducted “half-automated” by the use of an Integra ViaFlo equipped with a 96 well head with a 300 µL tip tray. The test compounds were all dissolved in DMSO, DBF was dissolved in Hank’s buffered salt solution (HBSS) exhibited in a tray. On the day of the assay, the supernatant of the cultured cells was removed. The cells got washed once with 50 µL pre-warmed HBSS buffer, which was removed again directly. Then the cells got preincubated with test compound of a final concentration of 10 µM dissolved in HBSS. For the method development of the fluorescence substrate assay, this was done manually. After a preincubation time of 5 min, the substrate DBF was added. The concentration ranged from 1.7-67 µM and the incubation time from 5-60 min. After the incubation at 37 °C, the supernatant was removed. The cells got washed once with ice-cold 150 mM ammonium formate buffer (pH 7.4, dissolved in HBSS)<sup>106</sup>. Fluorescence intensity was measured using an Envision plate reader using 485 nm as the excitation wavelength and 535 nm as the emission wavelength. The optimal screening conditions (30 min, 10 µM) were verified by the use of the standard inhibitor erlotinib.

#### 3.2.3.2 SCREEN FOR OATP2B1 INHIBITORS

A set of 294 compounds was selected from the top prescribed drugs in the US of the year 2017<sup>174</sup> excluding biologics and restricted substances, and was completed with

~100 literature small-molecule drugs known to interact with the transporter<sup>171, 175, 176</sup>. This compound set was used as the test inhibitors with each plate containing erlotinib (10  $\mu$ M final concentration) as the positive control and DMSO as the negative control. All of the compounds were dissolved in DMSO (1 mM) and on the assay day diluted to 20  $\mu$ M in HBSS. Cells were preincubated with the test compounds for 5 min and DBF dissolved in HBSS to 20  $\mu$ M was added in the same ratio leading to a final concentration of 10  $\mu$ M test compound and 10  $\mu$ M DBF. After incubation for 30 min, the supernatant was removed and the cells got washed once with 150 mM ice-cold ammonium formate buffer (pH 7.4, dissolved in HBSS)<sup>106</sup>. Fluorescence intensity was measured using the method explained above.

### 3.2.3.3 pIC<sub>50</sub> DETERMINATION

Drugs that produced an inhibition of DBF uptake of  $\geq 50$  % were serially diluted (5 nM-100  $\mu$ M) to analyse the concentration-dependent effect on the inhibition of the uptake. The experiment was conducted as described in 3.2.3.2. pIC<sub>50</sub> values were determined with GraphPad Prism v8.0.0 using the “response vs log(inhibitor concentration) – variable slope” equation with no constraints on all parameters (IC<sub>50</sub>, Hill Coefficient, Bottom, Top)<sup>177</sup>.

$$Y = bottom + \frac{top - bottom}{1 + 10^{\wedge}IC_{50} - X} * hillcoefficient)))$$

Each experimental run created a pIC<sub>50</sub> value that was compared to show assay reproducibility.

### 3.2.3.4 FLUORESCENCE MICROSCOPY

In order to validate the plate reader output of the fluorescence-based assay, fluorescence microscopy was done with the black-well 96-well plates right after treatment and measurement by the plate reader. Pictures were taken in Nomarski microscopy and in the excited state from both vector control and OATP2B1 cell lines treated with the substrate DBF. The wavelengths for excitation were comparable to the plate reader measurement (481 nm excitation, 515 nm emission). Nomarski



interference contrast pictures, which enhance the contrast in unstained, transparent samples, were compared to excited shots.

### 3.2.3.5 AUTOFLUORESCENCE AND QUENCHING MEASUREMENTS

For exclusion of possible false-negatives and -positives due to autofluorescence and quenching effects during the fluorescence-based assay, the 294 drug set was analysed and compared with the fluorescence of DBF itself. For testing the autofluorescence, the compounds were dissolved in HBSS to a final concentration of 10  $\mu\text{M}$  and 100  $\mu\text{M}$  in separate wells. DBF in a concentration of 10  $\mu\text{M}$  in separate wells served as a comparison. The fluorescence intensities were compared at the usual excitation and emission wavelengths. For the calculation of the relative values, the fluorescence intensity of the investigated compounds was respectively divided through the mean fluorescence intensity of 3 DBF wells and expressed as a % value. For the evaluation of a quenching effect, DBF was additionally given to each of the compound wells and it was checked if there was a decrease in the fluorescence compared to DBF alone. Therefore, the measurement was also done at 485 nm excitation and 535 nm emission and relative values calculated like mentioned before. Compounds with a decrease of 30 % of the intensity, which would lead to a final value of 70 % and lower, were considered to have a quenching effect.

### 3.2.4 MALDI MASS SPECTROMETRY WHOLE CELL MEASUREMENTS

#### 3.2.4.1 SAMPLE PREPARATION FOR METHOD DEVELOPMENT

A MALDI MS measurement in general was conducted on a 384-well MTP. Before usage of the plate, it got rinsed 2x with soap-water, 2x with methanol and 2x with acetone using extra low-lint wipers, then the plate got air-dried.

For a sample preparation, the cell pellet was taken out of  $-80\text{ }^{\circ}\text{C}$  and resuspended with acetonitrile (ACN)/ $\text{H}_2\text{O}$  leading to a final concentration of 2500 cells/spot. For the later in method development used normalisation, a final concentration of 0.3  $\mu\text{M}$  D<sub>4</sub>-E3S was supplemented to the solvent. One spot contained 1  $\mu\text{L}$  cell suspension. Cells were applied in eight measurement replicates. A different cell pellet that was treated the

same day is referred to as technical replicate. A biological replicate is here defined as a cell pellet of a different passage number that was treated on another day.

### 3.2.4.2 MATRIX APPLICATION FOR METHOD DEVELOPMENT

In the course of method development, several matrices were tested in their ability to detect the two different substrates, DBF or E3S. All of them were either applied Dried Droplet, via PrimaDrop<sup>168</sup>, as Sandwich or with a sprayer. For Dried Droplet application, the resuspended cells were mixed in a ratio of 1:1 with the matrix and applied onto the target plate. In case of PrimaDrop application, the cell suspension was applied manually onto the target plate and let dry before manually applying matrix on top. Sandwich application included coating the MTP with matrix first and then applying the cell suspension together with the matrix in a Dried Droplet way. For spraying the matrix, the cell suspension got applied and dried before using a spraying device to coat the samples. 20 mg/mL sDHB were used in 50 % ACN supplemented with 0.5 % TFA. 20 mg/mL DHB were used in 50 % ACN supplemented with 0.2 % TFA and the composition of 2,5-DHAP and Ph-CCA-NH<sub>2</sub> varied in the course of method development from different solvents to different concentrations. When sprayed, DHB, sDHB and Ph-CCA-NH<sub>2</sub> were coated with the SunCollect matrix sprayer. The HTX M5 sprayer was used for coating with 2,5-DHAP.

<b>Matrix spray protocol SunCollect sprayer</b>	
Spray-head height	28 mm
Distance between sprayed lines	2 mm
Matrix flow rate	10-25 µL/min
Speed while spraying	850 mm/min
Sprayed layers	9

<b>Matrix spray protocol HTXM5 sprayer</b>	
Spray head velocity	1000 mm/min
Spray-head height	40 mm
Distance between sprayed lines	2.5 mm
Matrix flow rate	100 $\mu$ L/min
Sprayed layers	2
Spray nozzle temperature	50 °C
Gas flow rate	2 l/min
Pressure	10 psi

### 3.2.4.3 AUTOMATED SAMPLE PREPARATION AND MATRIX APPLICATION FOR SCREENING

The automation of the method was done together with Lena Schumacher during her bachelor thesis. For automated sample preparation the CyBio FeliX pipetting platform 96-60  $\mu$ L tip tray was used. The 96-well plate with the treated cells was taken out of the -80 °C freezer and placed onto the instruments thermal mixer, BioShake. They directly got resuspended with 20  $\mu$ L ddH<sub>2</sub>O at room temperature and maximal pipetting speed was used to pipet the cell suspension up and down two times. Then, 20  $\mu$ L of 2.5 mg/mL Ph-CCA-NH<sub>2</sub> in 70 % ACN supplemented with a final concentration of 0.3  $\mu$ M D<sub>4</sub>-E3S were added. For improvement of resuspension, the BioShake mixed the sample for 7 s. A 5 s pause upon sample aspiration helped to saturate the gas phase above the liquid phase in the pipetting tip leading to improved pipetting. One  $\mu$ L of the suspension was applied to a MTP leading to a final concentration of 2500 cells per  $\mu$ L. The plate was air-dried before measurement. The pipetting steps took 2 min. Out of one well, there were four spots on the MTP pipetted, leading to four measurement replicates. In case of other wells with the same treatment, this was here referred to as technical replicate, treated on the same day. A biological replicate here is described as a different passage number of cells being treated on another day.

#### 3.2.4.4 MALDI-TIME OF FLIGHT MASS SPECTROMETRY DATA ACQUISITION

All of the experiments were measured with a rapifleX MALDI-TOF mass spectrometer. A 10 kHz smartbeam 3D laser is installed in the instrument. Automation of the data acquisition was possible due to the use of the AutoXecute function of the flexControl 4.0 software and later on by MALDI Pharma Pulse (MPP) 2.2. Spectra for method optimisation and inhibitor screen were acquired in the  $m/z$  range from 340-900. Random walk mode was used to create a preferably homogeneous overview of the sample spot at 40 different positions using the sum spectra of 4000 laser shots per measuring spot. The laser focus was adjusted to "MS thin layer" whereas the sampling rate amounts to 5 giga samples per second. E3S and D<sub>4</sub>-E3S were used as internal calibrants and a linear calibration on those two was performed.

#### 3.2.5 VIABILITY TEST: CELLTITER-GLO

For both assays, fluorescence-based and MALDI MS, an investigation of cell viability after compound addition was done. In the case of the fluorescence-based assay, all of the compounds that were further analysed in their concentration-dependent effect on the uptake of DBF were also tested in their effect on the viability of the cells. For that purpose, after the measurement with the Plate Reader, the same amount of CellTiter-Glo reagent (mixed out of two components, as instructed by the manufacturer) was given to the already existing amount of ammonium formate (100  $\mu$ L per well). After a mixing step, the plate was placed on a shaker for 2 min to induce cell lysis. Subsequently, the plate got incubated 10 more min at room temperature before measuring the luminescence with a plate reader. In case of the MALDI MS assay, the viability test could not be done after the measurement, but plates had to be treated with compounds and CellTiter-Glo reagent just for the viability measurement and could not be used further. The viability test was done once for each technique, because the incubation times with compounds varied in the two different assays (35 min in total with fluorescence-based assay, 12 min in total for MALDI MS assay) leading to possible differences in cell viability.

### 3.2.6 DATA ANALYSIS USING COMMERCIAL SOFTWARE

For the method optimisation before the establishment of the automated assay, FlexAnalysis batchprocess mode was used to analyse the data. Therefore, a method was used, where first the baseline was subtracted (TopHat) and then the spectra were processed with a centroid peak detection algorithm and a peak width of 0.02  $m/z$ . Peaks over a S/N of 2 were displayed. The algorithm for smoothing was set to SavitzkyGolay with a width of 0.2  $m/z$  and 1 cycle. For the automated screening assay, MPP was used to perform an internal calibration on E3S and D<sub>4</sub>-E3S and extracting the desired intensity values of the masses of interest, in this case always E3S and D<sub>4</sub>-E3S. The resulting Excel file included intensity, resolution and S/N of both peaks and a peak ratio resulting of the intensities of E3S vs D<sub>4</sub>-E3S. This normalised peak value was used for further calculations in Excel and GraphPad Prism. pIC<sub>50</sub> values were calculated as already mentioned in 3.2.3.3.

The search for a substrate during the screen for inhibitors was evaluated with R version 3.5.1<sup>178</sup> by Thomas Enzlein. The data were normalised to the intensity of D<sub>4</sub>-E3S after baseline correction and an average spectra of four measurement replicates was calculated. The respective compound masses were extracted from OATP2B1 and the vector control. The generated Excel file was then further analysed by determining a ratio of at least 1.5 (OATP2B1 vs. vector) and in addition the normalised peak of OATP2B1 had to be higher than the normalised peak of other samples at the respective compound mass. Compounds that were identified as eventual hits were further analysed in an inhibition experiment.

## 4 RESULTS

The results of this thesis are presented in two chapters with 3 parts each:

The first part focuses on a fluorescence-based assay, which was developed to be a reference method for the later developed MALDI MS assay. Throughout the course of experiments, there were three major goals to achieve:

- A) Checking the overexpression by a Western Blot
- B) Development of the assay
- C) Application to a screen and DDI analysis

The second and major part focuses on the MALDI MS method. It was developed to be a label-free alternative to the currently used technologies. A condition for the assay was to be automatable and therefore have a possible application in industry. The MALDI MS experiments can also be divided into three parts

- A) Development of the method
- B) Automation of the method
- C) Application to a screen and comparison of the results with fluorescence-based screen

### 4.1 WESTERN BLOT CONFIRMING THE OVEREXPRESSION OF OATP2B1

A prerequisite for transporter characterisation was the confirmation of the overexpression of the transport protein compared to the vector control (cells transfected with non-expressing plasmid), so that both cell lines could be compared in the following experiments and differences monitored could be attributed to the transport protein. A western blot was done to confirm the overexpression of OATP2B1 compared to its vector control. As OATP2B1 has a size of 76.6 kDa, a band should be noticed at this height in the overexpressing cell line, but not in the vector control cell line. As it can be seen in **Figure 10**, there is a smeared band with an accumulation of intensity at 76.6 kDa for the OATP2B1 cell line. The vector control cell line did not show a band at this height. A comparison of two different amounts of total protein (15 µg vs 25 µg) showed a higher intensity at 25 µg. The reason for the smeared band can be various ranging from too concentrated protein / antibody to problems with the sample buffer using too less SDS. It is also likely that the smear in the bands were caused by genomic DNA strands, which were left in the samples. In this protocol, the cells were harvested and then directly lysed, where also a short centrifugation step was included. The digestion was done at 37 °C and after the SDS buffer addition, the samples were heated to 95 °C and centrifuged to remove the precipitated material. An additional sonication step or shearing the probes through a needle could have improved the breakup of the cells and reduced the smear in the band. Despite the lacking quality of the western blot, the overexpression of the transport protein was confirmed. As the goal here was only to confirm the overexpression and focus did not lie on the improvement of the western blot, the results are sufficient. With the confirmation of the overexpression of OATP2B1, all following experiments comparing the transporter overexpressing cell line with its vector control therefore lead to results, which can be attributed to the transport protein.

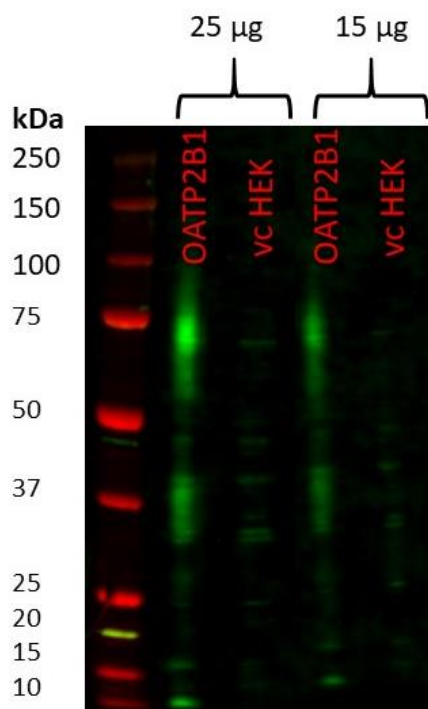


**Figure 10: Western blot as confirmation of the overexpression of OATP2B1:** A comparison of the OATP2B1 cell line and its vector control in a Western Blot showed a smeared band with an accumulation of the intensity at 76.6 kDa for OATP2B1 and none for the vector control. Two amounts of total protein (15 and 25 µg) were compared.

## 4.2 FLUORESCENCE-BASED ASSAY

Since fluorescence-based assays are still the most common method for transporter investigation, the goal was to establish a fluorescence-based assay for OATP2B1 as a reference assay. Due to the easy readout and applicability to high-throughput, this method is still used a lot.

### 4.2.1 DEVELOPMENT OF A FLUORESCENCE-BASED ASSAY FOR THE UPTAKE OF DIBROMOFLUORESCEIN THROUGH OATP2B1

For the development of the fluorescence-based assay, an existing protocol from the working group of Anne Nies was modulated and applied to the cells. Cells were treated with sodium butyrate 24 h prior to the assay in order to increase the expression of OATP2B1<sup>179</sup>. As a washing solvent for stopping of the uptake, ice-cold ammonium formate (pH 7.4) was utilised<sup>106</sup>. The usage of a pipetting platform (ViaFlo) improved



the Z' of the assay and led to acceptable values  $\geq 0.5$ . The Z' is a factor describing the quality of an assay system and leading to a value between 0.5 and 1 for a valid assay. It is dependent on the standard deviation and the mean value of the positive and negative control and calculated as following.

$$Z' = 1 - \frac{3 * (STDEV(positivecontrol) + STDEV(negativecontrol))}{|mean(positivecontrol) - mean(negativecontrol)|}$$

Confirmation of the uptake of DBF<sup>173</sup> through OATP2B1 was done by fluorescence microscopy. Therefore, the overexpressing cell line was compared to the vector control. A differential interference contrast picture, also known as Nomarski microscopy named after its inventor, was compared with a visible light (481 nm) excited version that led to the possible detection of the fluorescence of DBF (emission: 515 nm). Nomarski microscopy is based on a prism splitting up the polarised light into two rays. The following condenser focuses the rays for passage through the sample, the distance between the rays is about 0.2  $\mu\text{m}$  and thus, they hit two adjacent points on the object. In the following prism, the rays are merged again and interfere. This interference of the two rays, which have travelled through different path lengths due to variation in the thickness and refractive index of the analysed object, leads to the contrast in the picture.

The goal of the experiment was to detect a fluorescence only in the cells overexpressing the transport protein and not in the vector control confirming the uptake through the transporter. Therefore, OATP2B1 and the vector control were treated with the substrate DBF for 30 min. By a comparison of the Nomarski transmitted light microscope picture of DBF-treated OATP2B1-overexpressing cells (**Figure 11,A**) with the excited version, clearly showed the fluorescence in the cells (**Figure 11,B**). The comparison of the Nomarski microscopy picture of the vector control treated with DBF (**Figure 11,C**) with the excited one (**Figure 11,D**) made clear that no fluorescence could be seen in the vector control. This finding supports the uptake of DBF through the transport protein OATP2B1, due to the fact that a fluorescence could only be detected with the presence of the transporter.

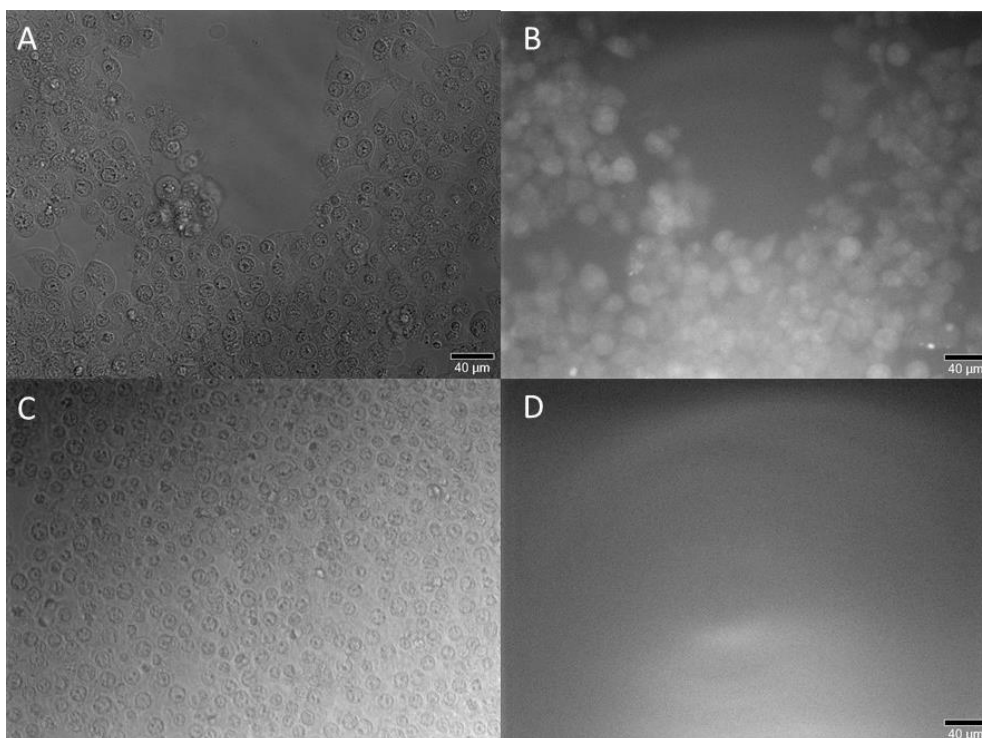


**Figure 11: Fluorescence microscopy supports uptake of DBF through OATP2B1:** (A) Nomarski microscopy, HEK293-OATP2B1 with DBF incubation. (B) Excited with 481 nm, emission at 515 nm, HEK293-OATP2B1 with DBF incubation. (C) Nomarski microscopy, HEK293-vec with DBF incubation. (D) Excited with 481 nm, emission at 515 nm, HEK293-vec with DBF incubation.

After the confirmation of overexpression and DBF uptake through OATP2B1, the overexpressing cell line was compared to its vector control and a concentration- and time-dependence of the DBF uptake was investigated in order to characterise the transport process. The goal of this experiment was the identification of the optimal assay conditions for investigating uptake and inhibition through OATP2B1, which lie in the linear range of the time-dependence and below the determined  $K_M$  value. A comparison with the vector control is done to ensure that the transport is only mediated through OATP2B1. Therefore, OATP2B1 and vector control cells were treated with various concentrations of DBF during the concentration-dependence test and for various time points during the time-dependence test. The uptake process showed to be time-dependent, indicating also a clear difference to the vector control uptake. A plateau could be seen after about 1 h (**Figure 12,A**). The uptake process also showed to be concentration-dependent. A Michaelis-Menten curve fit was done in GraphPad

Prism to determine the  $K_M$  value. Using the signal intensity to determine the  $K_M$  is less common than using the velocity of the uptake. Nevertheless, the  $K_M$  is the concentration at which the signal intensity describing the activity of the transport is half-maximal. Therefore, measurement of the signal intensity is comparable to the velocity and therefore can be used to determine the  $K_M$ <sup>180-182</sup>. The  $K_M$  determination led to a value of  $10.5 \mu\text{M} \pm 1.6$ . In addition to the evaluation of concentration- and time-dependence, the optimal assay conditions were found out. 30 min incubation time still lied in the linear range of the uptake, where transporter-activity is determined<sup>27</sup>, and  $10 \mu\text{M}$  DBF, which was beneath the  $K_M$  value, is a good condition ensuring that the transporter is not yet saturated and still actively involved in uptake. A general rule is to use a substrate concentration within twofold of the  $K_M$  value<sup>183</sup> (**Figure 12,B**).

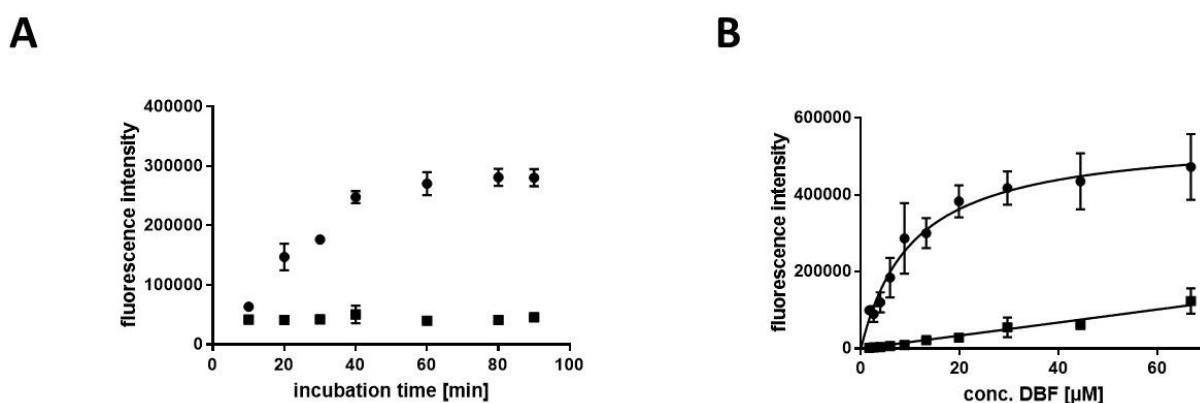


**Figure 12: Fluorescence-based evaluation of time- and concentration-dependence of DBF uptake through OATP2B1:** Uptake assay of DBF through OATP2B1 was done by treating OATP2B1-overexpressing and vector control cells with various concentrations of DBF for various time points. The uptake was stopped by aspiration of the compound dissolved in HBSS and washing with ice-cold ammonium formate. Fluorescence intensity was measured with an Envision plate reader using 485 nm as excitation and 535 nm as emission wavelength. **(A)** Cells were incubated with  $10 \mu\text{M}$  DBF for various time points ranging from 10 min to 90 min. HEK293-OATP2B1 (indicated as circles) are compared to HEK293-vec (indicated as squares). Mean  $\pm$  SEM for 4 technical replicates. **(B)** Cells were incubated with various concentrations of DBF ranging from  $1.7 \mu\text{M}$  to  $66.7 \mu\text{M}$  for 30 min. HEK293-OATP2B1 (indicated as circles) are compared to HEK293-vec (indicated as squares). Mean  $\pm$  SEM for 4 technical replicates. Figure adapted from<sup>170</sup>.

The development of a cell-based assay should follow important quality criteria that are applicable to a broad variety of laboratory experiments. In the case of a cell-based assay, the first step of course is the decision for a cell line that is suitable for the analysis. As monolayer forming cell lines are a common tool for the investigation of transport processes<sup>12</sup>, a cell line, which overexpresses the desired transport protein, and its respective vector control can be established in for example HEK293 cells, which generally have a low background expression of transporters<sup>184</sup>. The next important step is to confirm the expression of the transporter in comparison to the vector control, which was here shown with a western blot. The presence of suitable controls is one of the most important considerations. As the concentration- and time-dependence test already showed, the vector control acts as a good control for the OATP2B1 cell line. Additionally, in a screen, there should be a standard inhibitor involved, which acts as a suitable comparison to other substances investigated. The investigation of reproducibility is one of the key factors for the development of cell-based assays. It is confirmed when the investigated inhibitor shows a comparable pIC<sub>50</sub> in at least 3 biological replicates. Therefore, with the use of the optimised assay conditions, the pIC<sub>50</sub> value of the kinase inhibitor erlotinib, which is a known inhibitor for the uptake of OATP2B1<sup>171</sup>, was determined. Thus, a dilution series of erlotinib was added to the cells and preincubation was done for 5 min. DBF was then added for 30 min and the uptake was stopped by addition of ice-cold ammonium formate. During the assay validation, a pIC<sub>50</sub> of 7.0 ± 0.1 was determined (**Figure 13**). The determination of the value was done using a positive control (10 µM erlotinib) considered as 100 % inhibition and vehicle (DMSO) considered 0 % inhibition. The pIC<sub>50</sub> value was calculated with GraphPad Prism v8.0.0 using the “response vs log (inhibitor concentration) – variable slope” equation with no constraints on all parameters (IC<sub>50</sub>, Hill coefficient, bottom, top).

$$Y = bottom + (top - bottom) / (1 + 10^{\wedge}((LogIC_{50} - X) * hillcoefficient))$$

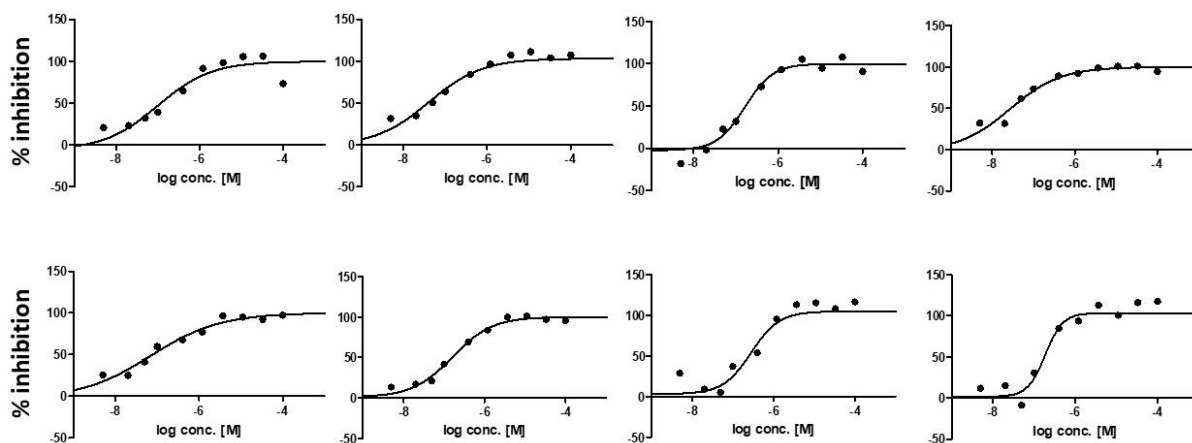


**Figure 13: pIC<sub>50</sub> generation of erlotinib during assay validation:** Uptake assay was done by preincubation of the cells with a dilution series of erlotinib in HBSS for 5 min. 10  $\mu$ M DBF was added for 30 min. After stopping the uptake by aspiration and washing with ice-cold ammonium formate, the plate was measured with an Envision plate reader at the mentioned wavelengths. Plotted is the % inhibition of DBF uptake with erlotinib control (10  $\mu$ M) as positive control considered 100 % inhibition and vehicle control as negative control considered 0 % inhibition of the uptake. pIC<sub>50</sub> of 7.0 was calculated using GraphPad Prism v8.0.0 using the “response vs log (inhibitor concentration) – variable slope” equation with no constraints on all parameters. Data represents 8 biological replicates.

With the reproducible determination of the pIC<sub>50</sub> and the evaluation of the optimal assay conditions, which led to an optimisation of the assay, the method was now applicable to a screening format, which also can be seen as a validation of the assay.

#### 4.2.2 SCREEN OF 294 DRUGS IDENTIFIES MANY INHIBITORS THAT ARE LIKELY TO CAUSE DRUG-DRUG INTERACTIONS

Through the use of a pipetting platform (ViaFlo), a high-throughput format was established and the transport protein could be investigated regarding possible DDIs. Screening formats of transport proteins are still lacking even though they confirmed to be related to human diseases in many ways<sup>33</sup> and therefore an interesting drug target. The goal therefore was the conduction of a screen, which was capable of testing 294 compounds as a reference assay. This compound set consisted of the top marketed drugs of the year 2017<sup>174</sup> plus ~100 additional compounds that are known to interact with the transporter OATP2B1<sup>171, 175, 176</sup>. The drugs were thus analysed in their ability

to inhibit the uptake of the fluorescent substrate DBF through OATP2B1. An alarming outcome of that experiment would be the identification of a high number of inhibitors that could also possibly lead to DDIs when coadministered. In order to enlighten the clinical relevance of the drugs in the compound set, OATP2B1 cells were preincubated with those test drugs for 5 min and then concomitantly incubated with 10  $\mu$ M DBF for 30 min. Uptake was stopped by washing with ice-cold ammonium formate and plates were measured in an Envision plate reader. There were 66 hits (inhibition  $\geq 50$  %) identified, meaning more than 20 % of the compounds in the data set showed an inhibition on the uptake (**Figure 14**). Compounds that led to an inhibition of more than 50 % were advanced to detailed analysis through  $pIC_{50}$  determination. A noticeable detail about the figure below is the existence of negative inhibition values. This effect may indicate stimulation of uptake and is a known phenomenon for OATP2B1 transporter<sup>185</sup>.

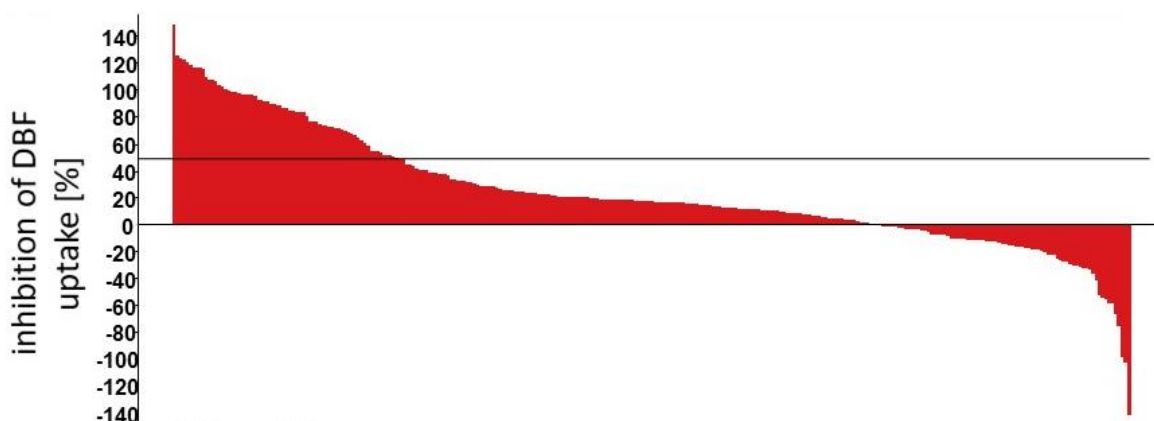


**Figure 14: Visual depiction of fluorescence screening results:** A set of 294 compounds was tested in its ability to inhibit the uptake of the fluorescent substrate DBF through OATP2B1. Therefore, the cells were incubated for 5 min with the test compound and then concomitantly incubated with 10  $\mu$ M DBF for 30 min before the uptake was stopped by aspiration and washing with ice-cold ammonium formate. 10  $\mu$ M erlotinib were used as a positive control considered 100 % inhibition and DMSO as a negative control considered 0 % inhibition. Compounds with an % inhibition of DBF uptake  $\geq 50$  % were considered a hit and were further analysed through the determination of their  $pIC_{50}$ . Figure adapted from <sup>170</sup> and done by Friedrich Reinhard.

As the potency of the identified inhibitors was of great interest, a detailed analysis by a determination of the  $pIC_{50}$  was conducted, which can also be seen as a confirmation of the hits. The  $IC_{50}$  is the half maximal inhibitory concentration and describes the concentration of an inhibitor for which a half maximal inhibition of the target is reached. It is often used in pharmacology in order to rate the potency of a drug. The  $pIC_{50}$  is the negative decadic logarithm of the  $IC_{50}$  and is like the pH better comparable.

For the  $pIC_{50}$  determination, the hit compounds were serially diluted and applied to the cells like mentioned before. The detailed analysis of the screening results showed an occurrence of 57 inhibitors in total meaning 9 inhibitors could not be confirmed during concentration-dependent measurements. Those were amiodarone, cetirizine, ceritinib, cyclosporine, fenofibrate, gliquidon, meloxicam, pioglitazone and trimethoprim. For gliquidone, there was no  $pIC_{50}$  determined, because the compound was forgotten to be included. Pioglitazone, ceritinib and trimethoprim were close to 50 % inhibition in the screen and it was therefore not unlikely that they did not produce a  $pIC_{50}$ . The others showed % inhibition values >73 % in the screen, but produced  $pIC_{50}$  curves with a high scatter or showed an inhibition less than 50 % for the highest concentration tested. Nevertheless, there were 8 potent inhibitors with a  $pIC_{50} \geq 6$  found (**Figure 15, Table 1**). Those were acemetacin, atorvastatin, benzbromarone, erlotinib, fluvastatin, montelukast, tipranavir and tropesine. Acemetacin is a known OATP1B1 inhibitor<sup>186</sup> and atorvastatin<sup>187</sup>, benzbromarone, erlotinib, fluvastatin<sup>171</sup>, montelukast<sup>188</sup> and tipranavir<sup>189</sup> are known OATP2B1 inhibitors. Tropesine was not known as OATP2B1 inhibitor before.

## Results

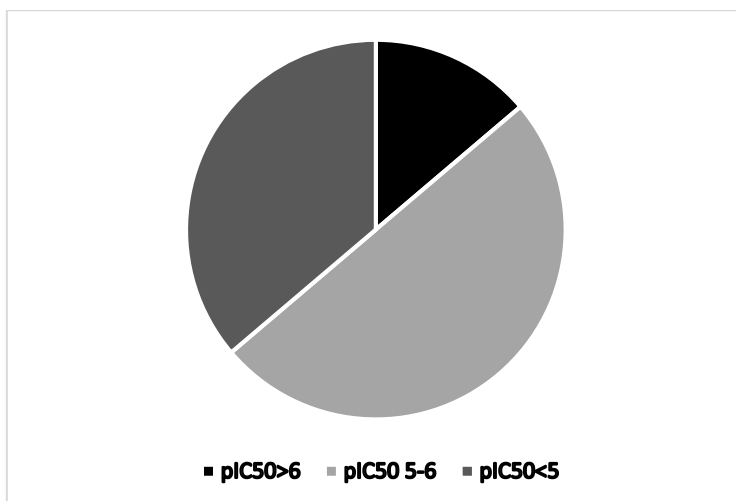


**Figure 15: Analysis of the fluorescence-based screening results:** From 294 screened compounds, there were 57 confirmed inhibitors in total, 21 with a pIC<sub>50</sub> < 5, 29 with a pIC<sub>50</sub> between 5-6 and 7 potent inhibitors with a pIC<sub>50</sub> > 6. pIC<sub>50</sub> are the average from two independent pIC<sub>50</sub> determinations.

**Table 1: pIC<sub>50</sub> determination results of fluorescence-based screen:** 57 inhibitors could be confirmed in 2 biological replicates, 8 potent inhibitors with mean pIC<sub>50</sub> > 6 identified.

Compound	n=1	n=2	Compound	n=1	n=2
Acemetacin	7.2	7.1	Ketoconazole	5.2	5.3
Amsacrine	4.7	5.0	Latanoprost	5.1	5.3
Atorvastatin	7.2	6.9	L-Thyroxine	5.0	5.0
Benzbromarone	6.6	7.4	Loratadine	4.7	5.0
Bicalutamide	4.9	4.7	Losartan Potassium	5.1	5.1
Calcitriol	4.9	5.5	Lovastatin	4.9	5.0
Celecoxib	4.7	5.0	Mometasone Furoate	5.2	4.9
Clobetasol Propionate	5.1	5.0	Montelukast	6.6	6.4
Desogestrel	4.9	4.1	Norethindrone	4.9	4.7
Diacerein	4.8	4.6	novobiocin	5.4	5.5
Diethylstilbestrol	5.4	6.5	Olmesartan Medoxomil	5.4	5.4
Diffunisal	5.0	4.9	Olsalazine	5.4	5.8
Dipyridamole	5.6	6.0	Oxaprozin	4.8	4.9
Doxazosin Mesylate	4.7	5.0	Oxybutynin	4.7	4.5
Drospirenone	4.7	5.4	P-3004Unergol	4.7	4.9
Erlotinib	7.0	7.4	Prasugrel Hydrochloride	5.2	5.3
Estradiol	5.3	5.9	Quetiapine Fumarate	4.8	4.7
Estrone-3-Sulfate	5.5	5.4	Raloxifene Hydrochloride	4.9	5.5
Ethinyl Estradiol	6.2	5.4	Reserpine	5.3	5.6
Ezetimibe	5.7	5.8	Silymarin	5.7	5.5
Felodipine	5.3	5.8	Simvastatin	4.7	5.6
Flutamide	4.4	4.5	Sulfasalazine	5.5	5.6
Fluvastatin	6.9	6.8	Ticagrelor	5.5	5.2
Glimepiride	5.6	6.0	Tipranavir	6.6	6.7
Glyburide	5.5	6.0	Travoprost	5.3	5.5
Indomethacin	4.7	4.9	Tropesine	7.8	7.3
Ibuprofen	5.6	6.3	Vilazodone Hydrochloride	4.4	4.3
Irbesartan	6.1	5.8	Zafirlukast	5.8	5.9
Itraconazole	4.5	4.7			



Based on the results of that screen, Jennypher Mudunuru from the group of Maciej Zamek-Gliszczynski at GSK calculated the clinical relevance of those inhibitors taking into account the actual dose of the drug, the blood flow in the two possible interacting organs liver and intestine and other drug-specific parameters of the compounds according to an ITC white paper recommended calculation<sup>190</sup>. According to those calculations, 66 % of the identified inhibitors were clinically-relevant in the intestine and 29 % were clinically-relevant in the liver<sup>170</sup>. Those results clearly show the need to investigate transporter-mediated DDI.

As an important requirement for a cell-based screening assay is the validation of the data, an inter-assay correlation of the screening data was analysed. One of the concentrations tested during pIC<sub>50</sub> determination was 11.1 µM, which is a comparable concentration to the single screen conducted at 10 µM. For a comparison, only the compounds, which were further processed in pIC<sub>50</sub> determination could be used, which led to an occurrence of only values greater than 50 % listed in the figure (**Figure 16**). The resulting Spearman correlation coefficient of 0.71 was acceptable, but still indicated that the method was not perfectly adjusted. The CV % value of the comparison 11.1 µM and 10 µM was 26.4 and therefore showed to still need optimisation. Nevertheless, due to the uncommon setup of a comparison of 11.1 µM and 10 µM, differences could have arised also thereof.



**Figure 16: Inter-assay correlation of fluorescence experiment:** Comparison of 11.1 µM that resulted from the pIC<sub>50</sub> screen with 10 µM that resulted from the single screen. For the screen, a set of 294 compounds were tested in their ability to inhibit the uptake of the

fluorescent substrate DBF through OATP2B1. Therefore, the cells were incubated for 5 min with the test compound and then concomitantly incubated with 10  $\mu\text{M}$  DBF for 30 min before the uptake was stopped by aspiration and washing with ice-cold ammonium formate. 10  $\mu\text{M}$  erlotinib were used as a positive control considered 100 % inhibition and DMSO as a negative control considered 0 % inhibition. For the  $\text{pIC}_{50}$  determination, there were besides 11.1  $\mu\text{M}$  of the compound also several other compound concentrations tested. The handling was the same as in the screen.

Also the  $\text{pIC}_{50}$  determination acts as a validation of the method. For the determination of the  $\text{pIC}_{50}$  values, there were two biological replicates performed, so the analysis of intra-experimental reproducibility here could be performed by a comparison of the two data sets and a calculation of the linear regression  $r^2$ . It had a value of 0.78 (**Figure 17**), which was also acceptable. The results of the screen could be trusted and therefore analysed further.

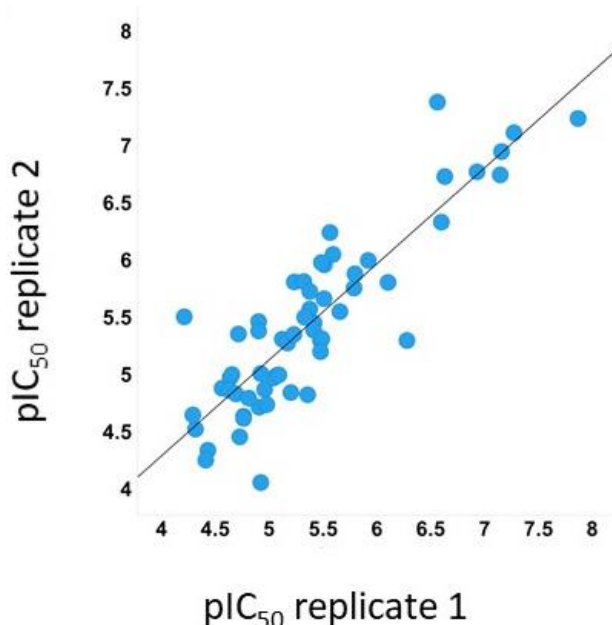


**Figure 17: Reproducibility of the screening data:**  $\text{pIC}_{50}$  values of two biological replicates plotted against each other to determine the reproducibility of the data. Figure adapted from<sup>170</sup>.

#### 4.2.3 AUTOFLUORESCENCE AND QUENCHING EFFECT TEST

A negative aspect about the fluorescence-based assays is that they can be prone to false-negatives and -positives due to photonic effects like quenching or autofluorescence of compounds. Autofluorescence of the investigated compounds can occur if the compounds themselves show a fluorescence emission measurable at 535 nm when being excited at 485 nm. In the case of the fluorescence-based screening assay, for the identification of an inhibitor, there is a decrease in the fluorescence intensity detectable, whereas a compound, which does not show an inhibiting effect would lead to the fluorescence intensity of the DBF signal maintaining. An autofluorescent compound could therefore act as such a maintain of the signal and would be interpreted as a non-inhibitor and therefore might be false-negative. Quenching of the compounds can occur when the compounds are excited at 485 nm and result in a fluorescing signal, which suppresses the DBF fluorescence intensity signal due to overlay effects. A quenching compound could therefore act as a reduction of the signal intensity even though it is a non-inhibitor and would be interpreted as an inhibitor and thus false-positive. Therefore, an evaluation of the autofluorescence and quenching effects of the investigated compounds was conducted in order to exclude those showing artefacts from the identified inhibitors.

For evaluation of autofluorescence of the compounds, they were solely diluted in HBSS, one compound per well, to a final concentration of 10  $\mu\text{M}$  and 100  $\mu\text{M}$ . Those two concentrations were used, because 10  $\mu\text{M}$  would be the final concentration of the compound in the assay system, but it could not be guaranteed that the concentration really stays that low in the cell assay due to accumulation effects, so 100  $\mu\text{M}$  was also tested. As a separate control in a separate well, DBF was diluted in HBSS to a final concentration of 10  $\mu\text{M}$ , like it was used in the assay system. The fluorescence was measured with a plate reader using 485 nm as excitation and 535 nm as emission wavelength. The resulting fluorescence intensity (FI) values for the compounds were divided through the mean of 3 DBF wells in order to get a relative value for each concentration.

$$\text{Autofluorescence [\%]} = \frac{\text{FI of compound}}{\text{Mean of FI of 3 DBF wells}} * 100$$

An alarming outcome of that experiment could be the identification of many autofluorescent inhibitors. This would be an error source that has to be investigated once more with a counter screen, because there might be many false-negatives that need to be reinvestigated. As **Table 2** shows, there were no compounds identified that showed a high autofluorescence (higher than 1.5 %) in comparison to the fluorescence of DBF, which makes clear that there are no false-negatives in the dataset due to this fluorescent effect.

For the evaluation of quenching, which was here defined as a DBF fluorescence signal reduction of more than 30 %, the diluted compounds from the autofluorescence measurement were additionally incubated with 10 µM DBF. The measurement was performed like mentioned above. For the calculation of the relative value, the fluorescence intensity (FI) of the compounds incubated together with DBF were divided through the mean FI of 3 DBF wells.

$$\text{Quenching [\%]} = \frac{\text{FI of compounds incub. together with DBF}}{\text{Mean of FI of 3 DBF wells}} * 100$$

Ideally, the resulting values of the quenching experiment would be at around 100 %, so no reduction of the fluorescence signal of DBF could be detected. In that case no false-positives would have been identified. As it can be seen in **Table 2** there were 5 compounds identified that showed a quenching effect on DBF fluorescence of more than 30 % at 100 µM leading to a DBF fluorescence signal reduction to 70 % and lower. Those were amlodipine, amsacrine, ceritinib, chlorhexidine and doxazosin mesylate. This means that through the simultaneous incubation with 100 µM of those compounds, a reduction up to 30 % in the fluorescence of DBF was observed. Those compounds therefore might be false-positives, because the quenching led to a reduction of the fluorescence that could falsely be interpreted as an inhibitory effect. This might have led to misinterpretations in the identification of inhibitors (**Table 2**).

**Table 2: Relative values of quenching and autofluorescence of 5 compounds:** Data of conspicuous compounds at two different concentrations (10  $\mu\text{M}$  and 100  $\mu\text{M}$ ) with relative values compared to DBF as a control. For autofluorescence, compounds were compared to DBF signal, for quenching, compounds were simultaneously incubated with DBF. Amlodipine, amsacrine, ceritinib, chlorhexidine and doxazosin mesylate showed a quenching effect of up to 30 % leading to a reduction of the fluorescence signal of 70% and more at 100  $\mu\text{M}$ .

Compound	Quenching		Autofluorescence	
	DBF fluorescence signal reduction Relative values [%]		Relative values [%]	
	10 $\mu\text{M}$	100 $\mu\text{M}$	10 $\mu\text{M}$	100 $\mu\text{M}$
Amlodipine	70.5	69.1	1.4	1.2
Amsacrine	77.7	48.7	1.2	1.1
Ceritinib	89.4	43.1	0.9	1.1
Chlorhexidine	107.9	59.2	1.3	1.2
Doxazosin Mesylate	94.3	68.2	1	1

Amlodipine, ceritinib and chlorhexidine were not identified as inhibitors during the fluorescence-based screen. Additionally to that, for the clinical relevance of the compounds doxazosin and amsacrine this quenching effect did not play a role, because they did not meet the criteria for clinical significance<sup>170</sup>, but this representation shows that there are 5 out of 294 compounds, which need at least a counter screen to be identified for certain.

#### 4.3 MALDI MASS SPECTROMETRY UPTAKE ASSAY

MALDI MS is a label-free method, which is HTS applicable and therefore represents a suitable tool to investigate transport proteins in a high-throughput manner also as a possible counter screen for fluorescence-based methods. Cell-based assays for MALDI MS already exist, nevertheless there is no MALDI MS-based unlabelled cellular uptake measurement existing yet. For that purpose, a WC method was developed, automated and validated. The applicability of the method is dependent on several critical steps. Cellular physiology might be affected by the number of cells used in an assay<sup>191</sup>. The incubation time with the drugs has to be chosen. For transporter assays, this incubation time has to lie in the linear range of the substrate uptake<sup>27</sup>. The resuspension is again a very critical step. The solvent for resuspension and matrix

have to be chosen carefully. Also the best-suited matrix has to be identified, as the co-crystallisation of matrix and analyte is a prerequisite for MALDI MS<sup>192</sup>. Those critical steps have to be kept in mind during assay development. This topic is manifold and diverse through the crystallisation patterns that can form dependent on the matrix, solvent and application technique that is used. Therefore, the method has to be developed and optimised on the best detection of the analyte thoroughly. All of those considerations have the aim to develop a method focused on the detection of the substrate in the cells. The intensity of the substrate signal paired with low noise values and CV % are crucial for the applicability of the method. Once the method has shown to be reproducible, it can be applied to a screen of drugs potentially inhibiting the uptake through the transporter to further characterise the transport process and be able to react to possible occurring DDIs.

### 4.3.1 DEVELOPMENT OF A WHOLE-CELL MALDI MASS SPECTROMETRY UPTAKE METHOD

First of all, it had to be decided which substrate is going to be used for the study of drug uptake through OATP2B1. In case of MALDI MS, there is of course no labelled substrate needed. In that case, other known substrates than DBF are possible. For that purpose, DBF and the physiological substrate estrone-3-sulfate (E3S) were compared in their possible detection by MALDI MS. The two possible substrates were spiked to a cell pellet in various concentrations ranging from 0.01  $\mu\text{M}$  to 10  $\mu\text{M}$ . It is likely that one of the substrates has an improved detection compared to the other. This is dependent on the use of matrix. Therefore, 2500 cells/spot were applied on a MTP and spray-coated with four different matrices. Intensity, S/N and crystallisation pattern were compared due to the fact that every matrix can lead to different outcomes in terms of homogeneity of crystallisation, measured intensity of the analyte peak and its S/N.

The direct comparison of the two possible substrates showed a higher signal intensity for E3S and also a detection at lower concentrations than DBF. The limit of detection for E3S was with a concentration of 0.01  $\mu\text{M}$  and usage of DHAP at an arb. u. of 1, whereas DBF showed poor signal intensity with DHAP matrix for all 3 lower concentrations (0.01  $\mu\text{M}$ , 0.1  $\mu\text{M}$ , 1  $\mu\text{M}$ ) at around 0.3 arb. u. With Ph-CCA-NH<sub>2</sub>, the

results were similar as E3S was still detected at 0.1  $\mu\text{M}$  (2.3 arb. u.) and DBF only showed possible detection until 1  $\mu\text{M}$  with a very low intensity of 0.5 arb. u. (**Figure 18,A**). The comparison of the detection of 0.1  $\mu\text{M}$  E3S with different matrices (DHAP, Ph-CCA-NH<sub>2</sub>, DHB and sDHB) showed the unsuitability of DHB and sDHB due to the low median S/N ratios of 8 (sDHB) and 19 (DHB) compared to 93 (Ph-CCA-NH<sub>2</sub>) and 250 (DHAP) (**Figure 18,B**) and patchy crystallisation (**Figure 18,C**). DHAP and Ph-CCA-NH<sub>2</sub> are both possible for the detection of E3S due to their good S/N ratio  $\geq 90$ , acceptable CV % (35 and 26 respectively) and homogeneous crystallisation pattern. Consequently, for further analyses, E3S was used as a substrate and the matrices DHAP and Ph-CCA-NH<sub>2</sub> were analysed further in their suitability. Analysing the physiological substrate E3S brings the advantage that identified inhibitors are more likely to cause pharmacologically relevant DDIs.

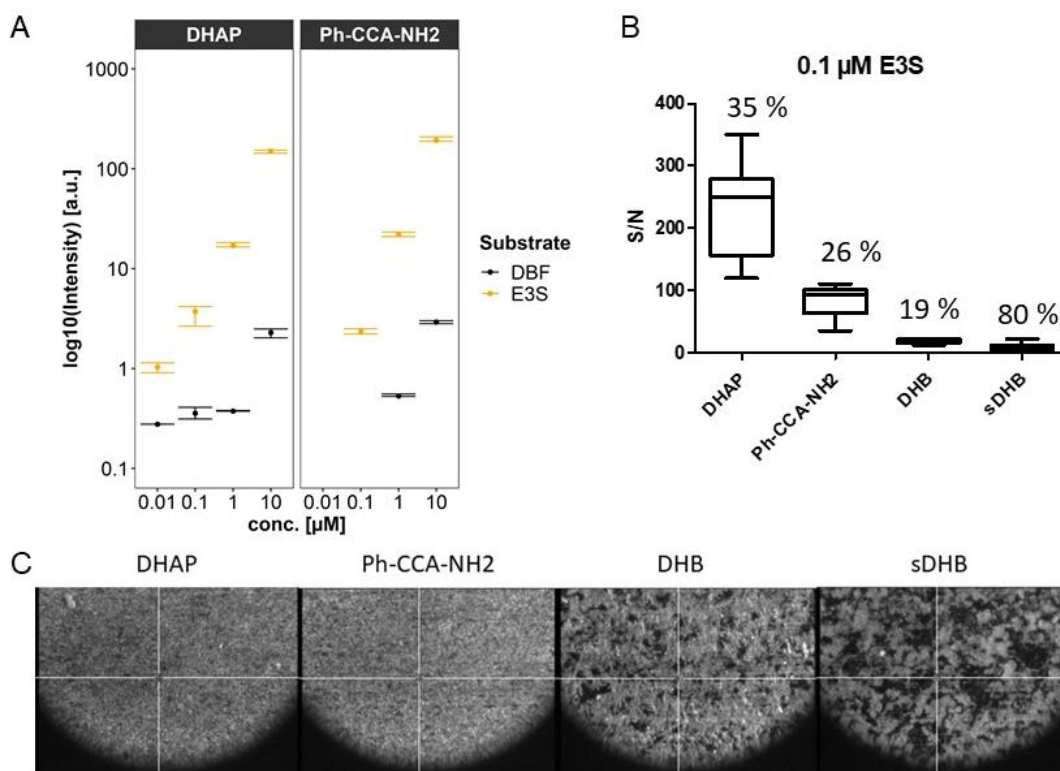


**Figure 18: Comparison of E3S and DBF as two possible substrates for OATP2B1 uptake renders E3S as better suited:** Cell pellets of HEK293 were resuspended at 2500 cells  $\mu\text{L}^{-1}$  in ACN/ddH<sub>2</sub>O. One microliter of the suspension was applied to a MALDI target plate, which was spray coated with either Ph-CCA-NH<sub>2</sub> (5 mg/mL in acetone/ddH<sub>2</sub>O (90/10)), DHAP (20 mg/mL in ethanol/DAHC (75/20)), DHB (20 mg/mL in ACN/ddH<sub>2</sub>O/TFA (50/50/0.2)) or sDHB

## Results

(20 mg/mL in ethanol/DAHC/TFA (75/25/0.2)). Samples were measured using a rapifleX MALDI. **(A)** E3S / DBF was spiked to the cell pellet in different final concentrations of 10, 1, 0.1 and 0.01  $\mu\text{M}$ . Plots were done in R. Plotted is the median and 25 to 75 quantile of 9 technical replicates. **(B)** Final spiked E3S concentration of 0.1  $\mu\text{M}$ , plotted is the median of 9 measurement replicates, whiskers are 5 to 95 percentile. CV % values indicated above boxes. **(C)** Matrix crystallisation of different matrices.

The availability of both ultrafleXtreme and rapifleX in the laboratory raised the question of usage for the conduction of the assay. The rapifleX is the first mass spectrometer that offers the speed to analyse a 1536 target plate within 8 min and therefore the possibility to conduct uHTS. With regard to a screen, which was the goal for the developed method, the rapifleX would be favoured. For an objective comparison of the two devices, a MTP was spotted with cells spiked with E3S and sprayed with DHAP. The measurement was conducted on both devices and the intensity of the analyte peak was compared. As **Figure 19** clearly shows, the use of the rapifleX did not only lead to a higher intensity of the analyte signal (100 arb. u. vs 55 arb. u.), but also to a higher resolution (17589 vs 7603). The rapifleX therefore was the favoured mass spectrometer for this analysis, owning also the possibility to conduct high-throughput.

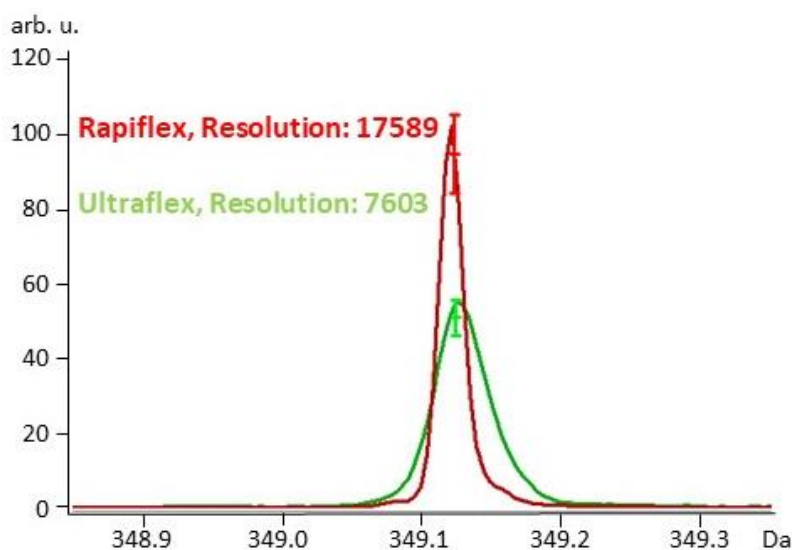


**Figure 19: Usage of rapifleX leads to higher intensity and resolution compared to ultrafleXtreme:** Analysis of the same MTP spotted with cell pellets spiked with 1  $\mu\text{M}$  E3S and



analysed with 20 mg/mL DHAP applied sprayed dissolved in ethanol/DAHC/TFA (75/25/0.2) with rapifleX and ultrafleXtreme. Resolution and peak intensity is higher using rapifleX.

As the result of detection is not only dependent on the matrix itself, but also the concentration of matrix and usage of solvent, the two well-performing matrices Ph-CCA-NH<sub>2</sub> and DHAP were optimised regarding their best suitable concentration, solvent and its composition in order to increase the detection of E3S. Important decision criteria were the S/N ratio of the E3S peak and its variability expressed in CV %. An ideal matrix and solvent composition would lead to a high S/N of the E3S signal combined with a low CV % value. For that purpose, cell pellets were spiked with 1 µM E3S and analysed with different matrix concentrations, solvent compositions and matrix application types.

For the optimisation of DHAP regarding detection of E3S, first the usage of different solvents was tested. The comparison of ethanol with acetone showed a clear advantage of acetone, despite the fact that they had a comparable highest median S/N of 222 and 205, respectively, as the variation using acetone was a lot lower (**Figure 20,A,B**). The CV % value for this experiment ranged from 37 to 52 for solvation in ethanol, with the lowest concentration of matrix having the highest CV % value. In comparison to that, the usage of acetone as solvent led to lower CV % values ranging from 11 (7.5 mg/mL) to 29 (10 mg/mL). The higher the DHAP concentration, the lower the median S/N got from 205 to 71 with acetone as a solvent rendering 7.5 mg/mL as best option, which also had the lowest CV % value (**Figure 20,B**).

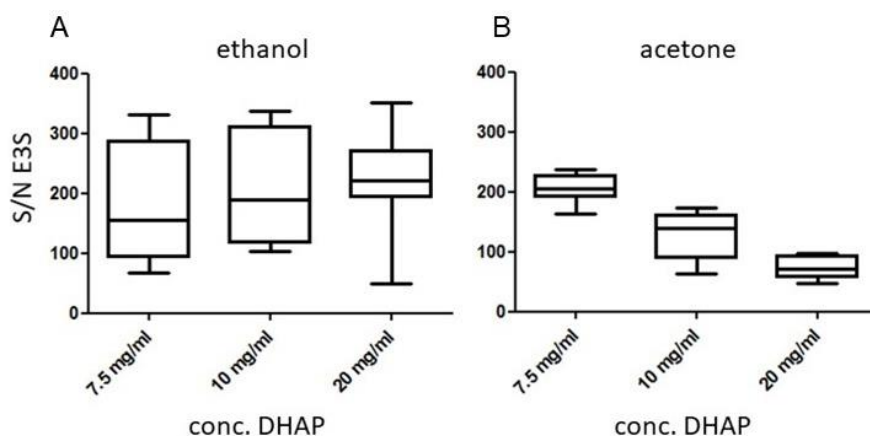


**Figure 20: Influence of the solvent for DHAP on S/N of E3S:** HEK293 cell pellets were resuspended at 2500 cells  $\mu\text{L}^{-1}$  in ACN/ddH<sub>2</sub>O. One microliter of the suspension was applied to a MALDI target plate, which was spray coated with DHAP used in differing concentrations from 7.5 mg/mL to 20 mg/mL dissolved either in 75 % ethanol (**A**) or acetone (**B**) together with 25 % DAHC. E3S was spiked to the cell pellet in the final concentration of 1  $\mu\text{M}$ . Samples were measured using a rapifleX MALDI. S/N of the E3S peak of 9 measurement replicates is shown in a boxplot with median, whiskers are 5-95 percentile.

With 7.5 mg/mL being identified as a good concentration of DHAP, also ACN was tested in comparison with acetone and a sandwich application was compared to a sprayed application. Both S/N and CV % were taken into account. The sandwich application of acetonitrile led to lower median S/N of 476 (75 % ACN) and 614 (60 % ACN) values than sprayed (1069 for 60 % ACN, 1237 for 70 % ACN) (**Figure 21,B**) and simultaneously to higher CV % values of 28-31 % compared to <10 % for sprayer application (**Figure 21,C**) leading to the exclusion of the sandwich application of ACN. The exclusion of the sandwich application was further supported by the crystallisation pattern, which showed a patchy crystallisation for sandwich application (**Figure 22**). The median S/N values for the sprayed application of DHAP with acetone were with values of 751 and 653 respectively comparable at 60 % and 75 % solvent rate (**Figure 21,A**). Comparing the CV % of the different two solvent percentages, 60 % acetone showed to be less variant with a CV % <5 compared to 75 % solvent with a CV % of 12 rendering the lower amount of solvent better suited (**Figure 21,C**). The direct comparison of 60 % acetone and the sprayed application of acetonitrile showed a good median S/N ratio of >750 for both. From two biological replicates, 60 % acetone showed a trend towards the lowest CV % value leading to the decision to choose this

## Results

composition for further investigations. The control with DMSO spiked in instead of E3S showed the applicability of the method leading to S/N ratios lower than 3, which is seen as the detection limit (**Figure 21,A,B**). DHAP was further used in the optimised conditions of a concentration of 7.5 mg/ml in 60 % acetone.

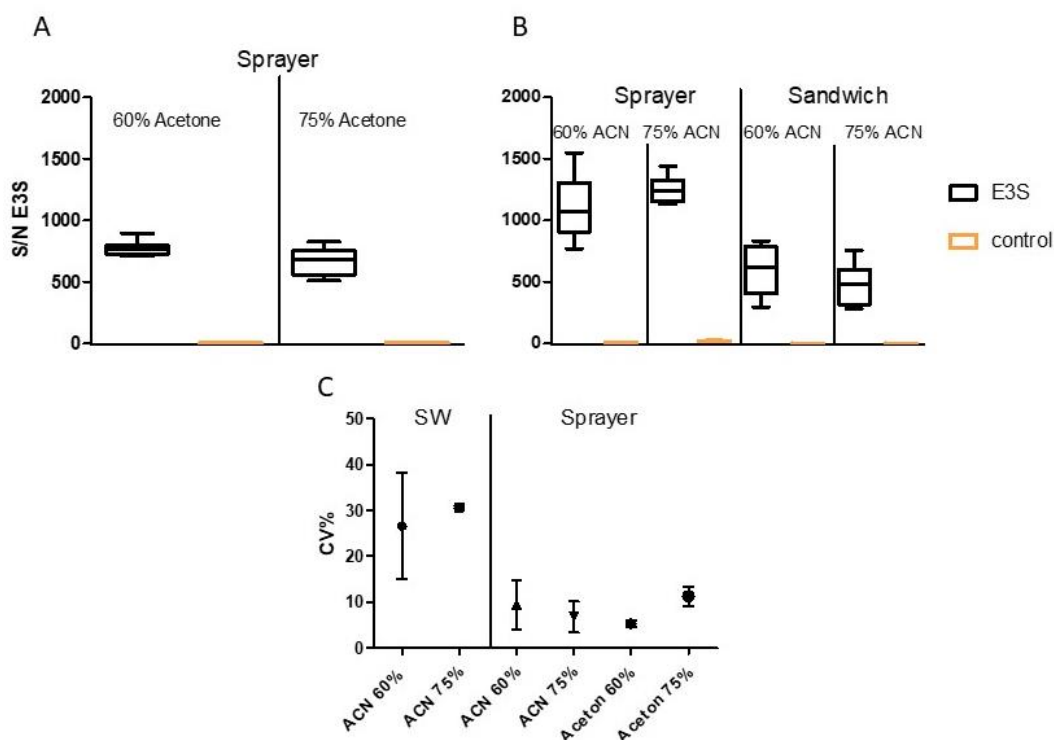


**Figure 21: Comparison of acetone and ACN as a solvent for DHAP:** HEK293 cell pellets were resuspended at 5000 cells  $\mu\text{L}^{-1}$  in ACN/ddH<sub>2</sub>O. In case of sandwich application, the MTP was coated with matrix first, then the analyte and matrix were applied dried droplet by resuspension of a cell pellet to 5000 cells  $\mu\text{L}^{-1}$  in ACN/ddH<sub>2</sub>O and mixing 1:1 with the matrix. One microliter of the suspension was applied to a MTP. In case of spray coating, the cell pellet was resuspended at a concentration of 2500 cells  $\mu\text{L}^{-1}$  in ACN/ddH<sub>2</sub>O and 1  $\mu\text{L}$  applied to the MTP, which was then spray coated with 7.5 mg/mL DHAP dissolved either in 75 % ACN or acetone together with 25 % DAHC. E3S was spiked to the cell pellet in the final concentration of 1  $\mu\text{M}$ . As a control, only DMSO was spiked to the cells, indicated as orange boxes. Samples were measured using a rapifleX MALDI. (**A,B**) S/N of the E3S peak of 9 measurement replicates is shown in a boxplot with median and whiskers of 5-95 percentile. (**C**) CV % of E3S peak of two biological replicates.

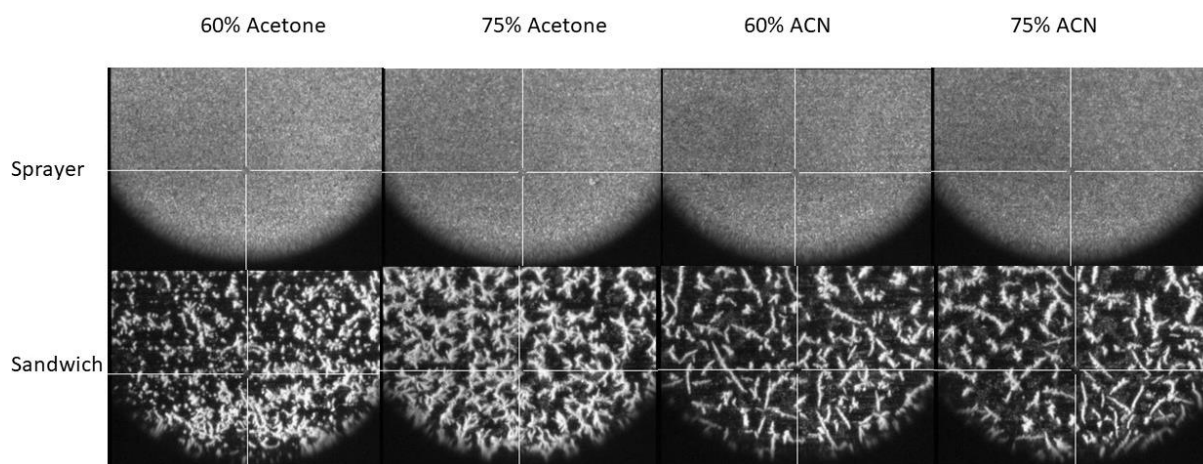


**Figure 22: Crystallisation pattern of DHAP with acetone and ACN renders sandwich application unsuitable:** HEK293 cell pellets were resuspended at  $5000 \text{ cells } \mu\text{L}^{-1}$  in ACN/ddH<sub>2</sub>O. In case of sandwich application, the MTP was coated with matrix first, then the analyte and matrix were applied dried droplet by resuspension of a cell pellet to a cell number of  $5000 \text{ cells } \mu\text{L}^{-1}$  in ACN/ddH<sub>2</sub>O and mixing 1:1 with the matrix. One microliter of the suspension was applied to a MTP. In case of spray coating, the cell pellet was resuspended at a concentration of  $2500 \text{ cells } \mu\text{L}^{-1}$  in ACN/ddH<sub>2</sub>O and  $1 \mu\text{l}$  applied to the MTP, which was then spray coated with  $7.5 \text{ mg/mL}$  DHAP dissolved either in  $75 \%$  ACN or acetone together with  $25 \%$  DAHC. E3S was spiked to the cell pellet in the final concentration of  $1 \mu\text{M}$ . As a control, only DMSO was spiked to the cells, indicated as orange boxes. Samples were measured using a rapifleX MALDI.

Also the Ph-CCA-NH<sub>2</sub> matrix had to be optimised for the detection of E3S in the cells. Therefore, the concentration of matrix and the solvent composition were analysed. This was done with a cell pellet spiked with  $1 \mu\text{M}$  E3S and analysed with different compositions of matrix and solvent. Ethanol only led to a median S/N ratio of 18-31 using different concentrations of matrix (**Figure 23,A**) leaving only acetone and ACN as possible solvents, which both led to a good S/N ratio of up to 45 (**Figure 23,C**) and 79 (**Figure 23,B**), respectively, whereas the lower concentrations of matrix ( $2.5 \text{ mg/mL}$  and  $5 \text{ mg/mL}$ ) performed better in terms of S/N. The low concentrations of  $2.5$  and  $5 \text{ mg/mL}$  matrix in either acetonitrile or acetone were decided to be analysed further due to the higher S/N of around 70 for the low concentrations dissolved in ACN compared to below 50 for the high concentrations (**Figure 23,B**). Since all of the matrix

compositions here were applied sprayed, they had to be investigated once more with dried droplet, which is better suitable for HTS intentions.

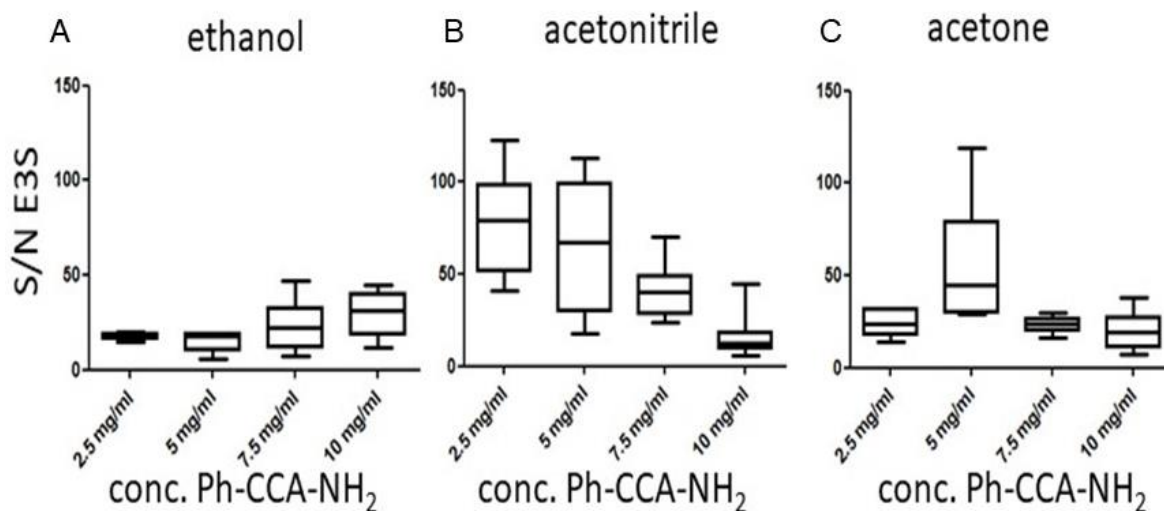


**Figure 23: Solvent and matrix concentration has an influence on the S/N of E3S detection:** Comparison of detection of E3S with Ph-CCA-NH<sub>2</sub> dissolved in three different solvents, all 90 %: ethanol (A), ACN (B) and acetone (C). Different concentrations of matrix were tested out ranging from 2.5 mg/mL to 10 mg/mL. For the evaluation of the best matrix composition, cell pellets of HEK293 were resuspended at 5000 cells  $\mu\text{L}^{-1}$  in ACN/ddH<sub>2</sub>O. The cells were mixed 1:1 with matrix dissolved in either ethanol, ACN or acetone before the manual dried droplet application onto the target plate. E3S was spiked to the cell pellet in the final concentration 1  $\mu\text{M}$ . Samples were measured using a rapifleX MALDI. S/N of 9 measurement replicates of the E3S peak is shown in a boxplot with median and whiskers of 5-95 percentile.

Further analysis of Ph-CCA-NH<sub>2</sub> matrix showed that both S/N and CV % had to be taken into account during the decision of the best matrix composition. The application of different concentrations of Ph-CCA-NH<sub>2</sub> dissolved in acetone showed the applicability of both concentrations when sprayed due to a comparable S/N of around 130 (Figure 24,A). Compared to that, acetonitrile led to higher median S/N ratios of around 190 when applied sprayed (Figure 24,B). The analysis of the CV % values showed the suitability of both acetonitrile and acetone as solvents for Ph-CCA-NH<sub>2</sub> (Figure 24,C). The dried droplet application of acetonitrile had a trend towards higher S/N ratios with acetonitrile (266 with 2.5 mg/ml Ph-CCA-NH<sub>2</sub> compared to 180 with the

## Results

same concentration of matrix dissolved in acetone). The direct comparison of dried droplet vs sprayed application showed higher S/N ratios for dried droplet with 2.5 mg/mL Ph-CCA-NH<sub>2</sub> in 90 % acetonitrile compared to the sprayed application. Besides the fact that the dried droplet application led to higher CV % values in general (33 for 2.5 mg/ml Ph-CCA-NH<sub>2</sub> in ACN compared to 11 %) (**Figure 24,C**) when applied in the same concentration and solvent sprayed, both application types seemed to be possible. The low concentration of 2.5 mg/mL Ph-CCA-NH<sub>2</sub> dissolved in 90 % ACN was chosen for further analyses due to its high S/N ratio of 200 when sprayed and even 275 when applied dried droplet paired with a low CV % value <10 for sprayed application and 30 for dried droplet application.

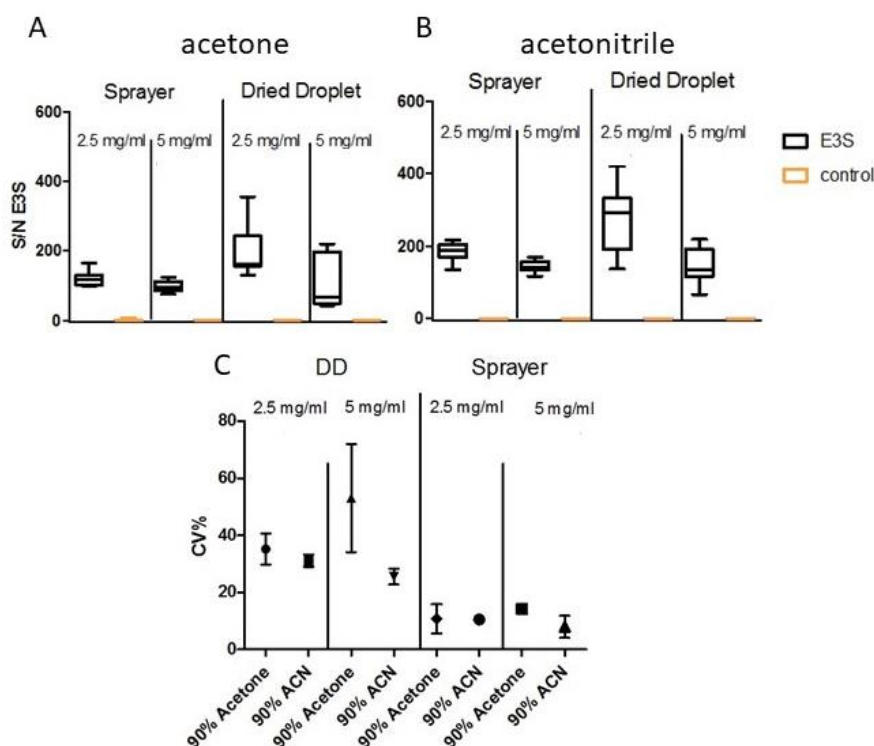


**Figure 24: Apart from S/N investigation, also CV % has to be taken into account for matrix decision:** Optimisation of solvent and comparison of sprayer against dried droplet of Ph-CCA-NH<sub>2</sub>. (**A,B**) For Dried Droplet application, cell pellets of HEK293 were resuspended at 5000 cells  $\mu\text{L}^{-1}$  in ACN/ddH<sub>2</sub>O. The cells were mixed 1:1 with matrix dissolved in either 90 % ACN or acetone before the manual application onto the target plate. For sprayed application, cell pellets were resuspended at 2500 cells  $\mu\text{L}^{-1}$  in ACN/ddH<sub>2</sub>O. One microliter of the suspension was applied to a MALDI target plate, which was spray coated with Ph-CCA-NH<sub>2</sub>. E3S was spiked to the cell pellet in the final concentration 1  $\mu\text{M}$ . As a control, only DMSO was

## Results

spiked to the cells, indicated as orange boxes. Samples were measured using a rapifleX MALDI. S/N of the E3S peak of 9 measurement replicates is shown in a boxplot with median and whiskers of 5-95 percentile. (C) CV % of E3S peak of two biological replicates.

The two matrices best suited for the analysis of E3S in the cells were identified and optimised on the E3S detection leading to 2.5 mg/mL Ph-CCA-NH<sub>2</sub> in 90 % ACN and 10 mg/mL DHAP in 60 % acetone as best options. As the positive influence of salts, which acidify / alkalyfy the sample on the detection in whole cell assay is known<sup>139, 193</sup>, this option was also tried out. The change in analyte detection through the acidification or alkylation of the samples comes due to the modified proton affinity, which again has an influence on the ionisation due to the lucky survivor model. Therefore, the matrices were additionally mixed with a dilution series of ammoniumformiate (pH 8.0). Neither for PhCCA-NH<sub>2</sub> (**Figure 25,A**), nor for DHAP (**Figure 25,B**), there was an improvement of S/N through the addition of ammoniumformiate seen. Therefore, the matrices will be used without the addition of salts for alkylation.

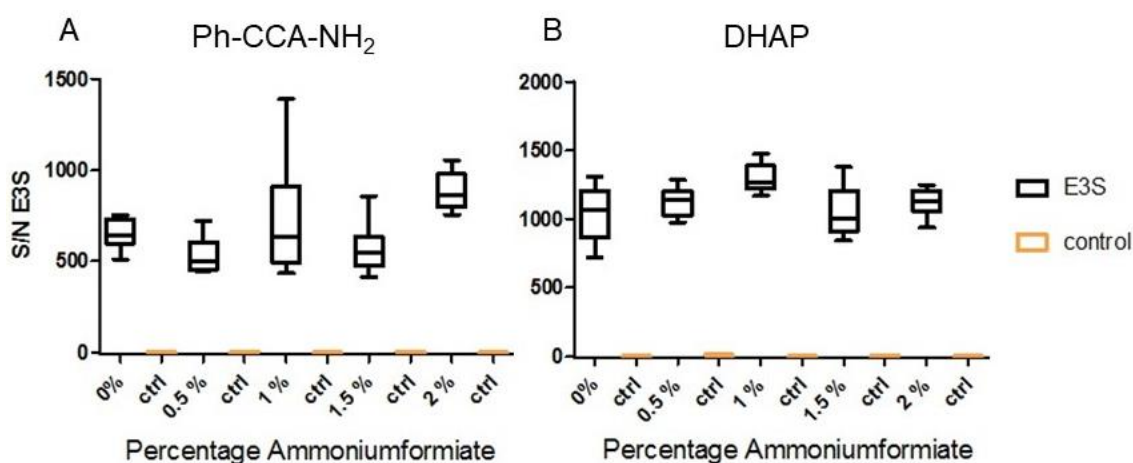


**Figure 25: Addition of ammoniumformiate to the matrix solvent did not improve S/N:** Optimisation of solvent and comparison of sprayer against dried droplet of Ph-CCA-NH<sub>2</sub>. (A,B) Cell pellets were resuspended at 2500 cells  $\mu\text{L}^{-1}$  in ACN/ddH<sub>2</sub>O. One microliter of the suspension was applied to a MALDI target plate, which was spray coated with 2.5 mg/mL Ph-CCA-NH<sub>2</sub> in 90 % ACN/ddH<sub>2</sub>O or 10 mg/mL DHAP in 60 % acetone/40 % DAHC. The matrices contained varying concentrations (0-2 %) 150 mM ammoniumformiate, pH 8.0. E3S was spiked to the cell pellet in the final concentration 1  $\mu\text{M}$ . As a control, only DMSO was spiked to the cells, indicated as orange boxes. Samples were measured using a rapifleX MALDI. S/N

of the E3S peak of 9 measurement replicates is shown in a boxplot with median and whiskers of 5-95 percentile.

All of the previous experiments were conducted due to method optimisation only as “spiked in” experiments of E3S. As the aspired experiments would be done in the course of real cell assay treatments, the two optimised matrix compositions, 10 mg/mL DHAP in 60 % acetone and 2.5 mg/mL Ph-CCA-NH<sub>2</sub> in 90 % ACN, which both seemed to be suitable for the detection of E3S, were used to analyse OATP2B1 and “vector control cells” in a real treatment with E3S. With this experiment, it should be ensured that the matrices, which worked best in method optimisation, still work in the real treatment case. Possible struggles due to the cell treatment are endogenous peaks that could affect the detection of the analyte. In case of the cell treatment, the cells got treated with the substrate (the analyte), which was washed away again. The cells were broken up due to freezing, resuspension in solvent and shooting with the MALDI laser. The resulting concentration of analyte, which was taken up by the cells is most likely lower than in “spiked in” experiments. This could lead to possible issues with the detection limit. OATP2B1 and vector control were therefore treated with E3S and also concomitantly with the standard inhibitor erlotinib to investigate the effect of inhibition on the uptake. Additionally, there was a control group only treated with DMSO.

As it can be seen in the following figure (**Figure 26,B**), the usage of DHAP led to the identification of a disturbing peak in close proximity to the analyte peak, indicated with an arrow. Also, the matrix crystallisation rendered DHAP inappropriate for a dried droplet application because of a very unhomogeneous crystallisation, which made an automated measurement difficult (**Figure 26,C**). A fully automated method can't be realised by using the sprayer for the matrix application, therefore Ph-CCA-NH<sub>2</sub> is the matrix of choice for the analysis of E3S uptake through OATP2B1. The figure also demonstrates the uptake through the transport protein. The red spectrum resulted from the incubation of OATP2B1 cells with the substrate, whereas there is a clear inhibition of the peak seen with concomitant incubation of erlotinib as an inhibitor. Also, the vector control treated with the substrate showed a significantly lower peak than the overexpressing cell line of 2.5 arb. u. compared to 30 (**Figure 26,A**). These findings showed that the uptake of the substrate through the transport protein can be measured



with the cell-based MALDI MS assay and DHAP is inappropriate as a matrix in the real cell-treatment case due to the background peak in close proximity to the analyte and patchy crystallisation.

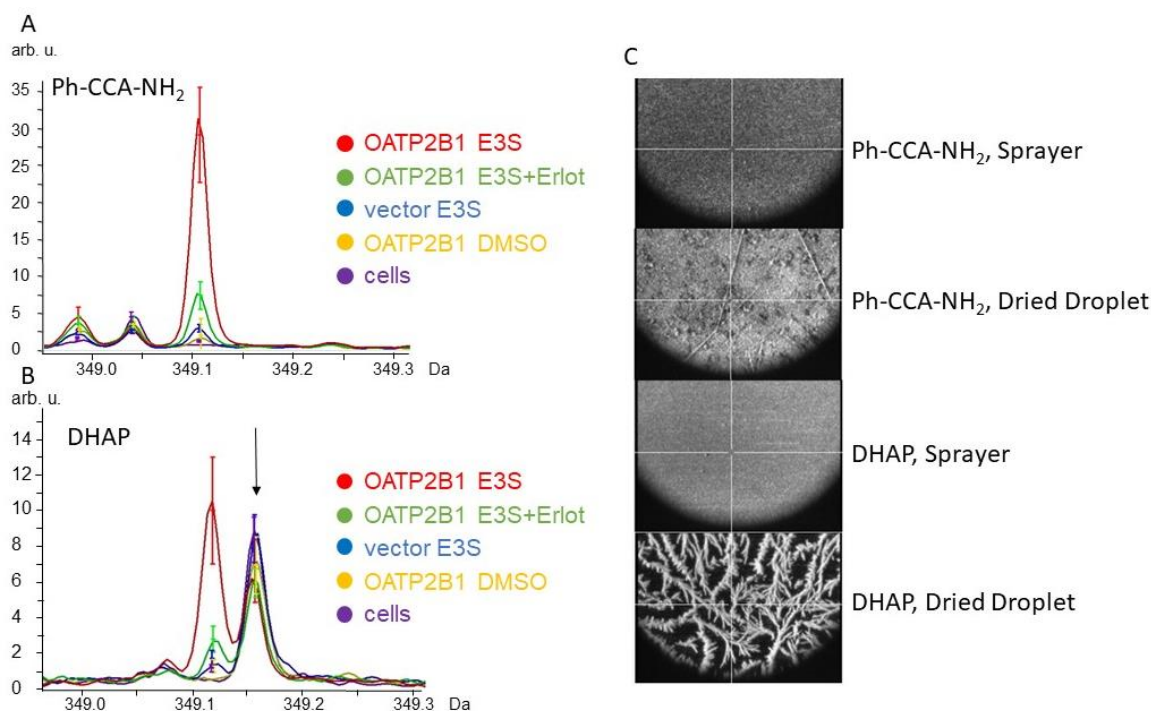


**Figure 26: Treatment of cells with E3S renders DHAP inappropriate due to background peak in close proximity to analyte peak:** HEK293-OATP2B1/HEK293-vc cells were treated with 20  $\mu\text{M}$  E3S (with and without 20  $\mu\text{M}$  erlotinib) or only DMSO for 30 min. For dried droplet application, cell pellets of HEK293 were resuspended at 5000 cells  $\mu\text{L}^{-1}$  in ACN/ddH<sub>2</sub>O. The cells were mixed 1:1 with either 7.5 mg/mL DHAP in 60 % acetone, 40 % DAHC or 2.5 mg/mL Ph-CCA-NH<sub>2</sub> in 90 % ACN/ddH<sub>2</sub>O. For sprayed application, cell pellets were resuspended at 2500 cells  $\mu\text{L}^{-1}$  in ACN/ddH<sub>2</sub>O. One microliter of the suspension was applied to a MALDI target plate, which was spray coated with the matrices respectively. Samples were measured using a rapifleX MALDI. **(A,B)** Spectra of 9 measurement replicates are shown in ClinPro Tools. **(C)** Matrix crystallisation of different matrices, both applied by sprayer and dried droplet.

After evaluation of the best matrix and solvent composition for the analyte, the application technique of matrix was investigated once more, as the method optimisation already showed the different effects of matrix application. Ideally, an assay should have a high signal window, defining the range between the positive and

the negative control. The higher the signal window, the easier it is to determine slight differences in concentration like a  $pIC_{50}$ . Therefore, OATP2B1 cells were incubated with E3S (positive control) and E3S+Erlotinib (negative control) with the optimised matrix composition of Ph-CCA-NH<sub>2</sub> with different application techniques and the signal window was compared. PrimaDrop, dried droplet, sprayer and sandwich application of 2.5 mg/mL Ph-CCA-NH<sub>2</sub> in 90 % ACN were compared. An analysis of the CV % values led to the conclusion not to choose PrimaDrop because of its high variation (**Figure 27,A**). The other application ways performed well leading to CV % <20 and therefore the factor between substrate uptake and inhibited substrate uptake were compared. The sandwich application of matrix led to a low factor of 1.5 (**Figure 27,D**), whereas the other two methods showed a comparable factor >4 (**Figure 27,B,C**). This led to the exclusion of sandwich as application technique. As already investigated, the CV % of the dried droplet application was higher compared to the sprayed version with values of 19 % and 11 % respectively. Both application types therefore showed suitability as it is of interest to establish an assay with a CV % < 20.

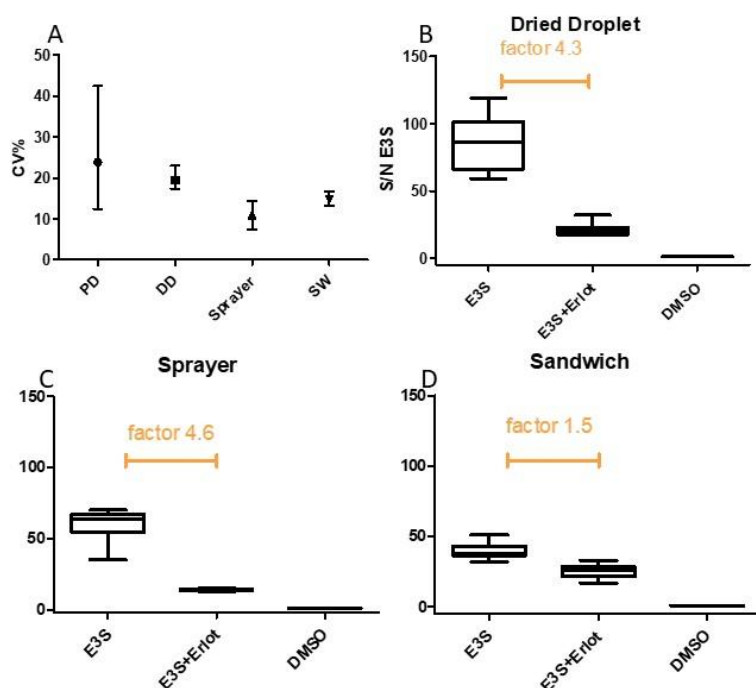


**Figure 27: Method of matrix application has an effect on E3S detection:** HEK293-OATP2B1/HEK293-vc cells were treated with 20  $\mu$ M E3S (with and without 20  $\mu$ M erlotinib) or only DMSO for 30 min. For sprayed and PrimaDrop application, the cell pellet was resuspended at 2500 cells  $\mu$ L<sup>-1</sup> in ACN/ddH<sub>2</sub>O. In case of spray-coating with matrix, one

microliter of the suspension was applied to a MALDI target plate and then spray-coated. In case of PrimaDrop application, the cells were manually applied to the target plate. The matrix was manually applied on top of the dried spot. For sandwich and dried droplet application, the cell pellet was resuspended at 5000 cells  $\mu\text{L}^{-1}$  in ACN/ddH<sub>2</sub>O. In case of sandwich application, first the MALDI target plate was coated with a layer of matrix, then matrix and analyte got mixed 1:1 and applied manually on top. For dried droplet application, matrix and analyte got mixed 1:1 and applied manually on to the MALDI target plate. In all cases, Ph-CCA-NH<sub>2</sub> (2.5 mg/mL in ACN/ddH<sub>2</sub>O (90/10)) was used as matrix. Samples were measured using a rapifleX MALDI. **(A)** CV % of 9 measurement replicates, shown is median with range. **(B,C,D)** Boxplot of 9 measurement replicates showing median of S/N of E3S signal. Whiskers are 5-95 percentile.

Due to the efforts to develop an automatable method, dried droplet would be the preferred application, because of its possibility to be automated. An option to decrease the intra-assay variability is the use of an internal standard. This procedure is very common in mass spectrometry imaging, where the internal standard is applied by a spraying device<sup>194</sup>. An internal standard is also a well-established method for quantification and normalisation in HPLC analysis<sup>195</sup>. For the internal standard, a molecule, which should ideally be preferably similar to the analyte molecule was chosen, in order to compensate measurement-related inaccuracies. In this case, the standard is applied by spiking it to the solvent, with which the cells got resuspended before application to the MTP. This has the advantage that no sprayed device is needed, which could have brought in another source of errors. D<sub>4</sub>-E3S is the deuterated standard of E3S and therefore resembles the analyte to a large extent. The use of 0.3  $\mu\text{M}$  internal standard led to a reproducible peak, which was high enough to be compared to the substrate peak and thus this concentration of internal standard was used further for normalisation (**Figure 28**).

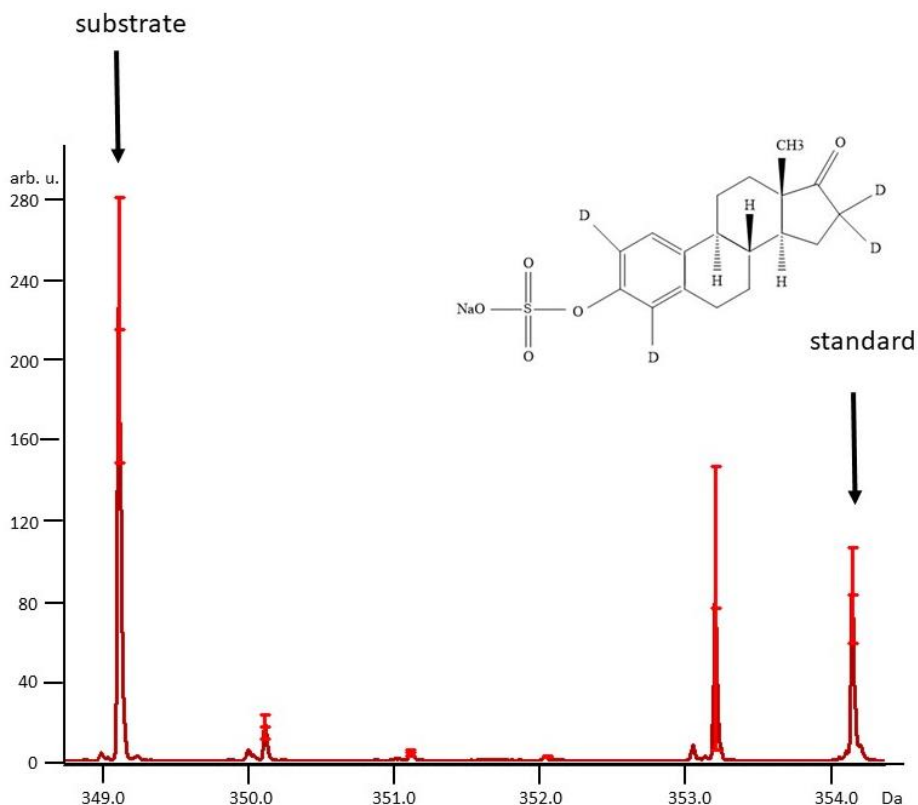


**Figure 28: Use of internal standard during uptake experiments:** HEK293-OATP2B1 cells were treated with 20  $\mu\text{M}$  E3S for 30 min. The cell pellet was resuspended at 5000 cells  $\mu\text{L}^{-1}$  in ACN/ddH<sub>2</sub>O. Matrix and analyte got mixed 1:1 and applied manually on to the MALDI target plate for dried droplet application. Ph-CCA-NH<sub>2</sub> (2.5 mg/mL in ACN/ddH<sub>2</sub>O (90/10)) was used as matrix. Samples were measured using a rapifleX MALDI. Shown are 9 measurement replicates in ClinPro Tools and the structure of D<sub>4</sub>-E3S.

The effect of the normalisation to the internal standard had to be investigated in the course of the assay treatment. Therefore, the normalisation of the peak intensity to D<sub>4</sub>-E3S was compared with the not normalised version. **Figure 29,A** clearly shows the effect of normalisation leading to a noticeable reduction of the CV % value from 52 to 15. As the matrix-analyte ratio is a key determinant of the detection of the analyte, the best amount of cells on a target spot had to be determined. This was also the first biological use case, on which the normalisation on the internal standard was transmitted to. Therefore, cell pellets of OATP2B1 treated with E3S or DMSO were resuspended with different amounts of ACN/ddH<sub>2</sub>O to achieve various cell numbers. After dried droplet application, there were cell numbers of 312 cells per spot up to 10000 cells per spot, which were included in testing. As it can be seen in **Figure 29**,

**B** and **C**, the saturation of the signal intensity looked a lot smoother when normalised to the internal standard. This again showed the advantage of normalisation and simultaneously showed that the higher the cell number per spot is, the greater the factor between DMSO control and E3S treatment. For the following experiments, a cell number of 2500 cells/spot was chosen, because a higher cell number was not possible due to practical handling in the 96-well plates, which should be used due to the need for automation. 2500 cells/spot still produced a stable and reproducible signal window between substrate treatment and control treatment. In addition, the internal standard was spiked in for normalisation in the following experiments.

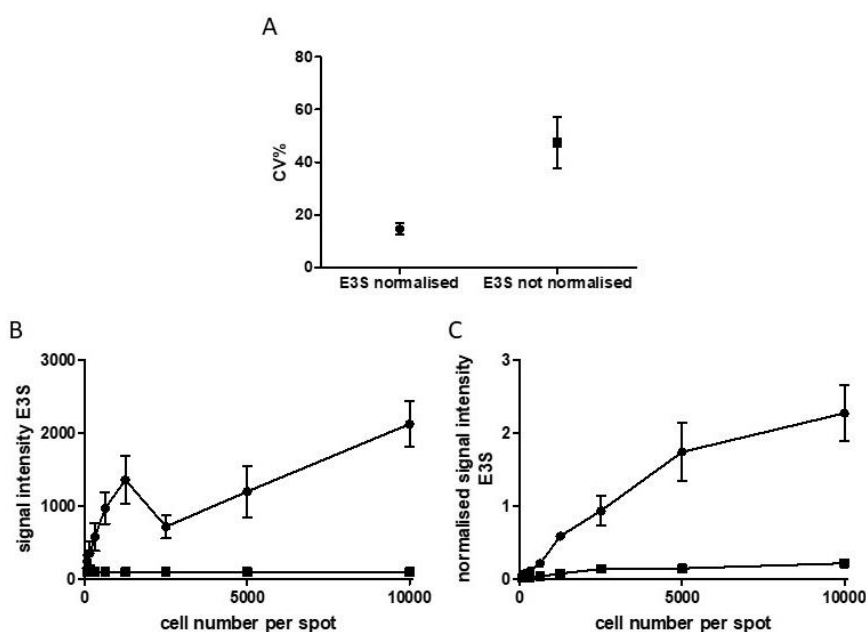


**Figure 29: Effect of normalisation of the spectra onto the internal standard D<sub>4</sub>-E3S:** (A) HEK293-OATP2B1 cells got treated with DMSO for 10 min. After that preincubation, cells were treated with E3S for 2 min, followed by removing the supernatant and washing with ice-cold PBS. The 96 well plate was snap-frozen in liquid nitrogen. Cells were resuspended at 5000 cells  $\mu\text{L}^{-1}$  in ddH<sub>2</sub>O. Before the automated Dried Droplet application with the CyBio pipetting platform, the cells got mixed 1:1 with Ph-CCA-NH<sub>2</sub> (2.5 mg/mL in ACN/ddH<sub>2</sub>O (70/30)). Samples were measured using a rapifleX MALDI. Automated measurement was performed by MPP. CV % is calculated from 3 biological replicates with 9 technical replicates each, normalised and not normalised CV % is compared. Shown is median and range. (B, C) HEK293-OATP2B1 cells were treated with 20  $\mu\text{M}$  E3S (circles) or only DMSO (squares) for 30 min. The cell pellet was resuspended at different cell numbers in ACN/ddH<sub>2</sub>O. Before the manual application onto the plate, the cells were mixed 1:1 with Ph-CCA-NH<sub>2</sub> (2.5 mg/mL in

## Results

ACN/ddH<sub>2</sub>O (90/10)) and thus applied dried droplet. Plots were done in GraphPad Prism, standard deviation of 9 measurement replicates.

The measurements were conducted on a MTP spot containing a complex matrix of cells including the analyte and the matrix-molecules. This complex mixture could have an effect on the detection of the analyte. This process is called matrix suppression effect and the assumption was that with an increase in cells per spot, the signal intensity of the analyte will decrease due to the effect. Furthermore, the optimal cell number per spot should be determined. This should ideally be a number, where the matrix suppression effect is moderate together with a high signal window which was determined in **Figure 29**. Therefore, different cell numbers per spot were analysed and a constant concentration of E3S was spiked to the cells. An analysis of different cell passages should investigate if the suppression effect is comparable in every passage. This was the case, as it could be seen in **Figure 30**. Even though there were slight differences between the passages, the effect was comparable. In all three cell passages, the decrease of the analyte intensity was observed with increasing cell number per spot. As 2500 cells/spot still showed high signal intensities of E3S (**Figure 30**) and also had a good signal window (**Figure 29**), it was chosen as the optimal cell number/spot.

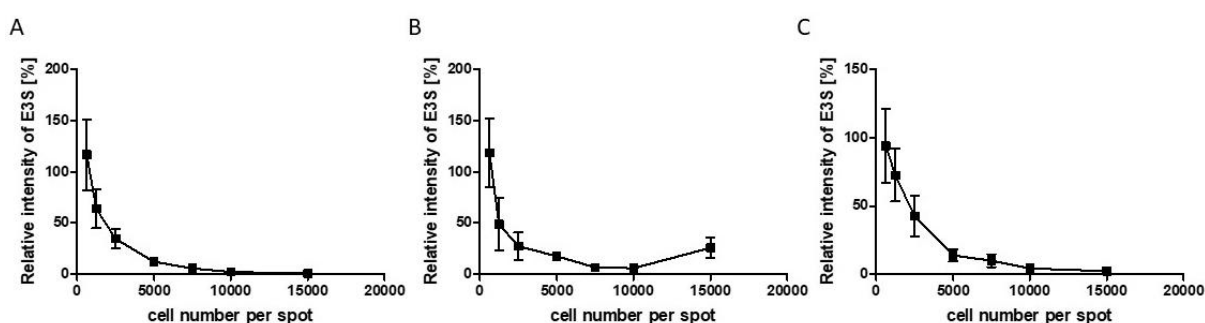


**Figure 30: Comparison of matrix suppression effect in three different cell passages:** (A,B,C) Analysis of differing cell numbers per spot. Cells were pelleted and resuspended in different amounts of suspension solution (ddH<sub>2</sub>O/matrix (50/50)). As matrix, 2.5 mg/mL Ph-CCA-NH<sub>2</sub> in 70% ACN was used. Final amount of 0.3  $\mu$ M D4-E3S and 1  $\mu$ M E3S were spiked to the matrix solvent. Cells were spotted manually and measured using a rapifleX MALDI.

Shown are 18 measurement replicates with standard deviation. Intensities were normalised to 312 cells set as 100 %.

### 4.3.2 AUTOMATION OF THE METHOD LEADS TO POSSIBLE HIGH-THROUGHPUT SCREENING

As the automation of the method plays a pivotal role with regard to high-throughput, this chapter of experiments was designed by the author and carried out by Lena Schumacher as part of her bachelor thesis. Effective drug screening requires an automated method<sup>153</sup>. Therefore, the goal was to switch from 24-well format to 96-well format to increase speed and amount of samples. In addition to this, the pipetting steps were intended to be automated by the usage of the CyBio FeliX pipetting platform. First, the resuspension and application of the cells was tested in three different versions. Plates were taken out of the freezer and immediately resuspended with

1. 40  $\mu$ L matrix solvent mixture and directly applied on the plate after shaking
2. first 20  $\mu$ L of water, then addition of 20  $\mu$ L matrix, shaking and application on plate
3. 20  $\mu$ L of water, then application on MTP and spot matrix on top.

A comparison of those three application techniques rendered the second version as the most fruitful because of the production of a very homogeneous matrix layer compared to the other two (**Figure 31,A**). The CV % and intensity values were with around 20 % and 0.6 normalised intensity comparable amongst the three methods (**Figure 31,B,C**).

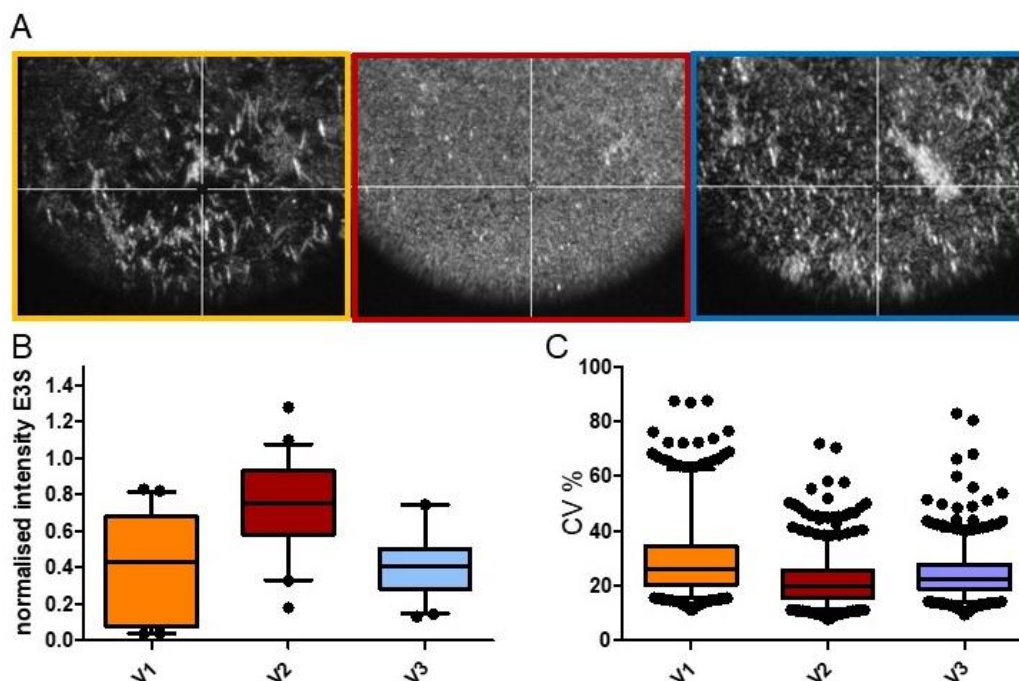


**Figure 31: Usage of CyBio FeliX pipetting platform for resuspension and application of cells:** HEK293-OATP2B1 cells were grown in a 96 well plate and treated with 20  $\mu$ M E3S for 30 min. After removing the supernatant and washing with ice-cold PBS, the plate was frozen in liquid nitrogen and stored at  $-80$   $^{\circ}$ C. Cells were applied in three different versions: Version 1 (V1): addition of 40  $\mu$ L matrix solvent mix to each well, then spotted; V2: add 20  $\mu$ L water first, shaken, then addition of 20  $\mu$ L matrix to each well, resuspended and spotted; V3: addition of 20  $\mu$ L water first, then spotted directly. Then spotted matrix on top. (A) Crystallisation pattern of three different resuspension versions. (B) Normalised intensity (on internal standard D<sub>4</sub>-E3S), 12 technical replicates, 4 measurement replicates each; box and whiskers from 5 to 95 percentile; outliers shown as circles. (C) CV % value of three different suspension versions; 2 biological replicates, 84 technical replicates with 4 measurement replicates each; box and whiskers from 5 to 95 percentile; outliers shown as circles. Done by Lena Schumacher.

Besides matrix, concentration, solvent composition and application, also the resuspension solvent plays a substantial role in the detection of the analyte and therefore was analysed during the automation of the method. As H<sub>2</sub>O already showed to be a suitable solvent for cell-based assays<sup>144, 145</sup>, it was compared with ACN/H<sub>2</sub>O, which was used before. Therefore, water was used as the resuspension solvent during CyBio FeliX application of the cells onto the MTP. This change in resuspension solvent led to a substantial increase in the assay window comparing the vector control and the



OATP2B1 overexpressing cell line. The resuspension with ACN/H<sub>2</sub>O only showed an assay window of 4 (**Figure 32,B**), whereas the resuspension with water led to a >5x increase of the assay window (**Figure 32,A**). Water was therefore further used as resuspension solvent during the drug uptake assay.

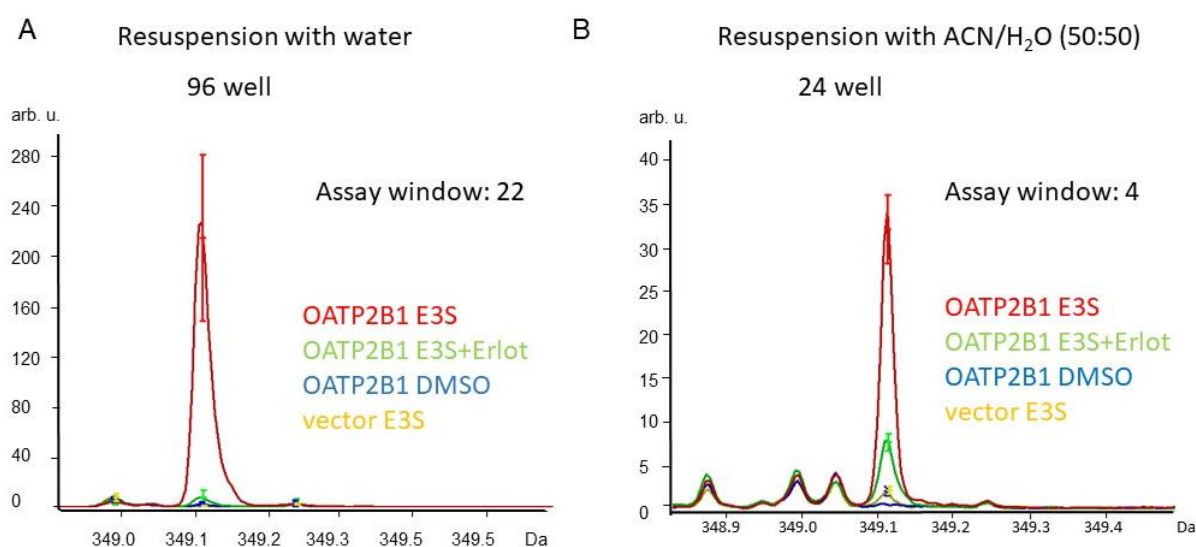


**Figure 32: Influence of resuspension solvent on detection of E3S and assay window:** HEK293-OATP2B1 and vec cells were treated with 20  $\mu$ M E3S with and without erlotinib or only DMSO for 30 min. 2.5 mg/mL Ph-CCA-NH<sub>2</sub> (ACN/H<sub>2</sub>O; 90/10) was used as a matrix. Samples were measured on a rapifleX. **(A)** Resuspension was done with water; 96 well plates were used and resuspension and cell application was performed by CyBio Felix. **(B)** Resuspension was done with ACN/H<sub>2</sub>O (50:50) in a 24 well plate and applied manually. 9 measurement replicates for each treatment are displayed in one spectrum. Done by Lena Schumacher.

In addition to the resuspension solvent, also the matrix solvent was once again investigated after automation of the method. The method had a relatively high concentration of organic solvent (90 % ACN), which could maybe lead to difficulties in the handling due to rapid evaporation, therefore also a lower concentration of 70 % ACN was investigated. The comparison of the different amounts of solvent for the matrix showed no clear difference in important criteria like S/N (**Figure 33,A**) and peak ratio of analyte peak (E3S) compared to the internal standard peak (D<sub>4</sub>-E3S) (**Figure**

**33,B).** Therefore, also 70 % solvent is a usable composition and was used for further analyses.

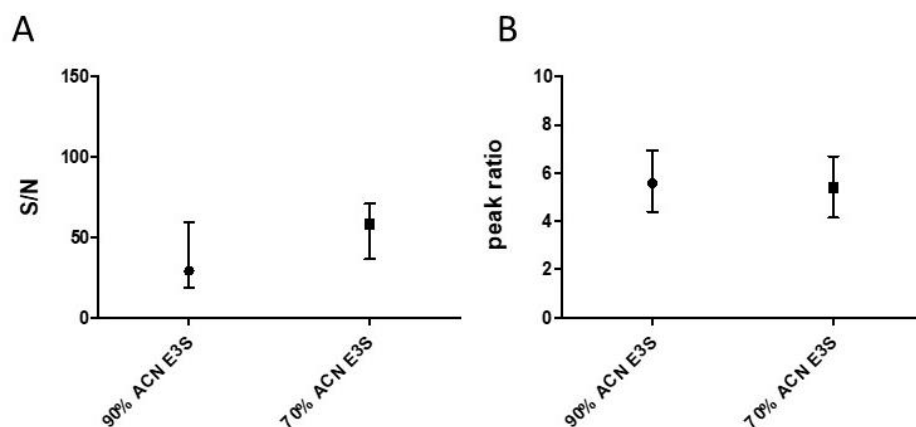


**Figure 33: Comparison of 70 % ACN and 90 % ACN as solvent for matrix:** HEK293-OATP2B1 cells were pretreated with DMSO for 10 min. Then cells were treated with 10  $\mu$ M E3S for 2 min. As solvent for 2.5 mg/mL Ph-CCA-NH<sub>2</sub> there were two different concentrations of ACN used: 90 % and 70 %. Cells were resuspended and applied automatically, plate was measured with a rapifleX. **(A)** S/N of 16 technical replicates with 4 measurement replicates each. Shown is median with interquartile range. **(B)** Peak ratio of 16 technical replicates with 4 measurement replicates each. Shown is median with interquartile range.

The automation of the method was a gain for the applicability of the assay due to the time saved and reduction of manual steps to a minimum. Before the automation, one well of a cell culture plate had to be converted to one Eppendorf cup, which had to be spun down and supernatant removed manually. Also, the application of one Eppendorf cup had to be done manually. This step took about 3 hours for one MTP. With the fully automated method, this could be reduced to just 2 min. With this in mind, a high-throughput approach can be pursued. This would not have been possible without automation. A comparison of the non-automated method with the automated method is shown in the following figures (**Figure 34,34**) and illustrates the ease of handling steps by the use of a pipetting robot for treatment and cell and matrix application (**Figure 35**).

## Results

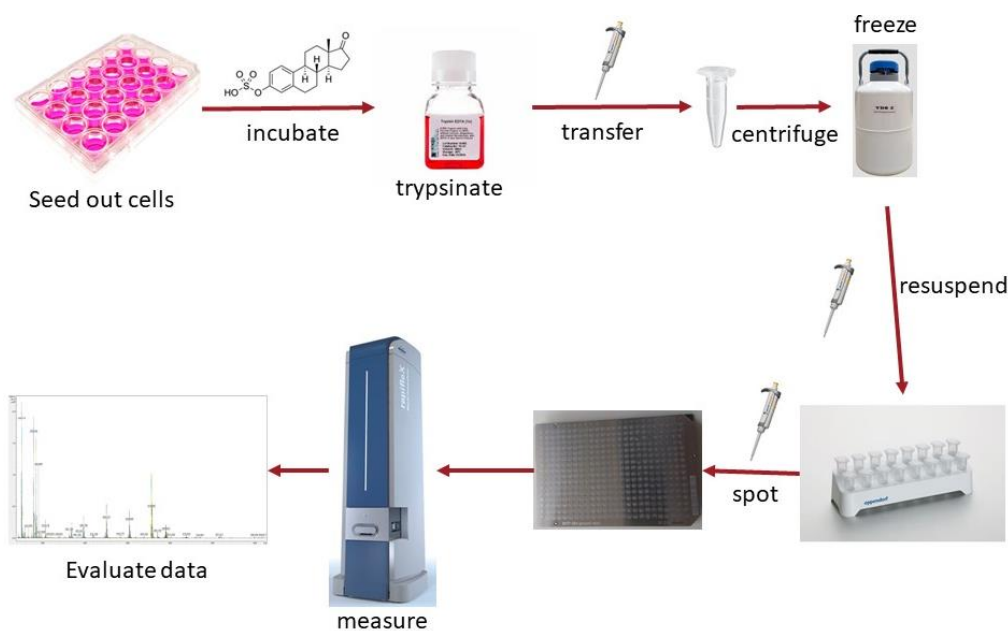


**Figure 34: Unautomated workflow of MALDI MS cell treatment assay:** Critical steps are seeding out of the cells, incubation, resuspension, spotting and measurement. Figure done by Lena Schumacher

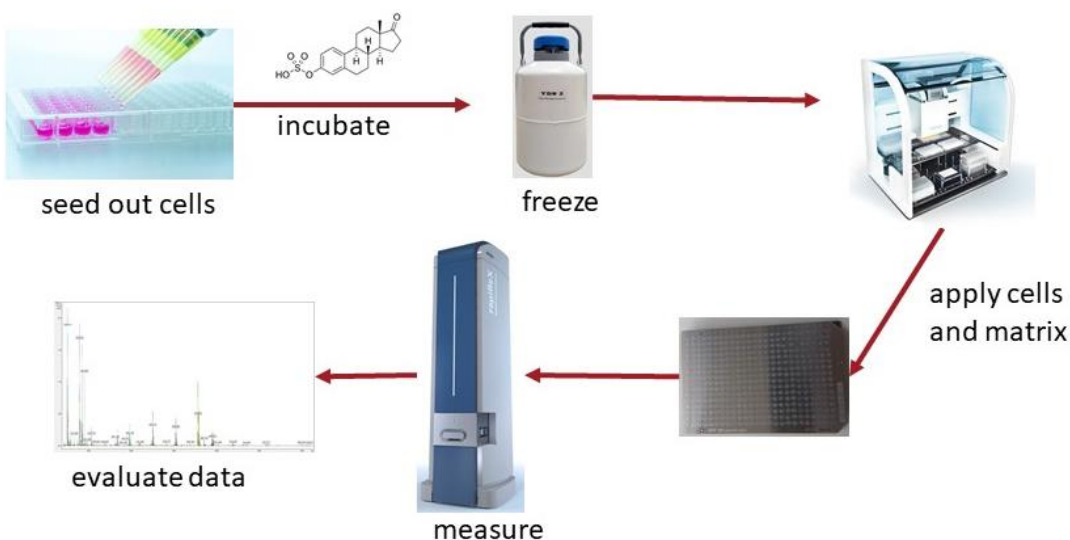


**Figure 35: Automated workflow of MALDI MS cell treatment assay:** Manual steps were noticeably reduced. Treatment with compound and application of cells and matrix are done with a pipetting robot. Figure done by Lena Schumacher

The fully automated method included the treatment of the cells with pharmaceuticals and sample resuspension together with dried droplet matrix application using the

CyBio pipetting platform. Data acquisition was done using a rapifleX MALDI MS and the developed method was now applicable to different use cases like the characterisation of the transport kinetics and also to the identification of new inhibitors (**Figure 36**).

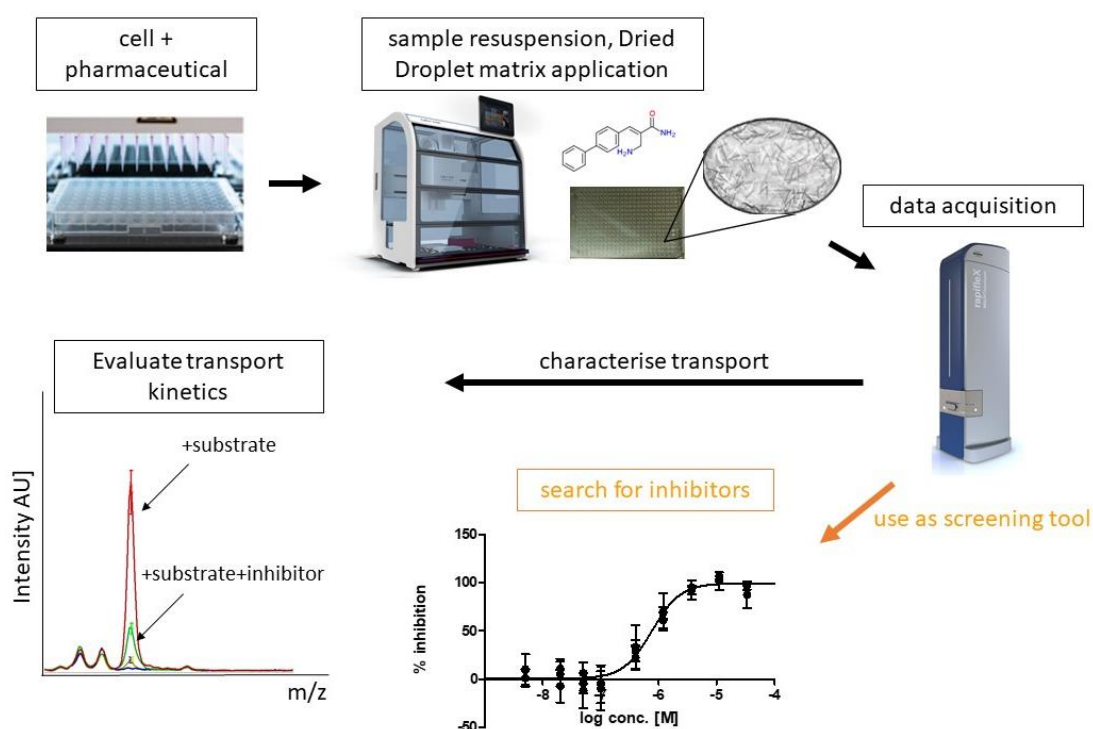


**Figure 36: Applicability of the fully automated method:** Cells are grown in a 96 well plate ( $0.5 \times 10^6$  cells/mL) for 24 hours. They are directly incubated with 5 mM sodium butyrate to increase the expression of the transporter. After 24 hours, the medium is changed to serum-free medium one hour prior to drug treatment. Then, cells are treated with inhibitor/test compound/DMSO for 10 min followed by treatment with substrate. To stop the uptake of the substrate, the supernatant is removed by a vacuum aspirator and cells are washed once with ice-cold PBS. The plate is snap-frozen in liquid nitrogen and stored at  $-80$  °C. Samples are resuspended in water and  $0.3$   $\mu$ M internal standard  $D_4$ -E3S is applied together with  $2.5$  mg/mL Ph-CCA-NH<sub>2</sub> (ACN/H<sub>2</sub>O 70/30).  $2500$  cells/ $\mu$ L are applied on one spot. Measurement is done with a rapifleX using the automated measurement function of the MPP software. Possibilities of application of this method are characterisation of transport kinetics or search for inhibitors.

#### 4.3.3 CHECK OF THE REPRODUCIBILITY THROUGH CONCENTRATION-/ TIME-DEPENDENCE AND $pIC_{50}$ DETERMINATION

The first step in drug uptake transporter assays always is the characterisation of the transport process. The time- and concentration-dependence of the uptake of the substrate have to be investigated in order to identify the optimal assay conditions for a possible screen. With the characterisation of the DBF uptake by the fluorescence-based measurement, the structure of this elucidation has already been shown. The characterisation of the substrate uptake including time- and concentration-dependence analysis is one of the possible applications of the automated and optimised MALDI MS method and therefore was the first real application example of the automation. The characterisation of E3S as OATP2B1 was also particularly of interest in comparison with DBF. Those two substrates could show completely different characteristics leading to different optimal assay conditions.

For the analysis of concentration-dependence, cells were treated with various concentrations of E3S for 1 min. As it can be seen in **Figure 37,A**, there was a saturation curve seen of the OATP2B1 overexpressing cell line. The uptake of E3S into the vector control stayed low apart from the increase at 100  $\mu$ M. The  $K_M$  value of the uptake was calculated and was 21.1  $\mu$ M. Hence, for the optimal assay condition, a concentration of 10  $\mu$ M E3S was chosen, being clearly lower than the  $K_M$  value and therefore not saturating the transport protein. The time-dependence was investigated by application of 10  $\mu$ M E3S for various time points. After 5 min, a flattening of the curve could be seen. An incubation time of 2 min still lied clearly in the linear range of the uptake, thus it was defined as the optimal assay condition where transporter-activity is determined<sup>27</sup>. Compared to DBF, this is a very short incubation time, highlighting the need to characterise every substrate before application in a screen (**Figure 37,B**). The first application of the automated assay was successful leading to a new methodological way of characterising a transport protein via a MALDI MS cell-based assay and the identification of the optimal assay conditions for E3S drug uptake (2 min, 10  $\mu$ M).

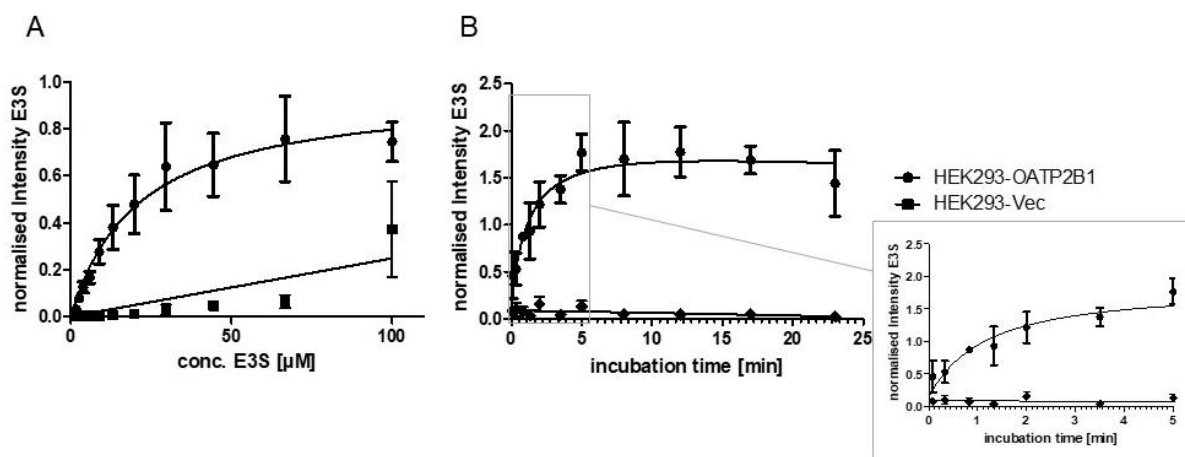


**Figure 37: Investigation of concentration and time-dependence of E3S uptake through OATP2B1:** (A) HEK293-OATP2B1 or vec cells were preincubated first with inhibitor/DMSO for 10 min and then the substrate was applied in different concentrations (1.7  $\mu\text{M}$  to 100  $\mu\text{M}$ ) for 1 min. 3 biological replicates with 3 technical replicates each and 4 measurement replicates for every technical replicate are shown. All replicates of one biological replicate were averaged, the 3 mean values of the biological replicates were then included in this graph. Fit was done in GraphPad Prism using the Michaelis Menten fit. (B) HEK293-OATP2B1 or vec cells were preincubated first with inhibitor/DMSO for 10 min and then 10  $\mu\text{M}$  E3S was applied for various time points (0.5-17 min). The cells were resuspended at 5000 cells  $\mu\text{L}^{-1}$  in ddH<sub>2</sub>O. Before the automated Dried Droplet application with the CyBio FeliX pipetting platform, the cells got mixed 1:1 with Ph-CCA-NH<sub>2</sub> (2.5 mg/mL in ACN/ddH<sub>2</sub>O (70/30)). Samples were measured using a rapifleX MALDI. 3 biological replicates with 3 technical replicates each and 4 measurement replicates for every technical replicate are shown. All replicates of one biological replicate were averaged, the 3 mean values of the biological replicates were then included in this graph. Time-dependence test done by Lena Schumacher.

The relationship between detector response and E3S concentration had to be shown in order to demonstrate the reliability of the developed method. A measurement in the linear range of the detector was the goal in order to ensure that the detector response was not saturated already. Therefore, E3S was spiked to the cells in different concentrations and the normalised intensity of E3S was analysed. Especially the optimal assay condition of 10  $\mu\text{M}$  that was determined during the concentration-dependence analysis should be investigated. **Figure 38** clearly shows a saturation of the detector response above 20  $\mu\text{M}$  and thus proves the linearity of the signal of E3S until 10  $\mu\text{M}$ , which can be seen in a close-up of the correlation. The resulting spearman

correlation coefficient of 0.95 makes clear that the linearity of the response is given and therefore the treatment with 10  $\mu\text{M}$  E3S still lied in the linear range of the detector.

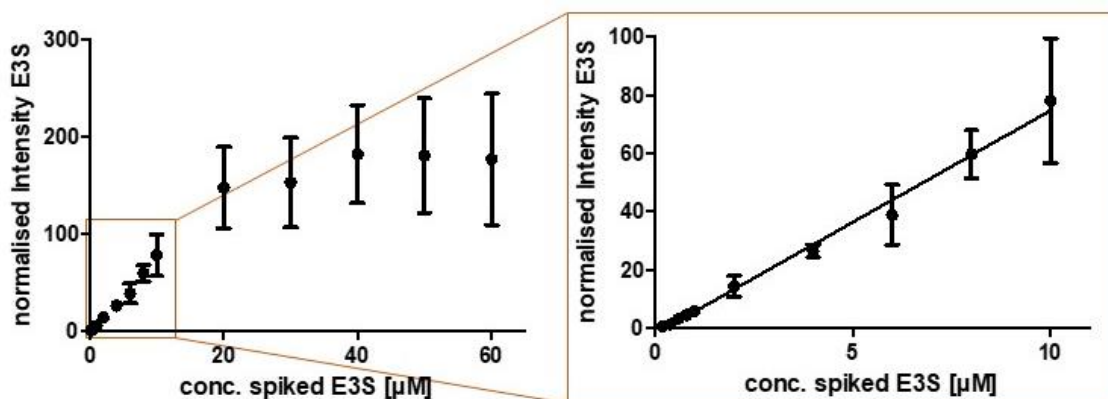


**Figure 38: Linearity of intensity and concentration of E3S:** HEK293 cells were seeded out at  $0.5 \cdot 10^6$  cells/mL and directly incubated with 5 mM sodium butyrate. After 24 h, the medium was aspirated and the cells got washed once with ice-cold PBS before snap-freezing in liquid nitrogen. Different concentrations of E3S were spiked to the cells during sample application and the matrix 2.5 mg/mL Ph-CCA-NH<sub>2</sub> was spiked with 0.3  $\mu\text{M}$  D<sub>4</sub>-E3S final for normalisation. Shown are average and standard deviation of 4 technical replicates with 4 measurement replicates each.

However, the reproducibility of the method still had to be shown. For this purpose, the cells were treated with a concentration range of erlotinib to see the variation of the inhibiting effect with differing concentration of inhibitor. The experiment was performed three times to see if the pIC<sub>50</sub> values were comparable. In case of a lack in reproducibility of pIC<sub>50</sub> determination, the method would have to be optimised again. The results showed a pIC<sub>50</sub> of 6.1 with a variance of just  $\pm 0.1$  (**Figure 39A,B,C**). This clearly showed the reproducibility of the method on the identification of inhibitors and rendered the method applicable for the screen of the compound set, which was already tested in the fluorescence-based assay.

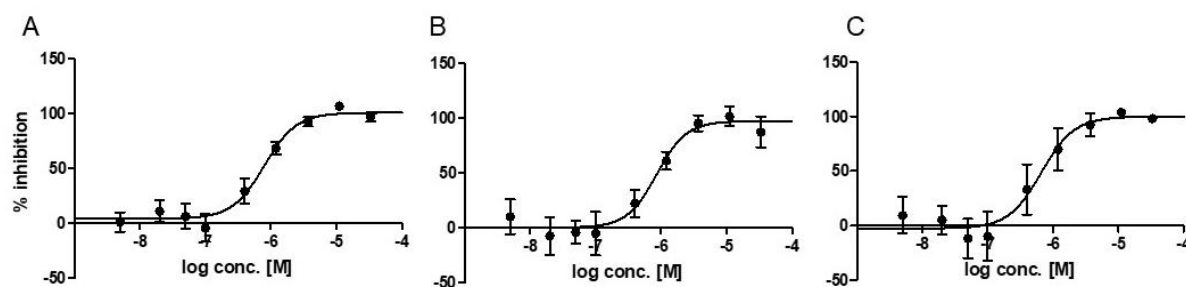


**Figure 39: Evaluation of the reproducibility of the method by determination of  $pIC_{50}$  of erlotinib:** (A,B,C) HEK293-OATP2B1 cells were preincubated first with different concentrations of inhibitor (5 nm to 33  $\mu$ M) for 10 min and then the substrate was applied for 2 min. The cells were resuspended at 5000 cells  $\mu$ L<sup>-1</sup> in ddH<sub>2</sub>O. Before the automated Dried Droplet application with the CyBio pipetting platform, the cells got mixed 1:1 with Ph-CCA-NH<sub>2</sub> (2.5 mg/mL in ACN/ddH<sub>2</sub>O (70/30)). Samples were measured using a rapifleX MALDI. Data shows 3 biological replicates with 8 technical replicates and 4 measurement replicates each.  $pIC_{50}$  value generation of erlotinib produced a  $pIC_{50}$  value of 6.1 $\pm$  0.1. Done by Lena Schumacher

#### 4.3.4 MALDI MASS SPECTROMETRY-BASED SCREENING OF INHIBITORS OF DRUG UPTAKE

The reproducibility of the developed, on E3S detection optimised and automated method was shown and was therefore applied to the screen of the compound set. Therefore, the overexpressing cell line was tested in two biological replicates and also the vector control was tested in one biological replicate with a single concentration of 10  $\mu$ M for all compounds. One of the reasons for also testing the vector control was the effect of the tested drugs on the enrichment of E3S in the vector-transfected cell line. An enriched uptake of E3S in the vector control could be due to passive membrane transport or other transporters, except OATP2B1, which are also expressed in the vector-transfected cell line<sup>12</sup>. In the case of an identification of a compound, which has an enriching effect on the E3S uptake in vc cells, for this compound, there has to be a subtraction of the vc intensity done in order to make a statement about the effect of OATP2B1. Based on an R calculation made by Thomas Enzlein, the E3S intensities in the vector control were analysed for all 294 compounds. Naproxen was identified as a compound, which exhibited a high E3S peak intensity for the vector control (normalised intensity: 0.86 compared to a mean value of 0.2 for all other compounds). Therefore, an attempt of reproduction of the finding was done



in a separate cell assay that had the same structure as the screen. Again, an enriched uptake of E3S in the vector-transfected cell line was observed, which can be seen by comparison of the blue spectrum, which resulted from the incubation of the vector control with naproxen and E3S and the purple spectrum, which resulted from the incubation of the vector control with one other drug as example (cholecalciferol). The blue spectrum led to an 3.5x increase in the intensity suggesting an enriched uptake of E3S through other transporters or passive transport (**Figure 40**). The OATP2B1-dependent effect of naproxen therefore has to be calculated by subtraction of the vector control intensity.

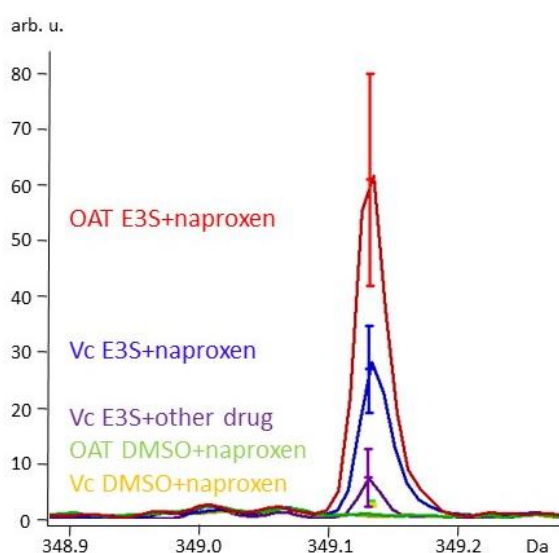


**Figure 40: Effect of treatment with naproxen on E3S uptake in vec cells:** OATP2B1 and vec cells were pretreated with 10  $\mu$ M naproxen/DMSO for 10 min before application of 10  $\mu$ M E3S/DMSO for another 2 min. Uptake was stopped by washing with ice-cold PBS and plates were snap-frozen in liquid nitrogen. Application of 2500 cells per spot was done dried droplet with 2.5 mg/mL Ph-CCA-NH<sub>2</sub> in 70 % ACN automated with the use of CyBio Felix. Shown are 8 measurement replicates of every treatment in ClinPro Tools.

The developed cell-based MALDI MS method is a completely new tool, which can also be applied to a screen of this large amount of compounds in order to classify them as inhibitors or non-inhibitors of the transport process of E3S through OATP2B1. In the fluorescence-based assay, there were 57 inhibitors confirmed. A possible outcome of that screen could be to identify the same 57 compounds as in the fluorescence-based

assay. Alternatively, a lower or higher amount of compounds could be identified due to the use of another substrate. The conduction of the screen in two biological replicates with a concentration of 10  $\mu$ M was done automated with the use of the CyBio FeliX pipetting platform. The cells were preincubated with the test compounds for 10 min followed by the application of substrate for another 2 min. Then the uptake was stopped by washing with ice-cold PBS and the cells were frozen and resuspended like already described. Every plate contained DMSO control (considered 0 % inhibition) and erlotinib control (considered 100 % inhibition), % inhibition values were calculated for every compound. Compounds, which showed a mean inhibition  $\geq 50$  % were identified as a hit. In **Table 3** all 76 compounds, which were counted as a hit are shown. A colour scale for the average value, on which the decision for hits is based, ranging from red (low % inhibition) to green (high % inhibition) is included and shows tendencies of potency of the inhibitors. All 76 compounds were further processed in  $pIC_{50}$  determination.

## Results

**Table 3: Cell-based MALDI MS screen results:** % inhibition values of 76 hits from two biological replicates of 294 compound set. Colour scale for the average, on which the decision of hit identification is based on, from red (low % inhibition) to green (high % inhibition).

Name	% inhibition n=1	% inhibition n=2	Average	Name	% inhibition n=1	% inhibition n=2	Average
Acemetacin	95.5	126.1	110.8	Irbesartan	65.1	77.6	71.3
Amiodarone	69.5	60.8	65.2	Itraconazole	104.6	104.8	104.7
Amlodipine	48.6	54.6	51.6	Ketoconazole	106.4	85.9	96.2
Amsacrine	73.3	87.9	80.6	Lansoprazole	68.0	46.3	57.2
Aripiprazole	70.0	80.1	75.1	Latanoprost	112.6	113.9	113.2
Atorvastatin	99.3	117.0	108.1	L-Thyroxine	108.7	103.5	106.1
Benzbromarone	110.2	115.6	112.9	Loratadine	93.5	118.0	105.8
Bicalutamide	89.3	88.6	88.9	Losartan	102.6	100.9	101.7
Budesonide	102.3	81.8	92.1	Lovastatin	99.6	106.7	103.1
Calcitriol	77.8	92.7	85.3	Medroxyprogesterone	65.2	60.1	62.6
Celecoxib	93.3	120.7	107.0	Mometasone Furoate	94.5	96.2	95.4
Ceritinib	74.7	57.5	66.1	Montelukast	109.4	101.8	105.6
Clobetasol Propionate	90.9	71.1	81.0	Nabumetone	58.4	55.8	57.1
Clopidogrel	116.0	106.2	111.1	Neбиволol	70.1	47.7	58.9
Cyclosporine	74.5	61.0	67.7	Norethindrone	85.5	103.1	94.3
Desogestrel	64.9	78.1	71.5	Novobiocin	32.1	68.3	50.2
Diacerein	76.7	72.3	74.5	Olsalazine	61.5	76.2	68.8
Diethylstilbestrol	102.2	110.4	106.3	Oxybutynin	80.4	106.2	93.3
Dipyridamole	111.2	111.3	111.3	P-30040 nergol	106.0	97.0	101.5
Doxazosin Mesylate	67.7	72.3	70.0	Parecoxib	56.2	68.3	62.2
Dronedarone	39.6	63.7	51.6	Pioglitazone	66.0	78.8	72.4
Drospirenone	76.7	70.2	73.4	Prasugrel	95.7	62.3	79.0
Efavirenz	83.7	70.8	77.3	Progesterone	63.5	81.6	72.5
Ergocalciferol	41.7	96.9	69.3	Quetiapine Fumarate	100.7	81.0	90.8
Erlotinib	105.0	108.7	106.8	Quinapril	70.1	75.5	72.8
Estradiol	98.6	106.8	102.7	Raloxifene	115.0	102.3	108.7
Ethinyl Estradiol	81.2	108.3	94.8	Reserpine	85.6	96.2	90.9
Ezetimibe	124.1	111.6	117.9	Silymarin	54.9	90.2	72.5
Felodipine	97.6	62.2	79.9	Simvastatin	70.5	81.3	75.9
Fenofibrate	107.1	121.4	114.3	Tacrolimus	77.8	125.8	101.8
Fluticasone	83.1	99.4	91.2	Tamoxifen Citrate	58.1	68.2	63.2
Fluticasone Propionate	102.3	119.3	110.8	Tianeptine	54.6	57.2	55.9
Fluvastatin	96.9	119.7	108.3	Ticagrelor	112.1	110.7	111.4
Glimepiride	87.2		87.2	Tipranavir	99.1	105.8	102.5
Gliquidone	104.3	95.2	99.7	Tolterodine Tartrate	60.2	53.1	56.6
Glyburide	96.3	98.2	97.2	Travoprost	112.1	105.3	108.7
Guacetasal	53.6	70.1	61.8	Vilazodone Hydrochloride	89.4	95.9	92.6
Ipriflavone	111.8	129.7	120.8	Zafirlukast	95.0	82.8	88.9

The fluorescence-based assay showed that a pIC<sub>50</sub> determination is needed for the determination of potency of the inhibitors, but also for the confirmation of hits, as some were not confirmed as hits in the pIC<sub>50</sub> determination. It was also of interest, if the inhibitors that were found in both assay types would be comparable in their potency. For the investigation of the potency of the identified inhibitors, a detailed concentration response analysis in the form of a pIC<sub>50</sub> determination had to be done. For pIC<sub>50</sub> determination, the cells were treated with a dilution series of the hit compounds ranging from 5 nm to 100 μM. Again, every plate contained positive and negative control. The determination was done for six biological replicates. The detailed analysis of the concentration-dependent inhibition confirmed 67 as inhibitors. The confirmation

was not possible for 9 compounds: Amiodarone, ceritinib, dronedarone, efavirenz, ergocalciferol, glyburide, lansoprazole, tamoxifen citrate and tolterodine tartrate. Apart from efavirenz and glyburide, all compounds that failed to be confirmed were close to 50 % inhibition. Some like dronedarone, ergocalciferol and lansoprazole showed a % inhibition value beneath 50 for one replicate confirming the struggle in hit confirmation. All of the compounds could not be confirmed as inhibitors, because they did not show an inhibition > 50% at the highest concentrations investigated in the pIC<sub>50</sub> determination. Nevertheless, 14 of the confirmed inhibitors can be seen as potent inhibitors with a pIC<sub>50</sub> ≥6 (**Figure 41, Table 4**), which showed the need for investigation of the inhibitors.

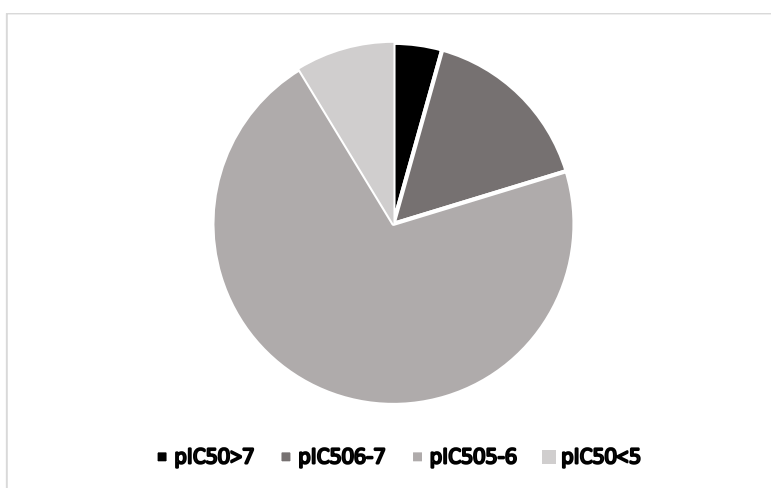


**Figure 41: MALDI MS results of the screen of 294 compounds:** pIC<sub>50</sub> determination of hits (≥50 % inhibition) revealed several potent inhibitors. For pIC<sub>50</sub> determination, HEK293-OATP2B1 cells were preincubated with a dilution series of hit compounds followed by treatment with substrate for 2 min. Every plate contained DMSO control (considered 0 % inhibition) and erlotinib control (considered 100 % inhibition). pIC<sub>50</sub> values were generated by using the “response vs log (inhibitor concentration) variable slope” equation with no constraint on all parameters (IC<sub>50</sub>, hill coefficient, bottom, top) in GraphPad Prism<sup>177</sup>. Screen was conducted together with Lena Schumacher.

The pIC<sub>50</sub> determination was conducted in six biological replicates. Thus, the reproducibility of the assay, which is an elemental factor of assay validation, could be assessed in a comparison of the replicates. With a mean standard deviation of 0.3 and

a CV % under 5.5 for the whole data set, the method clearly showed to be a reliable and reproducible tool for identification of drug uptake inhibitors. Indicated in red are the 14 most potent inhibitors that were identified (**Table 4**). Those were acetaminophen, atorvastatin, benzbromarone, cyclosporine, diethylstilbestrol, ezetimibe, fluticasone, fluvastatin, itraconazole, ketoconazole, montelukast, reserpine, tipranavir and zafirlukast (**Table 4**). Acetaminophen was already identified as a potent inhibitor in the fluorescence-based screen and is also a known inhibitor of OATP1B1<sup>186</sup>. Also atorvastatin<sup>187</sup>, benzbromarone, fluvastatin<sup>171</sup>, montelukast<sup>188</sup> and tipranavir<sup>189</sup> were already found as potent inhibitors in the fluorescence-based assays and are known OATP2B1 inhibitors. Cyclosporine<sup>196</sup>, diethylstilbestrol, reserpine and itraconazole<sup>171</sup> are known OATP2B1 inhibitors. Ezetimibe and ketoconazole were described as non-inhibitors of OATP2B1 in literature<sup>171</sup> and fluticasone and zafirlukast were not known as an inhibitor before. From the classification of those inhibitors, which range from statins over immunosuppressants (cyclosporine) to leukotriene receptor antagonists (montelukast and zafirlukast), it becomes clear that the inhibitors can't be predicted by the similarity of structure of pharmacological application. Nevertheless, there are also computer-based studies evolving, which predict inhibitors and non-inhibitors based on a training set of known compounds<sup>197, 198</sup>. Those approaches are called quantitative structure-activity relationship (QSAR) models and could also help to further investigate inhibitors of the transport protein.

## Results

**Table 4: Listing of the pIC<sub>50</sub> screening results for 6 biological replicates:** pIC<sub>50</sub> values were generated as already mentioned. Standard deviation and CV % were calculated for all six replicates (if available). Mean standard deviation was 0.3 and mean CV % 5.2. Indicated in red are potent inhibitors with a pIC<sub>50</sub> ≥6. Screen was conducted together with Lena Schumacher.

Name	pIC50						Mean	STDEV	CV%
	n=1	n=2	n=3	n=4	n=5	n=6			
Acemetacin	7.1	7.3	6.8	5.6	7.0	7.3	6.9	0.6	9.3
Amlodipine	4.9	4.8	4.8	4.8	4.9	5.0	4.9	0.1	1.9
Amsacrine	5.4	5.0	5.0	5.2	4.7	5.5	5.1	0.3	5.6
Aripiprazole	5.2	5.5	5.7	5.9	5.6	5.4	5.5	0.2	4.4
Atorvastatin	7.0	6.9	6.6	6.1	6.4	6.0	6.5	0.4	6.4
Benzbromarone	6.3	6.3	5.7	5.8	6.1	5.7	6.0	0.3	4.7
Bicalutamide	5.4			5.1	5.2	5.2	5.2	0.1	2.7
Budesonide	6.1	5.3	5.4	4.8	5.2	5.1	5.3	0.4	8.2
Calcitriol	5.5	5.7	5.6	5.7	5.6	6.0	5.7	0.2	2.7
Celecoxib	5.6	6.1	5.4	5.2	5.5	6.3	5.7	0.4	7.5
Clobetasol Propionate	5.6	5.3	5.7	5.7	5.5	5.7	5.6	0.2	3.2
Clopidogrel	5.3	5.3	5.6	5.5	5.3	6.1	5.5	0.3	5.6
Cyclosporine	6.5	7.0	6.5		6.5	6.2	6.5	0.3	4.6
Desogestrel	5.0	4.9	5.1	5.2	5.4	5.5	5.2	0.2	4.4
Diacerein	5.0	4.9	5.1	5.1	5.2	5.4	5.1	0.2	3.9
Diethylstilbestrol	7.2	7.0	7.0	6.1	6.7	6.4	6.7	0.4	5.9
Dipyridamole	5.9	5.4	5.4	5.4	5.8	5.4	5.6	0.2	3.8
Doxazosin Mesylate	5.4	4.8	5.1	5.4	5.0	5.4	5.2	0.3	5.4
Drospirenone	4.9	4.9	5.2	5.2	5.0	5.5	5.1	0.2	4.0
Erlotinib	5.4	5.2	5.7	5.7	5.9	6.1	5.7	0.3	5.6
Estradiol	5.5	5.4	5.5	6.1	5.3	5.0	5.5	0.4	6.5
Ethinyl Estradiol	5.8	5.4	5.6	5.8	5.7	5.3	5.6	0.2	3.6
Ezetimibe	7.0	6.4	6.4	6.4	6.5	6.9	6.6	0.3	4.0
Felodipine	5.9	5.8	6.2	5.9	5.9	5.7	5.9	0.2	3.0
Fenofibrate	6.0	5.5	6.0	5.9	5.9	5.4	5.8	0.3	4.9
Fluticasone	6.5	6.9	6.0	5.8	5.9	6.1	6.2	0.4	6.8
Fluticasone Propionate	6.5	6.1	5.6	5.0	5.7	6.4	5.9	0.6	9.5
Fluvastatin	6.4	5.9	6.3	5.3	6.3	6.0	6.0	0.4	6.9
Glimepiride	4.8	5.4	5.3	5.5	5.8	5.4	5.4	0.3	6.4
Gliquidone	5.9	5.9	5.5	5.7	5.5	5.6	5.7	0.2	3.3
Guacetasal	4.8	4.9	5.0	4.8	5.4	5.0	5.0	0.2	4.7
Ipriflavone	5.7	5.4	6.0	5.5	6.0	5.5	5.7	0.2	4.3
Irbesartan	5.7	6.0	5.9	6.1	5.5	5.5	5.8	0.3	4.4
Itraconazole	6.9	6.4	6.1	6.9	5.8	6.9	6.5	0.5	7.1
Ketoconazole	6.2	6.4	6.1	6.3	6.5	6.4	6.3	0.1	2.4
Latanoprost	6.2		5.0	5.8	6.3	5.9	5.8	0.5	8.6
Loratadine	6.0	5.7	5.5	6.1	5.9	5.9	5.8	0.2	3.7
Losartan	5.7	5.4	6.0	5.8	5.0	5.9	5.6	0.4	6.5
Lovastatin	4.9	5.0	5.0	4.7	4.7	5.0	4.9	0.1	2.6
L-Thyroxine	5.2	5.6	5.7	5.4	5.2	5.4	5.4	0.2	3.6
Medroxyprogesterone	6.1	5.7	5.5	5.0	5.3	5.6	5.5	0.4	6.7
Mometasone Furoate			5.3	5.7	5.6	5.3	5.5	0.2	3.6
Montelukast	7.8	7.8	7.7				7.8	0.0	0.5
Nabumetone	4.9	4.9	4.8	4.8	5.1	4.8	4.9	0.1	2.5
Nebivolol	4.6	5.2	5.8	5.3	5.4	4.9	5.2	0.4	8.2
Norethindrone	5.9	5.0	5.4	5.2	5.5	5.0	5.3	0.3	6.5
Novobiocin	4.6	4.6	4.7	4.3	5.0	5.0	4.7	0.3	5.8
Olsalazine	5.5	6.0	5.2	5.4	5.9	5.6	5.6	0.3	5.4
Oxybutynin	5.7	5.0	5.5	5.0	5.5	5.5	5.3	0.3	5.4
P 3004 Unergol	5.9	5.4	5.3	5.9	5.7	5.5	5.6	0.2	4.4
Parecoxib	5.0	4.8	5.0	5.4	5.4	5.4	5.2	0.3	5.2
Pioglitazone	5.4	5.0	4.8	4.9	5.9	5.4	5.2	0.4	7.7
Prasugrel	5.8	5.7	6.2	5.5	5.8	5.6	5.8	0.3	4.6
Progesterone		5.0	5.2	5.5	5.4	5.3	5.3	0.2	3.9
Quetiapine Fumarate	6.6	5.2	5.2	5.7	5.3	5.4	5.6	0.5	9.4
Quinapril	5.1	4.6	4.9	4.6	4.8	4.6	4.8	0.2	4.5
Raloxifene			6.2	5.6	5.9		5.9	0.3	4.5
Reserpine	7.0	7.3	7.0	7.2	6.9	7.5	7.2	0.2	3.1
Silymarin	5.0	5.0	5.3	4.9	4.6	5.2	5.0	0.2	5.0
Simvastatin	5.1	5.4	5.3	5.3	5.1	5.0	5.2	0.2	3.0
Tacrolimus	6.1	5.9	6.0	5.2	6.0	6.0	5.8	0.3	5.8
Tianeptine	4.3	4.7	5.0	4.7	4.6	4.9	4.7	0.2	4.8
Ticagrelor	5.9		5.4	5.2	5.4	5.6	5.5	0.3	5.0
Tipranavir	7.3	7.7	7.1		6.7	6.1	7.0	0.6	9.1
Travoprost	6.1	6.6	5.9	5.6	5.7	5.6	5.9	0.4	6.6
Vilazodone Hydrochlorid	6.3	5.7	6.0	5.8	5.6	6.0	5.9	0.3	4.6
Zafirlukast	6.6	6.5	6.4	5.6	6.3	5.5	6.2	0.5	7.6
Mean								0.3	5.2

Besides the confirmation of reproducibility through the comparison of the pIC<sub>50</sub> determination, the intra-assay reproducibility could also be analysed by a comparison of the % inhibition values of the two biological replicates of OATP2B1. With a Spearman correlation coefficient of 0.86, the assay showed to be reproducible and a good validation of the obtained results (Figure 42).

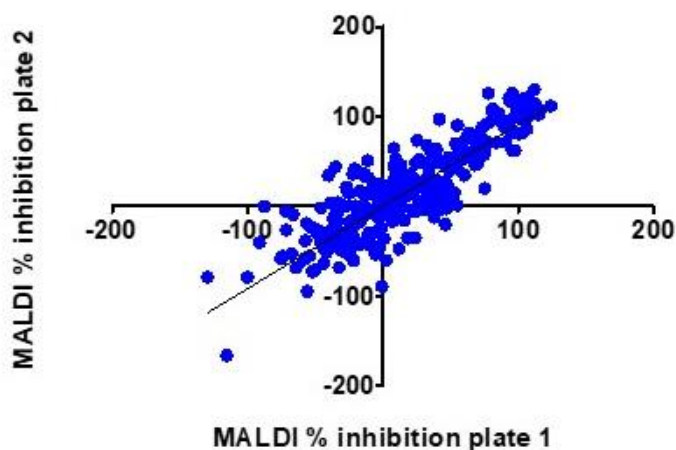


**Figure 42: Intra-assay reproducibility of MALDI MS screen:** Comparison of two biological replicates for screening of the compound set in MALDI MS. For the screen HEK293-OATP2B1 cells were preincubated with 10  $\mu\text{M}$  test compound for 10 min. After 2 min incubation with the substrate E3S, the cells were washed with ice cold PBS to stop the uptake. Cells were resuspended in ddH<sub>2</sub>O and 0.3  $\mu\text{M}$  D<sub>4</sub>-E3S dissolved in 2.5 mg/mL Ph-CCA-NH<sub>2</sub> (ACN/H<sub>2</sub>O 70/30). Via dried droplet performed by the CyBio Felix pipetting platform, 2500 cells per spot were applied and measured automated with the MPP software. Every plate contained DMSO control (considered 0 % inhibition) and erlotinib control (considered 100 % inhibition). % inhibition values were calculated for every compound and compared here. Spearman correlation coefficient is 0.86. Screen was conducted together with Lena Schumacher.

Due to the high concentrations used in this assay, a viability test in the form of a CellTiter-Glo assay was conducted. High concentrations could possibly lead to cell death resulting in disturbing signals. Therefore, the cells were treated with all 294 compounds in the same way like in the screen and after washing the cells after the treatment, they were incubated with 50  $\mu\text{L}$  PBS and the same amount of CellTiter-Glo reagent. A 10 min incubation at room temperature followed a shaking step and luminescence was measured in a plate reader thereafter. Cells that showed a viability of less than 80 % due to the treatment were excluded from the calculations (**Table 5**). This was the case for high concentrations of quetiapine fumarate, ticagrelor, tamoxifen citrate, dronedarone, amlodipine, ipriflavone, celecoxib, efavirenz, docusate, doxazosin mesylate, nebivolol, ketoconazole, travoprost and ceritinib.

**Table 5: CellTiter-Glo Viability measurement of pIC<sub>50</sub> determination:** Viability of the cells was measured at every concentration used during concentration-dependent analysis of inhibition on drug uptake. Values with viability less than 80 % were excluded from the data set. The compounds, which led to an exclusion of at least one concentration are listed below.

Compound	Viability [%]		
	Compound conc.	Compound conc.	Compound conc.
	100 $\mu$ M	33 $\mu$ M	11 $\mu$ M
Amlodipine	30.93	75.71	94.51
Amsacrine	79.22	101.53	105.38
Benzbromarone	78.23	93.87	98.7
Celecoxib	35.55	91.82	109.56
Ceritinib	23.79	32.44	82.43
Desogestrel	77.26	88.14	94.59
Dipyridamole	75.01	88.99	91.83
Docusate	24.38	43.88	88.43
Doxazosin Mesylate	40.64	96.32	93.45
Dronedarone	37.86	70.6	93.32
Efavirenz	24.38	61.35	85.8
Ethinyl Estradiol	79.97	74.63	87.52
Ezetimibe	78.79	75.23	90.1
Fenofibrate	77.2	76.575	84.9
Ipriflavone	68.19	85.06	88.17
Ketoconazole	32.26	58.19	88.69
Nebivolol	15.16	22.42	79.45
Norethindrone	84.65	76.8	95.01
Oxybutynin	79.62	87.22	96.75
Quetiapine Fumarate	32.24	87.05	89.27
Tamoxifen Citrate	61.51	89.34	95.63
Ticagrelor	44.44	80.76	103.03
Tolterodine Tartrate	76.53	92.85	95.72
Travoprost	102.49	48.09	75.69

Having two established methods for the analysis of inhibitors of E3S drug uptake through OATP2B1 now brought the possibility of comparison of the two assay types. Due to the use of different methods and substrates of OATP2B1 and differences in experimental setup, an inhibitor identification differing from each other is likely. A comparison of the % inhibition and the pIC<sub>50</sub> of the compounds for both assay types was therefore done. The comparison of the whole dataset by analysis of the % inhibition values for the compounds showed differences between the two methods. With MALDI MS, a total number of 67 hits could be verified, 47 of them were also identified with the fluorescence assay, 20 of them were just found with MALDI MS. For the fluorescence-based assay, a total number of 57 were found as hits, whereas 10 of



them were only found in fluorescence, not with MALDI MS. The methods were found to not overlap completely in regard to the identification of inhibitors (**Figure 43,A**). Also the detailed analysis of the ones being a hit in both assay types through a comparison of  $pIC_{50}$  values brought up some differences leading to a Spearman correlation coefficient of 0.44 (**Figure 43,B**). The fact that the two methods partly led to the identification of different inhibitors shows the need to have a reference method for testing inhibitors of drug uptake.

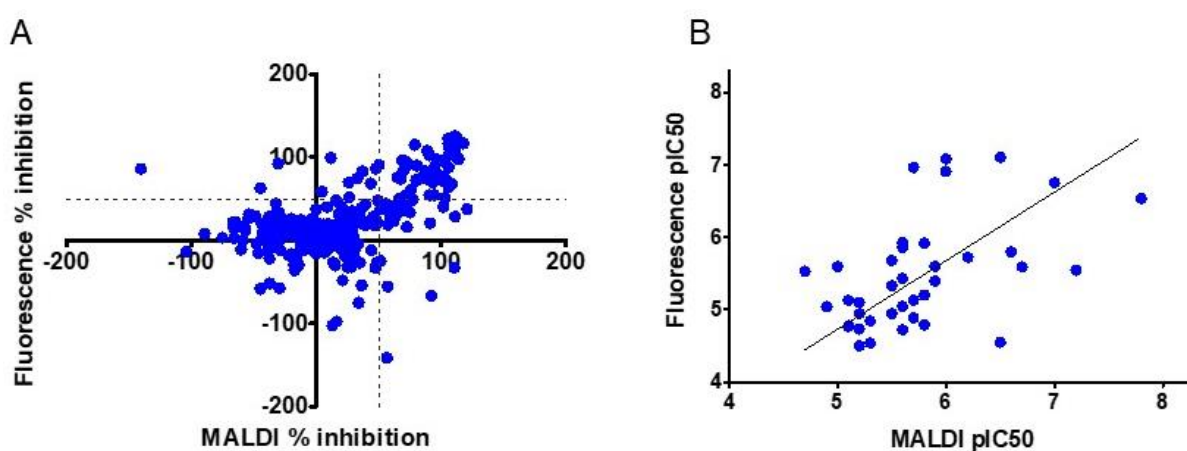


**Figure 43: Comparison of MALDI MS-based and fluorescence-based assay:** (A) Comparison of % inhibition values for both methods, for MALDI MS, the average of the two biological screening replicates was used, for fluorescence only the 10  $\mu$ M screening data. (B)  $pIC_{50}$  value comparison of both methods. Only the ones leading to a hit in both assay types could be compared. Screen was conducted together with Lena Schumacher.

A previously published radioactive-based study by Karlgren *et al.*<sup>171</sup> examined a comparable data set using also E3S as substrate for OATP2B1. As the use of the same substrate like in the MALDI MS assay leads to a better comparability of the assay types, a comparison of the two assays was done. A possible outcome could range from the identification of the same inhibitors in both assay types to a low overlap of inhibitors found in both methods. 75 compounds and their respective inhibition values were compared. Compounds  $\geq 50$  % inhibition were highlighted in orange. As it can be seen in some cases, the compound was identified as inhibitor in both methods, but the % inhibition values varied due to the differing method. Compounds

## Results

were counted as “consistent in both methods” when they were identified as a non-inhibitor <50 % inhibition or inhibitor >50 % inhibition with an additional consideration of  $\pm 5$  %. Only 13 of 75 compounds were based on this calculation identified as not consistent in both assays (**Table 6**).

**Table 6: Comparison of MALDI and Karlgren data:** % inhibition values of both methods are compared for 75 compounds. Compounds were counted as inhibitor/non-inhibitor as already described with an additional consideration of  $\pm 5$  %. Critical compounds (simvastatin, estradiol, doxazosin mesylate, genistein, tetracycline, ketoconazol), which lied in the limit of  $\pm 5$  % were counted as “consistent in both methods” due to their comparable result to the other assay format respectively. Cyclosporine revealed an  $IC_{50}$  of 37  $\mu$ M in the Karlgren assay and was therefore also counted as inhibitor.

Name	MALDI	Karlgren
Allopurinol	-24.9	8.4
Amitriptyline	-0.3	-8.9
Atenolol	-54.8	6.8
Atomoxetine Hydrochloride	21.8	16.3
Atorvastatin	108.1	98.3
Benzbromarone	112.9	76.3
Budesonide	92.1	30.3
Bupropion	34.0	17.0
Bupirone Hydrochloride	-22.3	-13.9
Carbamazepine	-15.0	17.3
Celecoxib	107.0	-69.0
Cetirizine Hydrochloride	-30.5	29.9
Colchicine	-39.8	24.4
Conjugated Estrogens	-140.6	20.8
Cyclosporine	67.7	14.0
Diclofenac	20.0	19.6
Diethylstilbestrol	106.3	68.1
Diltiazem Hydrochloride	48.6	-9.1
Dipyridamole	111.3	83.1
Doxazosin Mesylate	70.0	45.8
Enalapril Maleate	-20.8	19.7
erlotinib	106.8	93.7
Erythromycin	21.2	-19.0
Estradiol	102.7	47.4
Ezetimibe	117.9	-8.9
Felodipine	79.9	21.4
Fenofibrate	114.3	34.2
Fluconazole	-36.6	34.1
Fluoxetine Hydrochloride	31.2	22.6
flutamide	4.5	65.8
Fluvastatin	108.3	98.2
Furosemide	-60.3	34.5
Gemfibrozil	-50.2	15.1
genistein	49.4	67.9
Glipizide	15.2	22.0
Hydroxychloroquine Sulfate	5.7	23.5
Ibuprofen	-29.3	13.5

Name	MALDI	Karlgren
Indomethacin	25.9	-82.4
itraconazole	104.7	59.8
Ketoconazole	96.2	44.0
Lamotrigine	16.3	13.6
Levothyroxine	106.1	63.7
Lisinopril	-39.2	19.2
Loratadine	105.8	28.1
Lovastatin	103.1	-17.9
Metformin Hydrochloride	0.0	-4.5
Methotrexate	-5.4	-13.4
Metoprolol	-39.7	30.5
Nifedipine	7.9	-44.4
Nitrofurantoin	7.4	23.1
novobiocin	50.2	85.6
Ofloxacin	9.1	18.4
Olmesartan Medoxomil	43.6	-7.9
Omeprazole	-48.9	11.3
Pantoprazole Sodium	19.1	17.3
Paroxetine	28.1	37.5
Phenytoin	-32.5	11.1
Pioglitazone Hydrochloride	72.4	-9.9
Piroxicam	28.7	68.3
Pravastatin Sodium	-46.5	36.8
Prednisolone	-28.8	27.6
Probenecid	-24.9	26.4
Progesterone	72.5	-362.6
reserpine	90.9	72.3
Sildenafil	36.1	45.9
silymarin	72.5	74.0
Simvastatin	75.9	47.4
Spirolactone	34.4	-82.0
Sulfasalazine	11.6	92.3
Tetracycline	9.0	51.1
Tipranavir	102.5	99.0
Trimethoprim	-44.8	35.1
Valsartan	-32.1	12.3
Verapamil Hydrochloride	16.8	-62.6
Warfarin	17.9	31.6

The comparison of both datasets was done by classifying the compounds which were analysed in both assay types as “inhibitors” ( $\geq 50\%$  inhibition) or “non inhibitors” ( $< 50\%$  inhibition). Also values  $\pm 5\%$  were accepted in this classification. Generally, it could be stated that the data sets agreed well in 83% of the cases. Some compounds (12 %) were only found in the MALDI MS assay as inhibitors, even less (5 %) only in the Karlgren study based on a radioactive assay (**Figure 44**). The comparability to already published data rendered MALDI MS a possible screening tool.

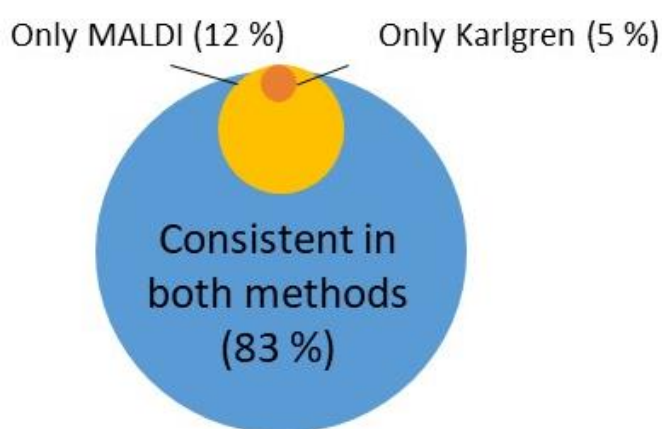


**Figure 44: Comparison of Karlgren publication with MALDI data:** Overlap of 83 % of consistently identified inhibitors/non-inhibitors. Compounds that showed an inhibition of  $50\% \pm 5\%$  in both methods were considered as inhibitor.

#### 4.3.5 SEARCH FOR SUBSTRATES OF OATP2B1 DURING SCREEN

As the SLC family is still an understudied drug target class<sup>9</sup> and a new consortium with 13 partners and the goal to de-orphanise transporters of the SLC family in a large scale has been established just recently<sup>199</sup>, there is a high interest in methods that tackle the de-orphanisation. By now, there are only fluorescence-, radio-labelled and LC-MS/MS methods in use for the detection of transporter substrates. A method, which identifies several substrates at once by analysing the mass spectrum does not exist yet and is therefore highly demanded. The developed and automatised cell-based MALDI MS assay is theoretically capable of serving this need. The uptake of one compound, E3S was confirmed in this study and because it is a mass spectrometric

analysis and the whole mass spectrum is gathered for every measurement, there is also the possibility for further analysis regarding identification of substrates.

The first reason of parallel conduction of the screen in the vector control was already described as the control of E3S enrichment in the vector control due to concomitant incubation with other drugs. The second reason of parallel conduction of the screen in the vector control was the search for a substrate of OATP2B1. The comparison of the mass spectrum of the vector control with the one of the overexpressing cell line could theoretically help to identify a substrate. Assuming one of the compounds ("compound A") in the 294 compound set has a chemical structure that leads to the  $m/z$  of 429.13, the mass spectrum is investigated at this value. Four different cases can occur. If the overexpressing cell line shows signal intensity at the sought-after  $m/z$  of 429.13 and simultaneously, the vector control does not show a peak at this  $m/z$  value, the signal window between these two peaks is analysed and has to be  $>1.5x$  in order to fulfil the criteria of a substrate (**Figure 45,A**). The signal window is analysed by division of the (normalised) peak intensity of the peak at 429.13  $m/z$  of OATP2B1 through the peak at this  $m/z$  obtained with the vector control. The simplicity of the MALDI based substrate identification concept gets clear by the awareness that in just one mass spectrum, the information of 294 compound is available at the same time, which could theoretically lead to a large scale identification of substrates. Nevertheless, the three other cases describe the situation where no substrate was found. A peak that was identified at the sought-after  $m/z$  only in the vector control and not in the OATP2B1 cell line does not lead to an identification of a substrate (**Figure 45,B**). This is also the case, when there is no peak at all identified at this respective  $m/z$  (**Figure 45,C**). Reasons for that could be that the substrate, which should be detected at this  $m/z$  does not fly (well enough) in the TOF. A last possible scenario is that in both cell lines a peak at the sought-after  $m/z$  is detected, which also does not lead to the identification of a substrate (**Figure 45,D**). This can also be due to the transport process occurring via passive transport or other transporters expressed in both cell lines. It is nevertheless not always possible to make a statement about the uptake of a drug into the cells by just identifying if a peak is present at the sought-after  $m/z$ . In the case of (**Figure 45,D**), this is not already a proof for the uptake of this substance into the cells in general, but it could also be an endogenous substance producing a peak at the  $m/z$ .

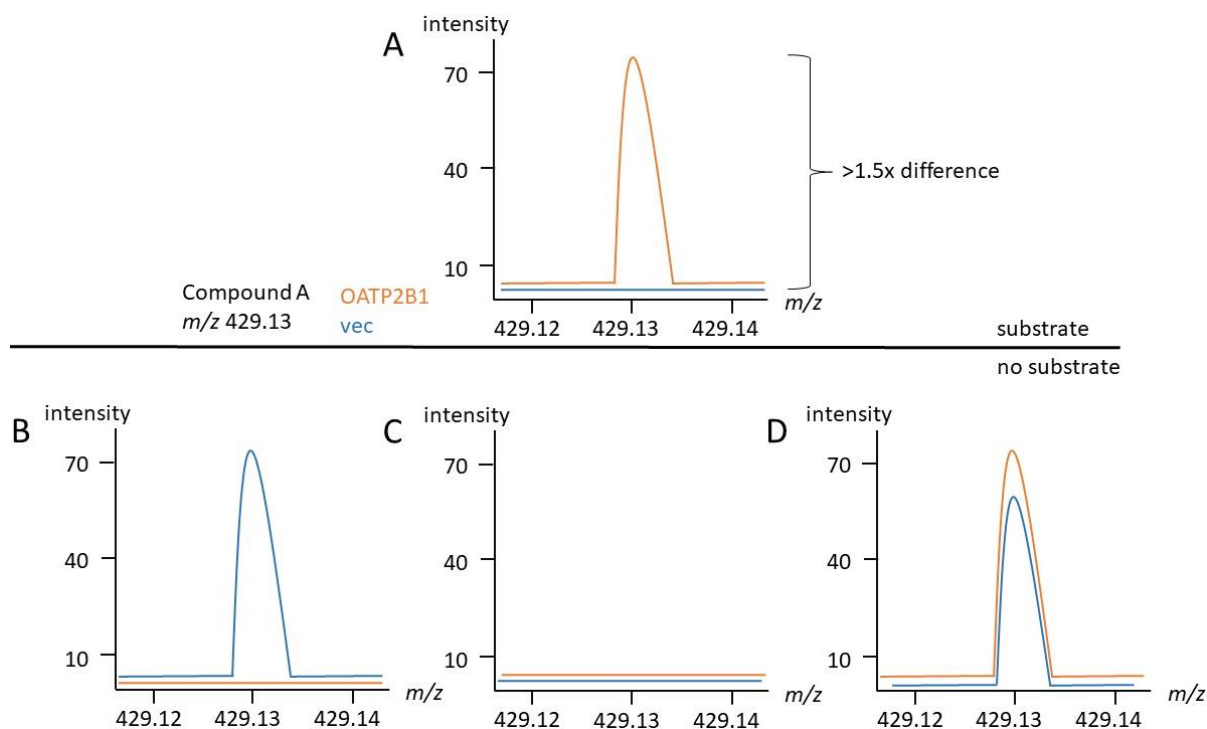


**Figure 45: Concept of OATP2B1 substrate identification in MALDI MS:** As an example drug, “Compound A” with an  $m/z$  of 429.13 is shown. Comparison of OATP2B1 overexpressing cell line with vector control can lead to three different cases. **(A)** OATP2B1 shows peak at the sought-after  $m/z$  and vec not. If the factor of signal intensities divided through each other  $>1.5$ , a substrate is identified. **(B)** Vec shows peak at the sought-after  $m/z$  and OATP2B1 not. No substrate was identified. **(C)** None of the cell lines show a peak at the sought-after  $m/z$ . No substrate was identified. **(D)** Both of the cell lines show a peak at the sought-after  $m/z$ . No substrate was identified.

The concept of this method was applied to the screen. Therefore, the results were normalised to the internal standard and the intensities of OATP2B1 and the vector control compared at different  $m/z$  – according to the respective compound mass. The criteria for substrates were defined as there needs to be a factor of  $> 1.5$  between the OATP2B1 peak intensity and vector control peak intensity. Based on those criteria, there were two compounds identified, which showed a high signal between OATP2B1 and the vector control based on the average of two biological replicates of OATP2B1. As it can be seen already, the reproducibility lacked as in the first run, both compounds produced a high normalised signal intensity, whereas the normalised signal intensity of the second biological replicate was comparable with the vector control (**Table 7**).

**Table 7: Compounds that meet the criteria of a candidate substrate for OATP2B1:** Signal window of OATP2B1 vs vector results from average of two replicates from OATP2B1 screening data. Data processed in R by Thomas Enzlein.

Compound	OATP2B1 N=1	OATP2B1 N=2	vector	Signal window
Fluvastatin	0.73	0.07	0.05	7.6
Sulfasalazin	5.8	0.03	0.02	161.9

The further goal was to verify those trends in a separate cell treatment once again. Therefore, the cells were pretreated with DMSO/erlotinib and treated 10 min with 10  $\mu\text{M}$  compound. The results show that none of the identified compounds could be verified as a substrate of OATP2B1. There was no significant difference between transporter overexpressing cell line and vector control seen, neither for sulfasalazine (**Figure 46,A**), nor for fluvastatin (**Figure 46,B**). This finding emphasised the assumption of the screen that the reproduction of the increased peak intensity in the OATP2B1 cell line cannot be achieved. Further, both compounds were investigated regarding their detection limit in MALDI-TOF. During the method optimisation, it was already shown that a high S/N is the basis for a reproducible detection. Thus, both compounds were analysed with a focus on their detection limit by analysing a dilution series of the compounds in cell background. Fluvastatin showed a low detection limit of about 8 arb. u. at a relatively high concentration of 2.5  $\mu\text{M}$ . Additionally, a peak is detected with the addition of just DMSO, which leads to the assumption that there is also an endogenous peak at this  $m/z$ , which could disturb the measurement (**Figure 46,D**). The detection limit of sulfasalazine is high with low concentrations as 0.6  $\mu\text{M}$  and 0.2  $\mu\text{M}$  still able to detect with arb. u. of 25 and 11 respectively. (**Figure 46,C**). Nevertheless, it was not possible of being identified as substrate during the screen and in the reproduction. Possible reasons for that are likely to be found in the method properties. As it was already shown multiple times during the assay development, the detection in cells is dependent on various factors ranging from matrix and solvent composition, to application of matrix and matrix analyte ratio. An optimised method for sulfasalazine is likely to show its uptake as a substrate, as it is also already a known substrate for OATP2B1<sup>200</sup>.

## Results

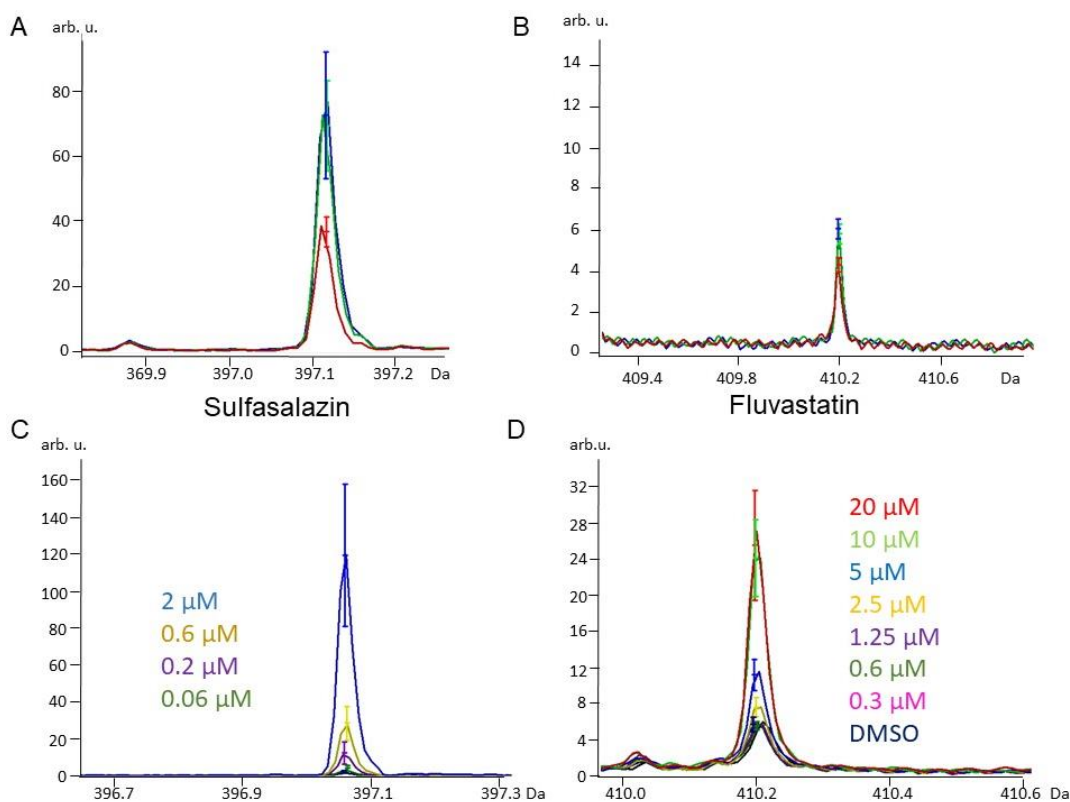


**Figure 46: Further testing reveals no possible substrates for OATP2B1: (A,B)** Comparison of sulfasalazine and fluvastatin. HEK293-OATP2B1 or “vector” cells were pretreated with DMSO/4 μM erlotinib for 10 min before 10 μM of the compounds was added for 10 min. Uptake was stopped and cells were frozen. Cells were resuspended in ddH<sub>2</sub>O/matrix (2.5 mg/mL Ph-CCA-NH<sub>2</sub> in 70 % ACN)/internal standard D<sub>4</sub>-E3S to a final cell number of 2500 cells/spot. Shown are 8 measurement replicates of each treatment in ClinPro Tools. **(C,D)** Flight test of sulfasalazine and fluvastatin. For the flight tests, there were different final concentrations of compound (0.2 μM-20 μM or only DMSO) added to a cell pellet of HEK293-OATP2B1. Shown are 8 measurement replicates of each concentration in ClinPro Tools.



## 5 DISCUSSION

### 5.1 FLUORESCENCE-BASED ASSAYS AND THEIR POSSIBLE DISADVANTAGES IN SCREENING

The success of a drug candidate during clinical trials is dependent on different aspects. They can be metaphorically summed up as four pillars of efficacy: high exposure at the site of action, sufficient target engagement, the functional pharmacology and the relevant phenotype<sup>201</sup>. If a drug candidate has a lack in one of those pillars, it is more likely to fail during clinical trials<sup>59</sup>. The process of clinical trials as such is a time- and cost-intensive work. During and also after the market launch of a drug, a special emphasis is given on possible adverse events, which could lead to a withdrawal of a product from the market in serious cases. Those processes show that, among many other things, it is important to conduct research on the uptake mechanism of cells, which are an important player of exposure at the site of action, namely the first pillar of efficacy, and of adverse events. OATP2B1 seems to be one of the key players of intestinal absorption<sup>202</sup>, even though it has already been discussed to be located at the basolateral membrane of enterocytes<sup>203</sup>. Therefore, it is of importance to investigate the transport protein regarding to substrates and inhibitors.

This was done in the first part of this thesis by the conduction of a fluorescence-based assay. Those assay types are besides radioactive measurements very common for transporter characterisation. Due to the western blot showing a clear overexpression of OATP2B1 compared to the vector control, those cell lines could be compared in order to characterise the transport protein. Another control was done by fluorescence microscopy, which clearly showed the uptake of DBF exclusively into OATP2B1-overexpressing cells. The vector control, which was also treated with DBF, showed no fluorescence, thus validating the method. The time-dependence of the DBF uptake was analysed in order to determine the kinetics of transport of DBF. A plateau of the fluorescence intensity in OATP2B1 cells could be seen after 60 min. Reported timepoints of plateauing intensity range from short timepoints like several seconds to few minutes<sup>204-206</sup> to long timepoints like 30-60 min, like in our case<sup>73, 207, 208</sup>. The analysis of the same transport protein with different substrates can lead to differences in plateauing time<sup>209</sup> and makes clear that the decision for the substrate is fundamental for transporter studies.



The  $K_M$  value was determined by investigation of a concentration range of DBF. The  $K_M$  value was found to be 10.5  $\mu\text{M}$  and is nearly identical with 10  $\mu\text{M}$  published by Izumi *et. al.*<sup>173</sup>. The uptake was neither time-dependent nor concentration-dependent in the vector control showing a clear effect of the transport protein OATP2B1. The verification of the assay was done with the determination of the  $\text{pIC}_{50}$  of the known inhibitor erlotinib<sup>171</sup>. The  $\text{pIC}_{50}$  in the assay validation resulting from eight separate occasions was  $7.0 \pm 0.1$ , which is slightly different to the value known from literature (6.3), which was obtained by usage of E3S as a substrate<sup>171</sup>. The conduction of the screen, which followed the characterisation of the transport, led to a  $\text{pIC}_{50}$  of 7.1 of two separate experimental assay runs showing the reproducibility of the method. The screen of the compound set revealed 66 compounds  $\geq 50\%$  inhibition. 57 hits were confirmed and 8 potent inhibitors with a  $\text{pIC}_{50} \geq 6$  identified.

As the intestine has a high risk of DDI because it has a special propensity to be exposed to high concentrations of drugs<sup>185</sup>, Jennypher Mudunuru from GlaxoSmithKline did a clinical extrapolation of the  $\text{pIC}_{50}$  data. This calculation also took the route of the drug, the molecular weight, the  $\text{pK}_a$ , the actual dose,  $I_{\text{in,max}}$  as the estimated maximum plasma inhibitor concentration at the inlet to the liver and the unbound fraction ( $f_u$ )<sup>210</sup> of the drug in plasma into account. For detailed description of calculation process, refer to<sup>170</sup>. For the extrapolation of intestinal clinical relevance, the  $I_{\text{gut}}$  was calculated. It is calculated as the dose of the drug divided through 250 mL and describes the intestinal luminal concentration of the interacting drug. Compounds with an  $I_{\text{gut}}/\text{IC}_{50} \geq 10$  are flagged as clinically relevant in the intestine. The influence of the hepatic drug uptake was calculated using the  $I_{\text{in,max}}$ . Drugs leading to  $1 + I_{\text{in,max}}/\text{IC}_{50} \geq 1.1$  were flagged as clinically relevant in the liver. This illustrates that the  $\text{IC}_{50}$  does not necessarily has to be very low, viz. potent, in order to also fulfil the needs for being accounted as clinically relevant. Flutamide for example had an  $\text{IC}_{50}$  of 32.4  $\mu\text{M}$ , which did not render it as a potent inhibitor. Nevertheless, the high  $I_{\text{gut}}$  of 3620 and high  $I_{\text{in,max}}$  of 56 led to a value of 112 for the intestinal analysis and 1.1 for the hepatic analysis and therefore counted as clinically relevant in both tissues. This makes the need to investigate inhibitors even more important, because also less potent inhibitors could lead to clinical effects.

The outcome of the clinical extrapolation was that 66 % of the identified inhibitors were clinically relevant in the intestine and 29 % in the liver. This is a really high number

possibly leading to DDI. Considering the fact that (when all medications are counted) more than 81 % of individuals would be taking at least 1 medication in a given week and more than 25 % would be taking at least 5 medications<sup>211</sup> and the population is getting older and thus it's coming to a worsening of that problem, attention to this is immensely important. The fluorescence-based assay, which was developed, can therefore act as a screening tool to classify the DDI potential of a drug set. In the end, a double verification with an *in vivo* test is intended and can shed another light onto the statement. For the conduction of the *in vivo* tests, OATP2B1 knockout mice would have to be created. They would be compared to the wildtype throughout the experiments. In the case of the study of Chen *et. al.*, erlotinib as the standard inhibitor was given to the mice 1 h before administration with fluvastatin. Serial blood samples were taken at several timepoints after administration of the substrate fluvastatin. The samples were analysed using LC-MS/MS and fluvastatin concentrations were determined<sup>212</sup>. Such a structure of a study could also be used for the dataset of the fluorescence-based assay. Of course this would have the negative side effect that the usage of many wildtype and knockout mice would be needed.

Bringing the research on the transporter to an even higher level, it could be possible to establish an individual dosing of patients according to their transporter availability in the genome<sup>213</sup>. Interindividual variability of transporters are a common phenomenon<sup>214</sup>, for which in the case of OCT1 for example the reasons are manifold ranging from genetic variants, epigenetic modifications and transcription factors to non-genetic factors, such as cholestasis. Metformin is a known important substrate of OCT1<sup>215</sup> and is postulated to be affected by the interindividual variability. Differences in its pharmacokinetics and response to metformin therapy can be possible results<sup>213</sup>. Addressing this interindividual variability of the transporters by analysis of transporter expression in individual patients and consequential administration of drug could be one of the possible key future aspects of transporter research in context with precision medicine.

Fluorescence-based readouts are most widely used in cell-based drug discovery<sup>216</sup>. A clear disadvantage of the assays is the possible occurrence of photonic artefacts like fluorescence quenching and autofluorescence requiring secondary assays. In this sense, also the autofluorescence and quenching properties of the investigated compounds was tested. 5 compounds (amlodipine, amsacrine, ceritinib, chlorhexidine

and doxazosin mesylate) were found to show a quenching effect at 100  $\mu\text{M}$  compound. This quenching effect might have led to the assumption of them being inhibitors while the interaction just led to a reduction of the DBF fluorescence signal. At 10  $\mu\text{M}$ , two compounds (amlodipine and amsacrine) showed a quenching effect of 20-29% fluorescence reduction. As this was the compound concentration at which the assay was conducted, these effects should be taken more into account than those at 100  $\mu\text{M}$ . Amlodipine had a  $\text{pIC}_{50}$  value of 4.9 and amsacrine 5.1 standing for a  $\text{IC}_{50}$  of 12.5  $\mu\text{M}$  and 8  $\mu\text{M}$  respectively. At 10  $\mu\text{M}$  compound concentration, they were therefore only at their halfmaximal inhibition. Nevertheless, a counter-screen for those substances may be needed, to ensure their inhibiting properties.

### 5.2 DEVELOPMENT OF FIRST LABEL-FREE UPTAKE ASSAY USING MALDI MASS SPECTROMETRY

A very recent publication in Nature once again highlighted the importance of SLC transporter research. A new consortium with 13 partners has been established with the ultimate goal to conduct a large scale de-orphanisation of the SLC superfamily. Most SLCs are difficult to access, also due to a lack of appropriate research tools<sup>199</sup>. The interaction of biomolecules can be investigated with several methods. The cellular thermal shift assay (CETSA) for example proved to be a suitable label-free method for the investigation of proteins and their binding partners by heat-induced protein stability changes. This method is based on the fact that a protein often gets stabilised by the binding of another molecule<sup>217, 218</sup> and could therefore be a useful tool for transporter investigation. Nevertheless, it is not a universal and easy tool for the investigation of transport proteins, because a direct stabilisation of transporters sometimes fails. A possible reason for that is that for large proteins, like transporters, the ligand binding just leads to a stabilisation of a part of the molecule and overall stability might stay the same leading to the impossibility of readout using this method<sup>219</sup>.

Another method, which is also dependent on temperature is the isothermal titration calorimetry (ITC), which is useful for the detection of biological interactions through an isothermal process. The structure of the device includes two separate chambers with thermally conductive material inside them. The temperature of the liquid surrounding the material can be measured using very sensitive thermometers. One of the

chambers acts as a reference chamber, whereas the probe is applied to the other chamber. The addition of the probe leads to the emission or absorption of heat to the liquid in the chamber. The measurement is based on the temperature recovery through a feedback loop. The disadvantage is that it is not really applicable to high-throughput screening, because the average duration of an experiment, where just one compound is tested is about 15-30 min<sup>220</sup>. Compared to analysis times of about 5 min for one 384-spot MALDI target plate, where a single screen of 384 compounds could be investigated at once, this is significantly slower.

Surface plasmon resonance (SPR) on the other hand is well suited for this due to its high throughput capacity<sup>221</sup>. It is a technique, which is often applied in drug discovery due to its ability to analyse interactions of molecules<sup>222</sup>. This works through the use of a goldsensor chip, on which the ligand is immobilised. Light passes through a prism and reflects off the backside of the chip surface and into a detector. The electrons in the metal of the gold sensor absorb the light of a certain incident angle and thus start to resonate leading to the formation of surface plasmons. The result is an intensity loss in the reflected beam, which appears as a dip in the SPR reflection intensity curve. Free analyte is given to the solution surrounding the goldsensor. If it binds to the immobilised ligand, the dip in the SPR curve shifts and a readout of the interaction of the biomolecular agents is possible. Optimisation of the technique also led to the possibility of the detection of smart molecules with their target macromolecules<sup>223</sup>. A disadvantage of the technique for the use case of transporter investigations is that a whole cell analysis is not possible. The target, in this case the transport protein, would have to be extracted and immobilised on the goldsensor chip. This may lead to changes in the binding situation and therefore artefacts. Also, the technique is rather suitable for the analysis of drug interactions of biomolecules than for the uptake of drugs into the cells. False assumptions could also happen due to the inhibitors that are also likely to bind to the transport protein. The SPR technique therefore represents an alternative with some drawbacks.

Another label-free approach would include mass spectrometric analysis. LC-MS/MS is a suitable label-free technique and in the course of a RapidFire assay showed to be applicable to the analysis of intracellular compound concentration<sup>109</sup>. The clear disadvantage of this assay format is the comparatively low throughput. Nevertheless, mass spectrometric methods as such are ideally suited for transporter characterisation

and as possible methods for the counter-screen of the fluorescence-based assay, because of their ease in handling and general applicability to higher throughput. As especially cell-based assays typically require labelling of the substrate via fluorescence or radioactivity, whole-cell assays with a simple sample preparation and automation of handling steps are highly desirable. MALDI-TOF MS represents a well-suited method for the label-free detection of drug uptake in whole cells as it is applicable to ADME processes<sup>224</sup> and the development of a high-throughput screen is possible<sup>152</sup>.

Previous work has showed that the method development part plays a crucial role in the detection of the analyte. The use of substrate, matrix and solvents have to be coordinated. For that purpose, our first approach was to determine the best substrate for the detection of uptake through OATP2B1. The dependence of detection on the use of different solvents was already a known phenomenon in MALDI MS<sup>225, 226</sup>. Therefore, the best matrix in terms of S/N ratio of substrate signal, CV % and matrix crystallisation was optimised in its concentration and also the solvent composition was optimised. The real cell treatment then showed the disability of the DHAP matrix due to a background peak in close proximity to the analyte peak. The problem of matrix peaks of certain matrices is often discussed. Especially in the low mass range, high matrix background signals are not unfamiliar. Therefore, projects that aim for the development of matrices with less background signals are ongoing<sup>227, 228</sup>. In that case, there was the option to switch to another matrix without a background peak. Another option could have been to switch to a higher resolution, which is possible by usage of the FT-ICR in combination with MALDI MS<sup>128</sup>. The possibility of the combination with FT-ICR leads to a wide range of applicability of cell-based MALDI MS assays. The disadvantage of it is the lack of speed that comes with the high resolution. Currently, there is still a compromise between the “4S criteria” required for mass spectrometry imaging, which could also be applied to biotyping. Those “4S criteria” include speed, spatial resolution, specificity and sensitivity<sup>110</sup>. High speed instruments like the rapifleX are supported by high specificity instruments like the FT-ICR. Nevertheless, for a screening application, FT-ICR is unsuitable due to its low throughput. A device that could bridge the gap is the timsTOF fleX as the next generation machine. It combines high speed and high spatial resolution and therefore could be an alternative to the screening done in the rapifleX.

During the real cell treatment, which led to the exclusion of DHAP, the first confirmation of the possibility of detecting the uptake of E3S through OATP2B1 was done. The vector control had a very low intensity at the  $m/z$  of E3S (349.14) and also the inhibition with the known inhibitor erlotinib led to a reduction of the peak intensity compared to the treatment with E3S only. Our next approach was to finalise the application of Ph-CCA-NH<sub>2</sub> for the drug uptake assay. As the success of a MALDI MS-based experiment is dependent on the matrix application technique<sup>229</sup>, different ways of application were tested. Even though dried droplet led to a higher CV % than sprayed application, it would theoretically be the method of choice due to its applicability in a high-throughput. For further optimisation of the method, an internal standard, D<sub>4</sub>-E3S was therefore used to normalise the spectra. This normalisation led to a decrease in the CV % value making dried droplet the method of choice.

Besides the solvent and matrix ratio, also the matrix-analyte ratio plays a pivotal role in the detection of the analyte<sup>230, 231</sup>. Therefore, differing cell numbers per spot were investigated. The method development and optimisation made MALDI MS a suitable method for a drug uptake assay and showed the possibility to be applied for transport characterisation and screening for inhibitors. The transport characterisation identified a time-dependence of the uptake with a plateau seen after about 5 min. Compared to the fluorescence-based assay, this is a short incubation time, but in general a plateau after about 5 min is very common, like it was already mentioned. Also a concentration-dependence of the uptake could be seen and resulted in the determination of the  $K_M$  of 21.1  $\mu\text{M}$ . As E3S is a very well-known and often used substrate of OATP2B1, it has been characterised often and has differing  $K_M$  values from 5  $\mu\text{M}$  to 38  $\mu\text{M}$ <sup>73, 171, 209, 232-234</sup>. Therefore, our determined value lies in the range and can be perfectly compared to the literature. The same cell line was also already investigated in a radiolabelled assay<sup>172</sup> and revealed a very comparable  $K_M$  of 16.9  $\mu\text{M}$ . The confirmation of reproducibility of the method was further done by pIC<sub>50</sub> determination of erlotinib. In three independent runs, a pIC<sub>50</sub> of 6.1  $\pm$ 0.1 was determined showing the reproducibility of the method and also the comparison to literature showed consistency with the data due to Karlgren *et al.* resulting in 6.3 as a pIC<sub>50</sub><sup>171</sup>. The method therefore showed to be a reliable and reproducible tool for the investigation of drug uptake and can be seen as the first unlabelled small molecule uptake assay by MALDI MS.

### 5.3 MALDI MASS SPECTROMETRY SCREENING OF INHIBITORS AS AN EMERGING METHOD FOR DRUG-DRUG INTERACTION TESTING

The development of the drug uptake assay has opened up completely new possibilities for the application of MALDI MS. Using MALDI MS as a screening technique is meanwhile an established procedure<sup>152, 153</sup>. Also the identification of inhibitors has been done in high-throughput MALDI MS screens already<sup>235</sup>, nevertheless, the inhibitors of cellular drug uptake have never been investigated with MALDI MS before. The method was just applied to monitor the drug uptake labelled with streptavidin-coated magnetic beads<sup>154, 155</sup> and the analysis of peptide transwell-uptake<sup>157</sup>. A label-free method conducted in whole cells for the direct measurement of the drug uptake of small molecules was nonetheless still lacking.

For the investigation of cellular drug uptake, in this case a recombinant cell line was used. This brings the possibility of investigation of a single transporter and is therefore the preferred method to study uptake transporters and their inhibitors/substrates. A clear disadvantage, which logically comes with this assay type, is that such a static study is not including all the other transport processes taking place in the cell. Besides that, also the lab-to-lab variability in expression levels of the studied transport protein has a negative effect on the comparability of literature data concerning transporters<sup>27,183</sup>. Nevertheless, an investigation of a single transport protein is a very common method and can give a hint about the influence of this transporter on the cellular processes. Our goal therefore was to use the assay as a screening tool and investigate the same compound set as in the fluorescence-based assay. A screening of transporters and their inhibitors is mostly conducted via *in vitro* testing and sometimes computational modelling beforehand<sup>236</sup>. Besides that, also quantitative structure-activity relationship (QSAR) studies are often conducted in the context of transporter screening<sup>237</sup>. This method is based on the comparability of the chemical structure of a molecule with its biological activity. For transporter studies, the machine-learning based technique can be fed with information about known inhibitors or substrates and their respective chemical structures. Based on structural similarities of various inhibitors regarding functional groups and vice versa, unknown compounds can be predicted as inhibitors or non-inhibitors. A first training set can therefore be confirmed or improved by testing *in vitro* again. The screening sets often encompass about 50-200 drugs<sup>238</sup>. So with testing nearly 300 compounds our compound set was

larger than average and together with the fact that it encompassed the top marketed drugs also very close to a real situation<sup>174</sup>.

Criteria for the assay performance of a cell-based assay had to be followed during method development. Those included in general the presence of suitable controls, the evaluation of  $Z'$  as an assay parameter, the involvement of a standard inhibitor, the check of the reproducibility and variability of the method and the validation of the data. The presence of suitable controls is especially important for conduction of experiments on a cell line with an overexpressing transport protein, because the background activity of transport also had to be taken into account. Therefore, the vector control was used as a control, which made assumptions about the transport protein itself possible.  $Z'$  is, like already described, an assay parameter describing the quality of an assay with special regard to standard deviation. It was monitored throughout the method development and ideally should have a value between 0.5-1. In fact, also values below this quality threshold were observed, which showed that especially the positive and negative controls used throughout the screen were not that stable in their intensity values. The CV %, which was also a quality parameter during checking variability of the method, ideally had to be below 20 % in order to represent valid data. With the screen leading to a mean CV % value of below 6, this result was very promising. Checking the reproducibility of the method was done with the determination of the pIC<sub>50</sub> of erlotinib. The intra-assay comparison of both the fluorescence-based and the MALDI MS assay still showed need for optimisation. Both assays are likely to need further stabilisation before being applied as industry standard operating procedure. This likely comes due to variability of the cells used in this assay. The HEK293 cells had issues with the adherence leading to problems throughout the workflow. Even an extra fixation step including coating of the plates with poly-L-lysine sometimes led to a detachment of the cells during the washing step. Apart from that, the overexpression of a protein can lead to several effects in the cell. Much energy is needed to assemble extra proteins in the cell<sup>239</sup>, which could lead to the disability to produce other proteins, which again has effects on the viability of a cell<sup>240</sup>. A way to improve the missing repeatability of the assay could be the use of another cell line, which is more stable in washing procedures due to better adherence.

Some of the identified inhibitors were already found to be clinically relevant in the intestine/liver during the fluorescence-based assay and especially statins are a known



cause for DDIs<sup>241, 242</sup>. Those analyses of inhibitors can give a hint about the DDI happening in the human body. The identified clinically relevant inhibitors can then be postponed to verification in an *in vivo* model, as the identification of DDIs which depend on a onedimensional cell-based assay are just a first approach for the confirmation of clinical relevance<sup>27</sup>. An idea for the future could be to use 3 dimensional cell cultures for the uptake assay instead. The organoids better mimic the processes in the human body<sup>243</sup>, which could also account for transport processes, and have also already been shown to be analysable via MALDI MS<sup>244</sup>. Another development that should be noted here is the design of “organs-on-chip”. Those biomimetic systems could clearly help to reduce animal-testing as it reconstitutes pathophysiology of organs *in vitro*<sup>245</sup>. Those chips could also be measured via MALDI MS and therefore display a possible future development in drug uptake and DDI assays. A general approach could also be the single-cell measurement, which could provide information about drug uptake in mixed cell cultures. The imaging of single cells was already achieved with SIMS-TOF<sup>106</sup> and with the improvement of spatial resolution in MALDI<sup>246, 247</sup>, such a scenario is also conceivable here.

Another important consideration for drug transporter screens is the before mentioned background of transport that has to be excluded. Due to the plethora of transport processes happening in the cellular organism, it has to be ensured that the conclusions drawn from the results are only due to the transporter itself and no passive transport processes are included. Therefore, the linear phase of the time-dependent plateau was identified during the characterisation and the screen was conducted at 2 min incubation and 10  $\mu$ M substrate concentration. Another indispensable action is the parallel screening of the vector control. Doing so, one can analyse directly the effect of the transport protein by analysis of the vector control data. In the case of naproxen treatment, there was an enriched E3S signal detected, which has to be subtracted in order to conclude about the inhibiting function of naproxen. All the other compounds did not lead to an enrichment in the vector control signal facilitating the analysis.

Another reason for parallel screening of the vector control can be the goal to identify a substrate during the screen. Theoretically, this should be possible with MALDI MS, because this technology has the advantage that the whole mass spectrum is measured and can be analysed. The recently founded consortium RESOLUTE shows

the ambition to de-orphanise and therefore characterise the whole SLC family<sup>199</sup>. OATP2B1 is less-well studied than its direct family members OATP1B1 and OATP1B3<sup>212</sup>, for which a considerable quantity of substrates are already known<sup>233, 248-250</sup>. Although there are some substrates known for OATP2B1<sup>251, 252</sup>, interest in a screening method for finding out new substrates is high. For the identification of possible substrates, the normalised peak intensities at the  $m/z$  of the respective compound given were compared in OATP2B1 and the vector control. Criteria for a substrate are a factor  $\geq 1.5$  between transporter and vector control and the nonexistence of other peaks at this defined  $m/z$ . Even though two compounds were identified that met the criteria, they failed to be confirmed as substrates during further experiments. A general remark about the substrate identification via MALDI MS is of course that for the detection of a compound, many factors must match. The compounds need to be detected and therefore have to be ionised by the use of a defined matrix and possible to fly within the TOF. In this screen, of course the for E3S optimised matrix and measurement conditions was used, which surely are not optimal for other compounds. During the optimisation of the method for E3S drug uptake, many conditions were observed that led to a high variability of E3S detection. In the case of the two identified possible substrates, this was also the case. The variability of the results was quite high and another negative aspect was that the vector control was just screened in one biological replicate. The detailed repetition showed that the difference to the vector control could not be reproduced. MALDI MS does not seem to be directly suitable for substrate identification. Nevertheless, the application of different matrices with different application techniques and measurement settings could maybe be able to identify a substrate. The success with the use of E3S also shows the general possibility of the use of this technique. The clear disadvantage is just the dependency on the matrix in this case. Other techniques for the identification of substrates are often radio-labelled<sup>253, 254</sup> or based on the determination of intracellular substrate by LC-MS/MS and therefore lack higher throughput. Although amongst others the group of Zhang *et al.* promotes the use of *in silico* approaches to identify new substrates<sup>255</sup>, which would definitely lead to a reduction of time, a method for identification of substrates in a screening manner is highly desirable. An amendment of the MALDI MS method to a multiple testing with different matrix conditions could be an option for substrate analysis.

#### 5.4 COMPARISON OF BOTH ASSAY TYPES REVEALS DIFFERENCES

The optimisation and conduction of two different technique-based screenings was done during this characterisation of OATP2B1. This suggests a comparison of the two screening results. This comparison has led to a quite unexpected outcome of just 47 overlapping hits in total and 20 hits more identified in MALDI MS in addition to 10 hits more identified with the fluorescence-based assay. The fact that the two assay systems did not overlap in their results brings up several questions and assumptions. The first one is the data quality of both methods. For both of the methods, the reproducibility of the data was shown in correlation analyses. Those did not render one of the methods as less applicable than the other. Still, both methods had only an acceptable correlation coefficient indicating noticeable issues with the reproducibility, which are most likely due to fluctuations of the cell line. The cell line had adherence issues and like it was already postulated, those adherence problems are a very likely cause for problems with repeatability. The second assumption is the quenching and autofluorescence that can be a reason for differences in the dataset. The compounds that showed quenching were amlodipine, amsacrine, ceritinib, chlorhexidine and doxazosin mesylate. Those compounds were due to their quenching effect maybe falsely interpreted as inhibitors during the fluorescence-based assay. Ceritinib could not be confirmed as a hit during the pIC<sub>50</sub> determination in the fluorescence-based assay, amlodipine and chlorhexidine were not found as a hit in the fluorescence-based assay. Amsacrine and doxazosin mesylate were found as a hit in both assay types and therefore do not explain the differences. The quenching effects maybe have happened during the fluorescence-based assay, but they do not explain the differences in the data sets. The situation is different for false positives of both assay types that could not be confirmed during pIC<sub>50</sub> determination. For the fluorescence-based assay, trimethoprim, cetirizine, fenofibrate, meloxicam, amiodarone, gliquidon, ceritinib and pioglitazone were falsely identified as hits in the first screening approach. Of those, only pioglitazone and gliquidon are true MALDI MS hits. For the MALDI MS assay, efavirenz, tolterodin tartrate, ceritinib, tamoxifen citrate, amiodarone, lansoprazole, glyburide and dronedarone were falsely identified as hits. Of those, only glyburide is a confirmed hit in the fluorescence-based assay. Also the presence of E3S itself in the compound set led to a big difference in the two different methods. For the

MALDI MS assay it was of course a substrate, therefore showing no inhibition and for the fluorescence-based assay, it was an inhibitor.

The comparison of the data sets with a known data set of the literature, which also encompasses a high number of our investigated compounds<sup>171</sup>, also showed differences. As already described, the overlap of the MALDI MS data with the Karlgren data set was 83 %. Taking also the fluorescence-based method into account, the overall comparable classification of inhibitors is 80 %. The missing ~20 % can most likely be explained either by the use of another substrate in the case of the fluorescence-based assay or by interlaboratory differences in general. Another assumption that has been discussed a lot in the transporter field might have effects on the different assay technologies. Some of the SLC transporters, among them also OATP1B1, have been found to have multiple binding sites with a high-affinity and a low-affinity<sup>232, 256, 257</sup>. This phenomenon of a multiple binding sites has also already been postulated for OATP2B1. The multiple binding sites seem to differ both in affinity and pH sensitivity<sup>79</sup>. The differing methodological setup of the Karlgren assay could have maybe also led to the investigation of a different binding site for OATP2B1. In a study of Hacker *et al.* it is also illustrated that the identification of inhibitors is dependent on the substrate used<sup>258</sup>. This study, which investigated OCT2 is similar to our comparison of screening results with once DBF and once E3S as a substrate. These results make obvious that the substrate and inhibitor interaction is a very complex system, which needs to be addressed closely in different investigations and with different substrate-combinations to uncover the mechanism and properties of a transport protein completely. Apart from that, interlaboratory differences are a common reason for variation in IC<sub>50</sub> determination. A study conducted by Bentz *et al.* revealed differences in the determination of the IC<sub>50</sub> up to 800 fold<sup>259</sup>. It was postulated that this is most likely due to interlaboratory differences. Those interlaboratory differences include culture conditions, seeding density, passage number and confluency. Also the ingredients of the cell culture media seem to affect the transport protein expression<sup>260</sup>. Comparing the MALDI MS assay and the fluorescence-based assay with the Karlgren assay, there are remarkable differences in the setup. Not only that there is a different cell line used, which could have a clear difference in transporter expression, also marked by the addition of sodium butyrate for our cells, which was not done in the Karlgren assay, but there were also other differences noted. The K<sub>M</sub> value of E3S in

the Karlgren study was with 38  $\mu\text{M}$  nearly 2 fold higher than our determined value of 21  $\mu\text{M}$ . Apart from that, also the concentration of the used substrate and inhibitor differed from our approach (1  $\mu\text{M}$  substrate and 20  $\mu\text{M}$  inhibitor in Karlgren assay vs. 10  $\mu\text{M}$  for both in MALDI MS). Those differences lead to the phenomenon of interlaboratory differences that result in the nonexistence of a 100 % comparable output. A variation in the transport protein expression could have also been a likely reason for the differences as it is already known that differences in transporter expression can lead to variation in DDI<sup>261</sup>. Besides the differences, there was also a consistent phenomenon observed. The addition of some compounds led to a negative % inhibition value suggesting a stimulation. Generally, this is a known occurrence in the transporter field<sup>185</sup>. For the MALDI MS assay, there were two drugs found with a stimulation greater than 100 %, namely E3S and fenbufen. E3S was used as a substrate and therefore is likely to appear as a stimulator, whereas also fenbufen is discussed as a drug increasing the uptake of prostaglandins by OATP2A1<sup>262</sup>. Hence, this finding fits well to the published literature. Nevertheless, a stimulation of the drug set on the uptake of E3S would have to be analysed separately once more.

### 5.5 CONCLUSION

During this project, I managed to build up a fluorescence-based assay with the verification via fluorescence microscopy and western blot showing the overexpression of OATP2B1. The fluorescence-based assay helped to characterise the uptake of DBF through OATP2B1 and showed to be both concentration- and time-dependent. The screen of a 294 compound set had an acceptable correlation and identified several hits, which were further analysed in a clinical extrapolation and showed the involvement of the transporter in DDI.

The main goal of the project was the development of a cell-based MALDI MS drug uptake assay. For this purpose, an optimisation of the method has been done and led to usage of E3S as a substrate and 2.5 mg/mL Ph-CCA-NH<sub>2</sub> as matrix dissolved in 70 % ACN. The method was automated and usage of internal standard was incorporated in the protocol for further reduction of variability. The uptake of E3S also showed to be concentration- and time-dependent and the determination of the pIC<sub>50</sub> of erlotinib showed the reproducibility of the method. The screen of the compound set

was conducted and showed an acceptable intra-assay reproducibility. The reliability of the newly developed method was above all underlined by the low CV % and standard deviation of the 6 biological replicates resulting from pIC<sub>50</sub> determination. The resulting identification of hits was not totally comparable to the results of the fluorescence-based assay. This is possibly due to the existence of multiple binding sites with differing pH sensitivity that has to be investigated further. A comparison with the data previously published by Karlgren *et al.* nevertheless showed an overlap of 83 % and represents the applicability of the MALDI MS assay as a new screening technology.

## 6 SUMMARY

For the longest time, there was the widely held belief that drug uptake into a cell is mainly due to diffusion, channels and carriers. Only in the 1940s, there was the first drug-transporter interaction discovered. As more transporter-related diseases were discovered and transport proteins identified that had an important connection to cancer, like the breast cancer resistance protein, the research field gained more interest. Drug-Drug interactions were identified and an International Transporter Consortium was founded that had the task to identify relevant transport proteins and closely work together with the drug approval by the FDA. The majority of transport proteins either belong to the class of ABC transporters, which are primary active export transporters or to the class of solute carrier (SLC) transporters, which are secondary active uptake transporters. OATP2B1 is an organic anion transporting polypeptide and is part of the group of SLC transporters. It is seen as an emerging transport protein and has gained attention due to many drug-fruit juice interactions. As the simultaneous intake of fruit juices and drugs are likely to happen in everyday life and OATP2B1 is a human transporter expressed mostly in liver and intestine, it is important to understand more about its uptake mechanism and possible inhibition.

Until now, the emerging field of transporters are examined by either radioactive or fluorescence-based assays. Radioactive assays render a rather unpopular method with many obstacles like cost, safety-issues, labelling and no possibility of high-throughput. Fluorescence-based assays are widespread and have the positive property that they can be automated and used in HTS. The negative aspects here are also labelling and the false negatives and positives prediction that comes through autofluorescence and quenching effects. Our goal therefore was to develop an alternative cell based assay based on a different technology: MALDI MS. MALDI MS brings the advantage that it is a label-free technique and it also is HTS-compatible, like it was already shown in the past. Cell-based MALDI MS assays have gained recognition in the last years in consequence of their speed, robustness and ease in setup and are suitable for the investigation of transport mechanisms due to the abundance of additional information gathered by this technique.

For the MALDI MS method development, the use of E3S as a substrate provided the best results. The optimal matrix composition for the detection of E3S in the cells had to be found. 2.5 mg/mL Ph-CCA-NH<sub>2</sub> in 70 % ACN were identified as the best

composition and were further used for transport characterisation with the confirmation of time-dependence and concentration-dependence of E3S uptake. The optimal assay conditions (2 min, 10  $\mu$ M E3S) were used to screen a set of 294 compounds consisting of the top 300 marketed drugs and a set of compounds that are known to interact with OATP2B1. The used compounds were tested in their ability to inhibit the uptake of E3S into the cells. There were 76 compounds found with an inhibition of more than 50 %, which were then further analysed by  $pI_{C_{50}}$  determination. 67 of those compounds could be verified as hits, leading also to 14 very potent inhibitors with a  $pI_{C_{50}}$  over 6. With an average CV % under 10 for 6 biological replicates, the method confirms reproducibility and reliability of the data.

As a reference assay to the aspired MALDI MS assay, also a fluorescence-based assay was developed to examine the uptake of DBF through OATP2B1. This assay was also used to screen the 294 compound set and 67 compounds with an inhibition  $\geq 50$  % were identified in the course of the experiments. 57 could be verified as a hit. There was a calculation being done to examine the clinical relevance of those transporters showing a clinical relevance of more than 60 % in the intestine reinforcing the meaning of transporter studies. By the comparison of the two techniques, it was found that only 47 inhibitors overlapped leading to compounds that were not found with one of both methods. This can eventually be explained by the use of different substrates and the multiple binding sites of OATP2B1, but still has to be addressed further. The comparison of the data with the previously published Karlgren *et al.* data set showed an overlap of 83 % and therefore shows the applicability of the MALDI MS method. To conclude, there were two assay systems developed that are suitable to examine the emerging transport protein OATP2B1. The importance of this transport protein has been shown through the amount of identified (clinically relevant) inhibitors. While the developed fluorescence-based method acts as a good reference method, the newly developed MALDI MS method represents a completely new way to analyse substrate and inhibitor of transporters. With its ease and speed in handling and most notably the label-free approach, the MALDI MS method is an indispensable tool for transporter characterisation and DDI analysis.



## 7 REFERENCES

1. Simons, K, Sampaio, JL: Membrane organization and lipid rafts. *Cold Spring Harbor perspectives in biology*, 3: a004697, 2011.
2. Hegner, D, Tellhelm, B: Studies on the isolation of plasma membranes of rumen forestomach epithelium and some properties of transport ATPases. *Zentralblatt fur Veterinarmedizin Reihe A*, 21: 112-131, 1974.
3. Rejman, J, Oberle, V, Zuhorn, IS, Hoekstra, D: Size-dependent internalization of particles via the pathways of clathrin- and caveolae-mediated endocytosis. *The Biochemical journal*, 377: 159-169, 2004.
4. Pelkmans, L, Helenius, A: Endocytosis via caveolae. *Traffic (Copenhagen, Denmark)*, 3: 311-320, 2002.
5. Rassow, JH, K.; Netzker, R.; Deutzmann, R.: *Duale Reihe Biochemie*, Thieme, 2012.
6. Pauletti, GM, Okumu, FW, Borchardt, RT: Effect of size and charge on the passive diffusion of peptides across Caco-2 cell monolayers via the paracellular pathway. *Pharmaceutical research*, 14: 164-168, 1997.
7. Giacomini, KM, Huang, SM, Tweedie, DJ, Benet, LZ, Brouwer, KL, Chu, X, Dahlin, A, Evers, R, Fischer, V, Hillgren, KM, Hoffmaster, KA, Ishikawa, T, Keppler, D, Kim, RB, Lee, CA, Niemi, M, Polli, JW, Sugiyama, Y, Swaan, PW, Ware, JA, Wright, SH, Yee, SW, Zamek-Gliszczynski, MJ, Zhang, L: Membrane transporters in drug development. *Nature reviews Drug discovery*, 9: 215-236, 2010.
8. Hediger, MA, Romero, MF, Peng, JB, Rolfs, A, Takanaga, H, Bruford, EA: The ABCs of solute carriers: physiological, pathological and therapeutic implications of human membrane transport proteins Introduction. *Pflugers Archiv : European journal of physiology*, 447: 465-468, 2004.
9. Cesar-Razquin, A, Snijder, B, Frappier-Brinton, T, Isserlin, R, Gyimesi, G, Bai, X, Reithmeier, RA, Hepworth, D, Hediger, MA, Edwards, AM, Superti-Furga, G: A Call for Systematic Research on Solute Carriers. *Cell*, 162: 478-487, 2015.
10. Perland, E, Fredriksson, R: Classification Systems of Secondary Active Transporters. *Trends in pharmacological sciences*, 38: 305-315, 2017.
11. Schlessinger, A, Yee, SW, Sali, A, Giacomini, KM: SLC classification: an update. *Clinical pharmacology and therapeutics*, 94: 19-23, 2013.
12. Sugano, K, Kansy, M, Artursson, P, Avdeef, A, Bendels, S, Di, L, Ecker, GF, Faller, B, Fischer, H, Gerebtzoff, G, Lennernaes, H, Senner, F: Coexistence of passive and carrier-mediated processes in drug transport. *Nature reviews Drug discovery*, 9: 597-614, 2010.
13. Kell, DB, Dobson, PD, Oliver, SG: Pharmaceutical drug transport: the issues and the implications that it is essentially carrier-mediated only. *Drug discovery today*, 16: 704-714, 2011.
14. Mc, KS, Peck, HM, Bochey, JM, Byham, BB, Schuchardt, GS, Beyer, KH: Benemid, p-(DI-n-propylsulfamyl)-benzoic acid; toxicologic properties. *The Journal of pharmacology and experimental therapeutics*, 102: 208-214, 1951.
15. Pascale, LR, Dubin, A, Hoffman, WS: Therapeutic value of probenecid (benemid) in gout. *Journal of the American Medical Association*, 149: 1188-1194, 1952.
16. Dubin, IN, Johnson, FB: Chronic idiopathic jaundice with unidentified pigment in liver cells; a new clinicopathologic entity with a report of 12 cases. *Medicine*, 33: 155-197, 1954.
17. Paulusma, CC, Kool, M, Bosma, PJ, Scheffer, GL, ter Borg, F, Scheper, RJ, Tytgat, GN, Borst, P, Baas, F, Oude Elferink, RP: A mutation in the human canalicular multispecific

## References

---

- organic anion transporter gene causes the Dubin-Johnson syndrome. *Hepatology (Baltimore, Md)*, 25: 1539-1542, 1997.
18. Juliano, RL, Ling, V: A surface glycoprotein modulating drug permeability in Chinese hamster ovary cell mutants. *Biochimica et biophysica acta*, 455: 152-162, 1976.
  19. Chen, CJ, Chin, JE, Ueda, K, Clark, DP, Pastan, I, Gottesman, MM, Roninson, IB: Internal duplication and homology with bacterial transport proteins in the *mdr1* (P-glycoprotein) gene from multidrug-resistant human cells. *Cell*, 47: 381-389, 1986.
  20. Dano, K: Active outward transport of daunomycin in resistant Ehrlich ascites tumor cells. *Biochimica et biophysica acta*, 323: 466-483, 1973.
  21. Xu, D, Kang, H, Fisher, M, Juliano, RL: Strategies for inhibition of MDR1 gene expression. *Molecular pharmacology*, 66: 268-275, 2004.
  22. Szakacs, G, Paterson, JK, Ludwig, JA, Booth-Genthe, C, Gottesman, MM: Targeting multidrug resistance in cancer. *Nature reviews Drug discovery*, 5: 219-234, 2006.
  23. Tsuruo, T, Iida, H, Yamashiro, M, Tsukagoshi, S, Sakurai, Y: Enhancement of vincristine- and adriamycin-induced cytotoxicity by verapamil in P388 leukemia and its sublines resistant to vincristine and adriamycin. *Biochemical pharmacology*, 31: 3138-3140, 1982.
  24. Okamura, N, Hirai, M, Tanigawara, Y, Tanaka, K, Yasuhara, M, Ueda, K, Komano, T, Hori, R: Digoxin-cyclosporin A interaction: modulation of the multidrug transporter P-glycoprotein in the kidney. *The Journal of pharmacology and experimental therapeutics*, 266: 1614-1619, 1993.
  25. Doyle, LA, Yang, W, Abruzzo, LV, Krogmann, T, Gao, Y, Rishi, AK, Ross, DD: A multidrug resistance transporter from human MCF-7 breast cancer cells. *Proceedings of the National Academy of Sciences of the United States of America*, 95: 15665-15670, 1998.
  26. Natarajan, K, Xie, Y, Baer, MR, Ross, DD: Role of breast cancer resistance protein (BCRP/ABCG2) in cancer drug resistance. *Biochemical pharmacology*, 83: 1084-1103, 2012.
  27. Zamek-Gliszczynski, MJ, Lee, CA, Poirier, A, Bentz, J, Chu, X, Ellens, H, Ishikawa, T, Jamei, M, Kalvass, JC, Nagar, S, Pang, KS, Korzekwa, K, Swaan, PW, Taub, ME, Zhao, P, Galetin, A: ITC recommendations for transporter kinetic parameter estimation and translational modeling of transport-mediated PK and DDIs in humans. *Clinical pharmacology and therapeutics*, 94: 64-79, 2013.
  28. Zamek-Gliszczynski, MJ, Taub, ME, Chothe, PP, Chu, X, Giacomini, KM, Kim, RB, Ray, AS, Stocker, SL, Unadkat, JD, Wittwer, MB, Xia, C, Yee, SW, Zhang, L, Zhang, Y: Transporters in Drug Development: 2018 ITC Recommendations for Transporters of Emerging Clinical Importance. *Clinical pharmacology and therapeutics*, 104: 890-899, 2018.
  29. Lin, L, Yee, SW, Kim, RB, Giacomini, KM: SLC transporters as therapeutic targets: emerging opportunities. *Nature reviews Drug discovery*, 14: 543-560, 2015.
  30. Hebert, SC, Mount, DB, Gamba, G: Molecular physiology of cation-coupled Cl<sup>-</sup> cotransport: the SLC12 family. *Pflugers Archiv : European journal of physiology*, 447: 580-593, 2004.
  31. Pramod, AB, Foster, J, Carvelli, L, Henry, LK: SLC6 transporters: structure, function, regulation, disease association and therapeutics. *Molecular aspects of medicine*, 34: 197-219, 2013.
  32. Grewer, C, Gameiro, A, Rauen, T: SLC1 glutamate transporters. *Pflugers Archiv : European journal of physiology*, 466: 3-24, 2014.

33. Hediger, MA, Clemencon, B, Burrier, RE, Bruford, EA: The ABCs of membrane transporters in health and disease (SLC series): introduction. *Molecular aspects of medicine*, 34: 95-107, 2013.
34. Dupuis, J, Langenberg, C, Prokopenko, I, Saxena, R, Soranzo, N, Jackson, AU, Wheeler, E, Glazer, NL, Bouatia-Naji, N, Gloyn, AL, Lindgren, CM, Magi, R, Morris, AP, Randall, J, Johnson, T, Elliott, P, Rybin, D, Thorleifsson, G, Steinthorsdottir, V, Henneman, P, Grallert, H, Dehghan, A, Hottenga, JJ, Franklin, CS, Navarro, P, Song, K, Goel, A, Perry, JR, Egan, JM, Lajunen, T, Grarup, N, Sparso, T, Doney, A, Voight, BF, Stringham, HM, Li, M, Kanoni, S, Shrader, P, Cavalcanti-Proenca, C, Kumari, M, Qi, L, Timpson, NJ, Gieger, C, Zabena, C, Rocheleau, G, Ingelsson, E, An, P, O'Connell, J, Luan, J, Elliott, A, McCarroll, SA, Payne, F, Roccascaccia, RM, Pattou, F, Sethupathy, P, Ardlie, K, Ariyurek, Y, Balkau, B, Barter, P, Beilby, JP, Ben-Shlomo, Y, Benediktsson, R, Bennett, AJ, Bergmann, S, Bochud, M, Boerwinkle, E, Bonnefond, A, Bonnycastle, LL, Borch-Johnsen, K, Bottcher, Y, Brunner, E, Bumpstead, SJ, Charpentier, G, Chen, YD, Chines, P, Clarke, R, Coin, LJ, Cooper, MN, Cornelis, M, Crawford, G, Crisponi, L, Day, IN, de Geus, EJ, Delplanque, J, Dina, C, Erdos, MR, Fedson, AC, Fischer-Rosinsky, A, Forouhi, NG, Fox, CS, Frants, R, Franzosi, MG, Galan, P, Goodarzi, MO, Graessler, J, Groves, CJ, Grundy, S, Gwilliam, R, Gyllensten, U, Hadjadj, S, Hallmans, G, Hammond, N, Han, X, Hartikainen, AL, Hassanali, N, Hayward, C, Heath, SC, Hercberg, S, Herder, C, Hicks, AA, Hillman, DR, Hingorani, AD, Hofman, A, Hui, J, Hung, J, Isomaa, B, Johnson, PR, Jorgensen, T, Jula, A, Kaakinen, M, Kaprio, J, Kesaniemi, YA, Kivimaki, M, Knight, B, Koskinen, S, Kovacs, P, Kyvik, KO, Lathrop, GM, Lawlor, DA, Le Bacquer, O, Lecoeur, C, Li, Y, Lyssenko, V, Mahley, R, Mangino, M, Manning, AK, Martinez-Larrad, MT, McAteer, JB, McCulloch, LJ, McPherson, R, Meisinger, C, Melzer, D, Meyre, D, Mitchell, BD, Morken, MA, Mukherjee, S, Naitza, S, Narisu, N, Neville, MJ, Oostra, BA, Orru, M, Pakyz, R, Palmer, CN, Paolisso, G, Pattaro, C, Pearson, D, Peden, JF, Pedersen, NL, Perola, M, Pfeiffer, AF, Pichler, I, Polasek, O, Posthuma, D, Potter, SC, Pouta, A, Province, MA, Psaty, BM, Rathmann, W, Rayner, NW, Rice, K, Ripatti, S, Rivadeneira, F, Roden, M, Rolandsson, O, Sandbaek, A, Sandhu, M, Sanna, S, Sayer, AA, Scheet, P, Scott, LJ, Sedorf, U, Sharp, SJ, Shields, B, Sigurethsson, G, Sijbrands, EJ, Silveira, A, Simpson, L, Singleton, A, Smith, NL, Sovio, U, Swift, A, Syddall, H, Syvanen, AC, Tanaka, T, Thorand, B, Tichet, J, Tonjes, A, Tuomi, T, Uitterlinden, AG, van Dijk, KW, van Hoek, M, Varma, D, Visvikis-Siest, S, Vitart, V, Vogelzangs, N, Waeber, G, Wagner, PJ, Walley, A, Walters, GB, Ward, KL, Watkins, H, Weedon, MN, Wild, SH, Willemsen, G, Witteman, JC, Yarnell, JW, Zeggini, E, Zelenika, D, Zethelius, B, Zhai, G, Zhao, JH, Zillikens, MC, Borecki, IB, Loos, RJ, Meneton, P, Magnusson, PK, Nathan, DM, Williams, GH, Hattersley, AT, Silander, K, Salomaa, V, Smith, GD, Bornstein, SR, Schwarz, P, Spranger, J, Karpe, F, Shuldiner, AR, Cooper, C, Dedoussis, GV, Serrano-Rios, M, Morris, AD, Lind, L, Palmer, LJ, Hu, FB, Franks, PW, Ebrahim, S, Marmot, M, Kao, WH, Pankow, JS, Sampson, MJ, Kuusisto, J, Laakso, M, Hansen, T, Pedersen, O, Pramstaller, PP, Wichmann, HE, Illig, T, Rudan, I, Wright, AF, Stumvoll, M, Campbell, H, Wilson, JF, Bergman, RN, Buchanan, TA, Collins, FS, Mohlke, KL, Tuomilehto, J, Valle, TT, Altshuler, D, Rotter, JI, Siscovick, DS, Penninx, BW, Boomsma, DI, Deloukas, P, Spector, TD, Frayling, TM, Ferrucci, L, Kong, A, Thorsteinsdottir, U, Stefansson, K, van Duijn, CM, Aulchenko, YS, Cao, A, Scuteri, A, Schlessinger, D, Uda, M, Ruukonen, A, Jarvelin, MR, Waterworth, DM, Vollenweider, P, Peltonen, L, Mooser, V, Abecasis, GR, Wareham, NJ, Sladek, R, Froguel, P, Watanabe, RM, Meigs, JB, Groop, L, Boehnke, M, McCarthy, MI, Florez,

- JC, Barroso, I: New genetic loci implicated in fasting glucose homeostasis and their impact on type 2 diabetes risk. *Nature genetics*, 42: 105-116, 2010.
35. Xu, C, Zhu, L, Chan, T, Lu, X, Shen, W, Gillies, MC, Zhou, F: The Altered Renal and Hepatic Expression of Solute Carrier Transporters (SLCs) in Type 1 Diabetic Mice. *PLoS one*, 10, 2015.
36. Kolz, M, Johnson, T, Sanna, S, Teumer, A, Vitart, V, Perola, M, Mangino, M, Albrecht, E, Wallace, C, Farrall, M, Johansson, A, Nyholt, DR, Aulchenko, Y, Beckmann, JS, Bergmann, S, Bochud, M, Brown, M, Campbell, H, Connell, J, Dominiczak, A, Homuth, G, Lamina, C, McCarthy, MI, Meitinger, T, Mooser, V, Munroe, P, Nauck, M, Peden, J, Prokisch, H, Salo, P, Salomaa, V, Samani, NJ, Schlessinger, D, Uda, M, Volker, U, Waeber, G, Waterworth, D, Wang-Sattler, R, Wright, AF, Adamski, J, Whitfield, JB, Gyllensten, U, Wilson, JF, Rudan, I, Pramstaller, P, Watkins, H, Doering, A, Wichmann, HE, Spector, TD, Peltonen, L, Volzke, H, Nagaraja, R, Vollenweider, P, Caulfield, M, Illig, T, Gieger, C: Meta-analysis of 28,141 individuals identifies common variants within five new loci that influence uric acid concentrations. *PLoS genetics*, 5: e1000504, 2009.
37. Flynn, TJ, Phipps-Green, A, Hollis-Moffatt, JE, Merriman, ME, Topless, R, Montgomery, G, Chapman, B, Stamp, LK, Dalbeth, N, Merriman, TR: Association analysis of the SLC22A11 (organic anion transporter 4) and SLC22A12 (urate transporter 1) urate transporter locus with gout in New Zealand case-control sample sets reveals multiple ancestral-specific effects. *Arthritis research & therapy*, 15: R220, 2013.
38. Ehret, GB, Ferreira, T, Chasman, DI, Jackson, AU, Schmidt, EM, Johnson, T, Thorleifsson, G, Luan, J, Donnelly, LA, Kanoni, S, Petersen, AK, Pihur, V, Strawbridge, RJ, Shungin, D, Hughes, MF, Meirelles, O, Kaakinen, M, Bouatia-Naji, N, Kristiansson, K, Shah, S, Kleber, ME, Guo, X, Lyytikainen, LP, Fava, C, Eriksson, N, Nolte, IM, Magnusson, PK, Salfati, EL, Rallidis, LS, Theusch, E, Smith, AJP, Folkersen, L, Witkowska, K, Pers, TH, Joehanes, R, Kim, SK, Lataniotis, L, Jansen, R, Johnson, AD, Warren, H, Kim, YJ, Zhao, W, Wu, Y, Tayo, BO, Bochud, M, Absher, D, Adair, LS, Amin, N, Arking, DE, Axelsson, T, Baldassarre, D, Balkau, B, Bandinelli, S, Barnes, MR, Barroso, I, Bevan, S, Bis, JC, Bjornsdottir, G, Boehnke, M, Boerwinkle, E, Bonnycastle, LL, Boomsma, DI, Bornstein, SR, Brown, MJ, Burnier, M, Cabrera, CP, Chambers, JC, Chang, IS, Cheng, CY, Chines, PS, Chung, RH, Collins, FS, Connell, JM, Doring, A, Dallongeville, J, Danesh, J, de Faire, U, Delgado, G, Dominiczak, AF, Doney, ASF, Drenos, F, Edkins, S, Eicher, JD, Elosua, R, Enroth, S, Erdmann, J, Eriksson, P, Esko, T, Evangelou, E, Evans, A, Fall, T, Farrall, M, Felix, JF, Ferrieres, J, Ferrucci, L, Fornage, M, Forrester, T, Franceschini, N, Duran, OHF, Franco-Cereceda, A, Fraser, RM, Ganesh, SK, Gao, H, Gertow, K, Gianfagna, F, Gigante, B, Giulianini, F, Goel, A, Goodall, AH, Goodarzi, MO, Gorski, M, Grassler, J, Groves, C, Gudnason, V, Gyllensten, U, Hallmans, G, Hartikainen, AL, Hassinen, M, Havulinna, AS, Hayward, C, Herberg, S, Herzig, KH, Hicks, AA, Hingorani, AD, Hirschhorn, JN, Hofman, A, Holmen, J, Holmen, OL, Hottenga, JJ, Howard, P, Hsiung, CA, Hunt, SC, Ikram, MA, Illig, T, Iribarren, C, Jensen, RA, Kahonen, M, Kang, H, Kathiresan, S, Keating, BJ, Khaw, KT, Kim, YK, Kim, E, Kivimaki, M, Klopp, N, Kolovou, G, Komulainen, P, Kooner, JS, Kosova, G, Krauss, RM, Kuh, D, Kutalik, Z, Kuusisto, J, Kvaloy, K, Lakka, TA, Lee, NR, Lee, IT, Lee, WJ, Levy, D, Li, X, Liang, KW, Lin, H, Lin, L, Lindstrom, J, Lobbens, S, Mannisto, S, Muller, G, Muller-Nurasyid, M, Mach, F, Markus, HS, Marouli, E, McCarthy, MI, McKenzie, CA, Meneton, P, Menni, C, Metspalu, A, Mijatovic, V, Moilanen, L, Montasser, ME, Morris, AD, Morrison, AC, Mulas, A, Nagaraja, R, Narisu, N, Nikus, K, O'Donnell, CJ, O'Reilly, PF, Ong, KK, Paccaud, F, Palmer, CD, Parsa, A, Pedersen, NL, Penninx, BW, Perola, M, Peters, A,

- Poulter, N, Pramstaller, PP, Psaty, BM, Quertermous, T, Rao, DC, Rasheed, A, Rayner, N, Renstrom, F, Rettig, R, Rice, KM, Roberts, R, Rose, LM, Rossouw, J, Samani, NJ, Sanna, S, Saramies, J, Schunkert, H, Sebert, S, Sheu, WH, Shin, YA, Sim, X, Smit, JH, Smith, AV, Sosa, MX, Spector, TD, Stancakova, A, Stanton, A, Stirrups, KE, Stringham, HM, Sundstrom, J, Swift, AJ, Syvanen, AC, Tai, ES, Tanaka, T, Tarasov, KV, Teumer, A, Thorsteinsdottir, U, Tobin, MD, Tremoli, E, Uitterlinden, AG, Uusitupa, M, Vaez, A, Vaidya, D, van Duijn, CM, van Iperen, EPA, Vasani, RS, Verwoert, GC, Virtamo, J, Vitart, V, Voight, BF, Vollenweider, P, Wagner, A, Wain, LV, Wareham, NJ, Watkins, H, Weder, AB, Westra, HJ, Wilks, R, Wilsgaard, T, Wilson, JF, Wong, TY, Yang, TP, Yao, J, Yengo, L, Zhang, W, Zhao, JH, Zhu, X, Bovet, P, Cooper, RS, Mohlke, KL, Saleheen, D, Lee, JY, Elliott, P, Gierman, HJ, Willer, CJ, Franke, L, Hovingh, GK, Taylor, KD, Dedoussis, G, Sever, P, Wong, A, Lind, L, Assimes, TL, Njolstad, I, Schwarz, PE, Langenberg, C, Snieder, H, Caulfield, MJ, Melander, O, Laakso, M, Saltevo, J, Rauramaa, R, Tuomilehto, J, Ingelsson, E, Lehtimaki, T, Hveem, K, Palmas, W, Marz, W, Kumari, M, Salomaa, V, Chen, YI, Rotter, JI, Froguel, P, Jarvelin, MR, Lakatta, EG, Kuulasmaa, K, Franks, PW, Hamsten, A, Wichmann, HE, Palmer, CNA, Stefansson, K, Ridker, PM, Loos, RJF, Chakravarti, A, Deloukas, P, Morris, AP, Newton-Cheh, C, Munroe, PB: The genetics of blood pressure regulation and its target organs from association studies in 342,415 individuals. *Nature genetics*, 48: 1171-1184, 2016.
39. Warren, HR, Evangelou, E, Cabrera, CP, Gao, H, Ren, M, Mifsud, B, Ntalla, I, Surendran, P, Liu, C, Cook, JP, Kraja, AT, Drenos, F, Loh, M, Verweij, N, Marten, J, Karaman, I, Lepe, MP, O'Reilly, PF, Knight, J, Snieder, H, Kato, N, He, J, Tai, ES, Said, MA, Porteous, D, Alver, M, Poulter, N, Farrall, M, Gansevoort, RT, Padmanabhan, S, Magi, R, Stanton, A, Connell, J, Bakker, SJ, Metspalu, A, Shields, DC, Thom, S, Brown, M, Sever, P, Esko, T, Hayward, C, van der Harst, P, Saleheen, D, Chowdhury, R, Chambers, JC, Chasman, DI, Chakravarti, A, Newton-Cheh, C, Lindgren, CM, Levy, D, Kooner, JS, Keavney, B, Tomaszewski, M, Samani, NJ, Howson, JM, Tobin, MD, Munroe, PB, Ehret, GB, Wain, LV: Genome-wide association analysis identifies novel blood pressure loci and offers biological insights into cardiovascular risk. *Nature genetics*, 49: 403-415, 2017.
40. Nyquist, MD, Prasad, B, Mostaghel, EA: Harnessing Solute Carrier Transporters for Precision Oncology. *Molecules (Basel, Switzerland)*, 22, 2017.
41. El-Gebali, S, Bentz, S, Hediger, MA, Anderle, P: Solute carriers (SLCs) in cancer. *Molecular aspects of medicine*, 34: 719-734, 2013.
42. Nakanishi, T, Tamai, I: Solute carrier transporters as targets for drug delivery and pharmacological intervention for chemotherapy. *Journal of pharmaceutical sciences*, 100: 3731-3750, 2011.
43. Matsumoto, J, Ariyoshi, N, Sakakibara, M, Nakanishi, T, Okubo, Y, Shiina, N, Fujisaki, K, Nagashima, T, Nakatani, Y, Tamai, I, Yamada, H, Takeda, H, Ishii, I: Organic anion transporting polypeptide 2B1 expression correlates with uptake of estrone-3-sulfate and cell proliferation in estrogen receptor-positive breast cancer cells. *Drug metabolism and pharmacokinetics*, 30: 133-141, 2015.
44. Huang, Y, Sadee, W: Membrane transporters and channels in chemoresistance and -sensitivity of tumor cells. *Cancer letters*, 239: 168-182, 2006.
45. Windt, T, Toth, S, Patik, I, Sessler, J, Kucsma, N, Szepesi, A, Zdrzil, B, Ozvegy-Laczka, C, Szakacs, G: Identification of anticancer OATP2B1 substrates by an in vitro triple-fluorescence-based cytotoxicity screen. *Archives of toxicology*, 93: 953-964, 2019.
46. Rask-Andersen, M, Almen, MS, Schioth, HB: Trends in the exploitation of novel drug targets. *Nature reviews Drug discovery*, 10: 579-590, 2011.

## References

---

47. Rask-Andersen, M, Masuram, S, Fredriksson, R, Schioth, HB: Solute carriers as drug targets: current use, clinical trials and prospective. *Molecular aspects of medicine*, 34: 702-710, 2013.
48. Liang, Y, Li, S, Chen, L: The physiological role of drug transporters. *Protein & cell*, 6: 334-350, 2015.
49. Backman, JT, Kivisto, KT, Olkkola, KT, Neuvonen, PJ: The area under the plasma concentration-time curve for oral midazolam is 400-fold larger during treatment with itraconazole than with rifampicin. *European journal of clinical pharmacology*, 54: 53-58, 1998.
50. Dawson, S, Stahl, S, Paul, N, Barber, J, Kenna, JG: In vitro inhibition of the bile salt export pump correlates with risk of cholestatic drug-induced liver injury in humans. *Drug metabolism and disposition: the biological fate of chemicals*, 40: 130-138, 2012.
51. Monahan, BP, Ferguson, CL, Killeavy, ES, Lloyd, BK, Troy, J, Cantilena, LR, Jr.: Torsades de pointes occurring in association with terfenadine use. *Jama*, 264: 2788-2790, 1990.
52. Dresser, GK, Bailey, DG, Leake, BF, Schwarz, UI, Dawson, PA, Freeman, DJ, Kim, RB: Fruit juices inhibit organic anion transporting polypeptide-mediated drug uptake to decrease the oral availability of fexofenadine. *Clinical pharmacology and therapeutics*, 71: 11-20, 2002.
53. Akamine, Y, Miura, M, Sunagawa, S, Kagaya, H, Yasui-Furukori, N, Uno, T: Influence of drug-transporter polymorphisms on the pharmacokinetics of fexofenadine enantiomers. *Xenobiotica; the fate of foreign compounds in biological systems*, 40: 782-789, 2010.
54. Huang, SM, Strong, JM, Zhang, L, Reynolds, KS, Nallani, S, Temple, R, Abraham, S, Habet, SA, Baweja, RK, Burckart, GJ, Chung, S, Colangelo, P, Frucht, D, Green, MD, Hepp, P, Karnaukhova, E, Ko, HS, Lee, JI, Marroum, PJ, Norden, JM, Qiu, W, Rahman, A, Sobel, S, Stifano, T, Thummel, K, Wei, XX, Yasuda, S, Zheng, JH, Zhao, H, Lesko, LJ: New era in drug interaction evaluation: US Food and Drug Administration update on CYP enzymes, transporters, and the guidance process. *Journal of clinical pharmacology*, 48: 662-670, 2008.
55. Tornio, A, Filppula, AM, Niemi, M, Backman, JT: Clinical Studies on Drug-Drug Interactions Involving Metabolism and Transport: Methodology, Pitfalls, and Interpretation. *Clinical pharmacology and therapeutics*, 105: 1345-1361, 2019.
56. Rekić, D, Reynolds, KS, Zhao, P, Zhang, L, Yoshida, K, Sachar, M, Piquette Miller, M, Huang, SM, Zineh, I: Clinical Drug-Drug Interaction Evaluations to Inform Drug Use and Enable Drug Access. *Journal of pharmaceutical sciences*, 106: 2214-2218, 2017.
57. Huang, SM, Lesko, LJ: Drug-drug, drug-dietary supplement, and drug-citrus fruit and other food interactions: what have we learned? *Journal of clinical pharmacology*, 44: 559-569, 2004.
58. Scannell, JW, Bosley, J: When Quality Beats Quantity: Decision Theory, Drug Discovery, and the Reproducibility Crisis. *PLoS one*, 11: e0147215, 2016.
59. Morgan, P, Van Der Graaf, PH, Arrowsmith, J, Feltner, DE, Drummond, KS, Wegner, CD, Street, SD: Can the flow of medicines be improved? Fundamental pharmacokinetic and pharmacological principles toward improving Phase II survival. *Drug discovery today*, 17: 419-424, 2012.
60. Cumming, JG, Davis, AM, Muresan, S, Haerberlein, M, Chen, H: Chemical predictive modelling to improve compound quality. *Nature reviews Drug discovery*, 12: 948-962, 2013.
61. Alluri, RV, Li, R, Varma, MVS: Transporter-enzyme interplay and the hepatic drug clearance: what have we learned so far? *Expert opinion on drug metabolism & toxicology*: 1-15, 2020.

## References

---

62. Hagenbuch, B, Gui, C: Xenobiotic transporters of the human organic anion transporting polypeptides (OATP) family. *Xenobiotica; the fate of foreign compounds in biological systems*, 38: 778-801, 2008.
63. Nishimura, M, Naito, S: Tissue-specific mRNA expression profiles of human ATP-binding cassette and solute carrier transporter superfamilies. *Drug metabolism and pharmacokinetics*, 20: 452-477, 2005.
64. Jetter, A, Kullak-Ublick, GA: Drugs and hepatic transporters: A review. *Pharmacological research*, 154: 104234, 2020.
65. Bronger, H, Konig, J, Kopplow, K, Steiner, HH, Ahmadi, R, Herold-Mende, C, Keppler, D, Nies, AT: ABCC drug efflux pumps and organic anion uptake transporters in human gliomas and the blood-tumor barrier. *Cancer research*, 65: 11419-11428, 2005.
66. Gao, B, Huber, RD, Wenzel, A, Vavricka, SR, Ismail, MG, Reme, C, Meier, PJ: Localization of organic anion transporting polypeptides in the rat and human ciliary body epithelium. *Experimental eye research*, 80: 61-72, 2005.
67. Kraft, ME, Glaeser, H, Mandery, K, Konig, J, Auge, D, Fromm, MF, Schlotzer-Schrehardt, U, Welge-Lussen, U, Kruse, FE, Zolk, O: The prostaglandin transporter OATP2A1 is expressed in human ocular tissues and transports the antiglaucoma prostanoid latanoprost. *Investigative ophthalmology & visual science*, 51: 2504-2511, 2010.
68. Kobayashi, D, Nozawa, T, Imai, K, Nezu, J, Tsuji, A, Tamai, I: Involvement of human organic anion transporting polypeptide OATP-B (SLC21A9) in pH-dependent transport across intestinal apical membrane. *The Journal of pharmacology and experimental therapeutics*, 306: 703-708, 2003.
69. Knauer, MJ, Urquhart, BL, Meyer zu Schwabedissen, HE, Schwarz, UI, Lemke, CJ, Leake, BF, Kim, RB, Tirona, RG: Human skeletal muscle drug transporters determine local exposure and toxicity of statins. *Circulation research*, 106: 297-306, 2010.
70. St-Pierre, MV, Hagenbuch, B, Ugele, B, Meier, PJ, Stallmach, T: Characterization of an organic anion-transporting polypeptide (OATP-B) in human placenta. *The Journal of clinical endocrinology and metabolism*, 87: 1856-1863, 2002.
71. McFeely, SJ, Wu, L, Ritchie, TK, Unadkat, J: Organic anion transporting polypeptide 2B1 - More than a glass-full of drug interactions. *Pharmacology & therapeutics*, 196: 204-215, 2019.
72. Shitara, Y, Maeda, K, Ikejiri, K, Yoshida, K, Horie, T, Sugiyama, Y: Clinical significance of organic anion transporting polypeptides (OATPs) in drug disposition: their roles in hepatic clearance and intestinal absorption. *Biopharmaceutics & drug disposition*, 34: 45-78, 2013.
73. Tamai, I, Nezu, J, Uchino, H, Sai, Y, Oku, A, Shimane, M, Tsuji, A: Molecular identification and characterization of novel members of the human organic anion transporter (OATP) family. *Biochemical and biophysical research communications*, 273: 251-260, 2000.
74. Hagenbuch, B, Stieger, B: The SLCO (former SLC21) superfamily of transporters. *Molecular aspects of medicine*, 34: 396-412, 2013.
75. Yu, J, Zhou, Z, Tay-Sontheimer, J, Levy, RH, Ragueneau-Majlessi, I: Intestinal Drug Interactions Mediated by OATPs: A Systematic Review of Preclinical and Clinical Findings. *Journal of pharmaceutical sciences*, 106: 2312-2325, 2017.
76. Johnson, M, Patel, D, Matheny, C, Ho, M, Chen, L, Ellens, H: Inhibition of Intestinal OATP2B1 by the Calcium Receptor Antagonist Ronacaleret Results in a Significant Drug-Drug Interaction by Causing a 2-Fold Decrease in Exposure of Rosuvastatin. *Drug metabolism and disposition: the biological fate of chemicals*, 45: 27-34, 2017.

## References

---

77. Al Sarakbi, W, Mokbel, R, Salhab, M, Jiang, WG, Reed, MJ, Mokbel, K: The role of STS and OATP-B mRNA expression in predicting the clinical outcome in human breast cancer. *Anticancer research*, 26: 4985-4990, 2006.
78. Laczko-Rigo, R, Jojart, R, Mernyak, E, Bakos, E, Tuerkova, A, Zdrzil, B, Ozvegy-Laczka, C: Structural dissection of 13-epiestrones based on the interaction with human Organic anion-transporting polypeptide, OATP2B1. *The Journal of steroid biochemistry and molecular biology*, 200: 105652, 2020.
79. Shirasaka, Y, Mori, T, Shichiri, M, Nakanishi, T, Tamai, I: Functional pleiotropy of organic anion transporting polypeptide OATP2B1 due to multiple binding sites. *Drug metabolism and pharmacokinetics*, 27: 360-364, 2012.
80. Gaus, HJ, Gupta, R, Chappell, AE, Østergaard, ME, Swayze, EE, Seth, PP: Characterization of the interactions of chemically-modified therapeutic nucleic acids with plasma proteins using a fluorescence polarization assay. *Nucleic acids research*, 47: 1110-1122, 2019.
81. Filburn, BH, Shull, VH, Tempera, YM, Dick, JD: Evaluation of an automated fluorescence polarization immunoassay for vancomycin. *Antimicrobial agents and chemotherapy*, 24: 216-220, 1983.
82. Shin, SB, Woo, SU, Lee, YJ, Yim, H: Comparative Analysis of a FRET-based PLK1 Kinase Assay to Identify PLK1 inhibitors for Chemotherapy. *Anticancer research*, 37: 1177-1183, 2017.
83. Ergin, E, Dogan, A, Parmaksiz, M, Elçin, AE, Elçin, YM: Time-Resolved Fluorescence Resonance Energy Transfer [TR-FRET] Assays for Biochemical Processes. *Current pharmaceutical biotechnology*, 17: 1222-1230, 2016.
84. Xu, Z, Nagashima, K, Sun, D, Rush, T, Northrup, A, Andersen, JN, Kariv, I, Bobkova, EV: Development of high-throughput TR-FRET and AlphaScreen assays for identification of potent inhibitors of PDK1. *Journal of biomolecular screening*, 14: 1257-1262, 2009.
85. Truong, K, Ikura, M: The use of FRET imaging microscopy to detect protein-protein interactions and protein conformational changes in vivo. *Current opinion in structural biology*, 11: 573-578, 2001.
86. Liu, J, Saw, CL, Olivo, M, Sudhaharan, T, Ahmed, S, Heng, PW, Wohland, T: Study of interaction of hypericin and its pharmaceutical preparation by fluorescence techniques. *Journal of biomedical optics*, 14: 014003, 2009.
87. Blacker, TS, Mann, ZF, Gale, JE, Ziegler, M, Bain, AJ, Szabadkai, G, Duchon, MR: Separating NADH and NADPH fluorescence in live cells and tissues using FLIM. *Nature communications*, 5: 3936, 2014.
88. Pflieger, KD, Eidne, KA: Illuminating insights into protein-protein interactions using bioluminescence resonance energy transfer (BRET). *Nature methods*, 3: 165-174, 2006.
89. Xu, Y, Piston, DW, Johnson, CH: A bioluminescence resonance energy transfer (BRET) system: application to interacting circadian clock proteins. *Proceedings of the National Academy of Sciences of the United States of America*, 96: 151-156, 1999.
90. Nguyen, VT, Morange, M, Bensaude, O: Firefly luciferase luminescence assays using scintillation counters for quantitation in transfected mammalian cells. *Analytical biochemistry*, 171: 404-408, 1988.
91. Jones, LR, Goun, EA, Shinde, R, Rothbard, JB, Contag, CH, Wender, PA: Releasable luciferin-transporter conjugates: tools for the real-time analysis of cellular uptake and release. *Journal of the American Chemical Society*, 128: 6526-6527, 2006.
92. Almqvist, H, Axelsson, H, Jafari, R, Dan, C, Mateus, A, Haraldsson, M, Larsson, A, Martinez Molina, D, Artursson, P, Lundbäck, T, Nordlund, P: CETSA screening



## References

---

- identifies known and novel thymidylate synthase inhibitors and slow intracellular activation of 5-fluorouracil. *Nature communications*, 7: 11040, 2016.
93. Shapiro, AB, Walkup, GK, Keating, TA: Correction for interference by test samples in high-throughput assays. *Journal of biomolecular screening*, 14: 1008-1016, 2009.
94. Shan, G, Huang, W, Gee, SJ, Buchholz, BA, Vogel, JS, Hammock, BD: Isotope-labeled immunoassays without radiation waste. *Proceedings of the National Academy of Sciences of the United States of America*, 97: 2445-2449, 2000.
95. Fardel, O, Le Vee, M, Jouan, E, Denizot, C, Parmentier, Y: Nature and uses of fluorescent dyes for drug transporter studies. *Expert opinion on drug metabolism & toxicology*, 11: 1233-1251, 2015.
96. Tegos, GP, Evangelisti, AM, Strouse, JJ, Ursu, O, Bologa, C, Sklar, LA: A high throughput flow cytometric assay platform targeting transporter inhibition. *Drug discovery today Technologies*, 12: e95-103, 2014.
97. Villena Gonzales, W, Mobashsher, AT, Abbosh, A: The Progress of Glucose Monitoring- A Review of Invasive to Minimally and Non-Invasive Techniques, Devices and Sensors. *Sensors (Basel, Switzerland)*, 19, 2019.
98. Thorne, N, Auld, DS, Inglese, J: Apparent activity in high-throughput screening: origins of compound-dependent assay interference. *Current opinion in chemical biology*, 14: 315-324, 2010.
99. Enjalbal, C, Maux, D, Combarieu, R, Martinez, J, Aubagnac, JL: Imaging combinatorial libraries by mass spectrometry: from peptide to organic-supported syntheses. *Journal of combinatorial chemistry*, 5: 102-109, 2003.
100. Jones, JJ, Stump, MJ, Fleming, RC, Lay, JO, Jr., Wilkins, CL: Investigation of MALDI-TOF and FT-MS techniques for analysis of Escherichia coli whole cells. *Analytical chemistry*, 75: 1340-1347, 2003.
101. Cooper, HJ, Marshall, AG: Electrospray ionization Fourier transform mass spectrometric analysis of wine. *Journal of agricultural and food chemistry*, 49: 5710-5718, 2001.
102. Glish, GL, Vachet, RW: The basics of mass spectrometry in the twenty-first century. *Nature reviews Drug discovery*, 2: 140-150, 2003.
103. Makarov, A: Electrostatic axially harmonic orbital trapping: a high-performance technique of mass analysis. *Analytical chemistry*, 72: 1156-1162, 2000.
104. Turteltaub, KW, Vogel, JS: Bioanalytical applications of accelerator mass spectrometry for pharmaceutical research. *Current pharmaceutical design*, 6: 991-1007, 2000.
105. Solon, EG, Schweitzer, A, Stoeckli, M, Prideaux, B: Autoradiography, MALDI-MS, and SIMS-MS imaging in pharmaceutical discovery and development. *The AAPS journal*, 12: 11-26, 2010.
106. Newman, CF, Havelund, R, Passarelli, MK, Marshall, PS, Francis, I, West, A, Alexander, MR, Gilmore, IS, Dollery, CT: Intracellular Drug Uptake-A Comparison of Single Cell Measurements Using ToF-SIMS Imaging and Quantification from Cell Populations with LC/MS/MS. *Analytical chemistry*, 89: 11944-11953, 2017.
107. Yokota, H: Applications of proteomics in pharmaceutical research and development. *Biochimica et biophysica acta Proteins and proteomics*, 1867: 17-21, 2019.
108. Wikoff, WR, Nagle, MA, Kouznetsova, VL, Tsigelny, IF, Nigam, SK: Untargeted metabolomics identifies enterobiome metabolites and putative uremic toxins as substrates of organic anion transporter 1 (Oat1). *Journal of proteome research*, 10: 2842-2851, 2011.
109. Gordon, LJ, Allen, M, Artursson, P, Hann, MM, Leavens, BJ, Mateus, A, Readshaw, S, Valko, K, Wayne, GJ, West, A: Direct Measurement of Intracellular Compound Concentration by RapidFire Mass Spectrometry Offers Insights into Cell Permeability. *Journal of biomolecular screening*, 21: 156-164, 2016.

## References

---

110. Schulz, S, Becker, M, Groseclose, MR, Schadt, S, Hopf, C: Advanced MALDI mass spectrometry imaging in pharmaceutical research and drug development. *Current opinion in biotechnology*, 55: 51-59, 2019.
111. Rao, T, Shao, Y, Hamada, N, Li, Y, Ye, H, Kang, D, Shen, B, Li, X, Yin, X, Zhu, Z, Li, H, Xie, L, Wang, G, Liang, Y: Pharmacokinetic study based on a matrix-assisted laser desorption/ionization quadrupole ion trap time-of-flight imaging mass microscope combined with a novel relative exposure approach: A case of octreotide in mouse target tissues. *Analytica chimica acta*, 952: 71-80, 2017.
112. Sun, N, Fernandez, IE, Wei, M, Wu, Y, Aichler, M, Eickelberg, O, Walch, A: Pharmacokinetic and pharmacometabolomic study of pirfenidone in normal mouse tissues using high mass resolution MALDI-FTICR-mass spectrometry imaging. *Histochemistry and cell biology*, 145: 201-211, 2016.
113. Dong, H, Shen, W, Cheung, MT, Liang, Y, Cheung, HY, Allmaier, G, Kin-Chung Au, O, Lam, YW: Rapid detection of apoptosis in mammalian cells by using intact cell MALDI mass spectrometry. *The Analyst*, 136: 5181-5189, 2011.
114. Kober, SL, Meyer-Alert, H, Grienitz, D, Hollert, H, Frohme, M: Intact cell mass spectrometry as a rapid and specific tool for the differentiation of toxic effects in cell-based ecotoxicological test systems. *Analytical and bioanalytical chemistry*, 407: 7721-7731, 2015.
115. Griffiths, IW: J. J. Thomson - the centenary of his discovery of the electron and of his invention of mass spectrometry. *Rapid communications in mass spectrometry : RCM*, 11: 2-16, 1997.
116. Griffiths, J: A brief history of mass spectrometry. *Analytical chemistry*, 80: 5678-5683, 2008.
117. Wolff, MM, Stephens, WE: A pulsed mass spectrometer with time dispersion. *Review of Scientific Instruments*, 24, 1953.
118. Guilhaus, M, Mlynski, V, Selby, D: Perfect timing: Time-of-flight mass spectrometry. *Rapid communications in mass spectrometry : RCM*, 11: 951-962, 1998.
119. Karas, H, Bachmann, D, Hillenkamp, F: Influence of the wavelength in high-irradiance ultraviolet laser desorption mass spectrometry of organic molecules. *Analytical chemistry*, 57: 2935-2939, 1985.
120. Karas, M, Hillenkamp, F: Laser desorption ionization of proteins with molecular masses exceeding 10,000 daltons. *Analytical chemistry*, 60: 2299-2301, 1988.
121. Karas, M, Bachmann, D, Bahr, U, F., H: Matrix-assisted ultraviolet laser desorption of non-volatile compounds. *International Journal of Mass Spectrometry and Ion Processes*, 78: 53-68, 1987.
122. Vestal, ML: Modern MALDI time-of-flight mass spectrometry. *Journal of mass spectrometry : JMS*, 44: 303-317, 2009.
123. Jaskolla, TW, Karas, M: Compelling evidence for Lucky Survivor and gas phase protonation: the unified MALDI analyte protonation mechanism. *Journal of the American Society for Mass Spectrometry*, 22: 976-988, 2011.
124. Karas, M, Glückmann, M, Schäfer, J: Ionization in matrix-assisted laser desorption/ionization: singly charged molecular ions are the lucky survivors. *Journal of Mass Spectrometry*, 35: 1-12, 2000.
125. Montaudo, MS: Mass spectra of copolymers. *Mass spectrometry reviews*, 21: 108-144, 2002.
126. Coates, ML, Wilkins, CL: Laser desorption Fourier transform mass spectra of malto-oligosaccharides. *Biomedical mass spectrometry*, 12: 424-428, 1985.
127. Cotter, RJ: TOF Mass Spectrometry: Instrumentation and applications in biological research. *American Chemical Society*, 1997.

## References

---

128. Marshall, AG, Hendrickson, CL, Jackson, GS: Fourier transform ion cyclotron resonance mass spectrometry: a primer. *Mass spectrometry reviews*, 17: 1-35, 1998.
129. Comisarow, MB, Marshall, AG: The early development of Fourier transform ion cyclotron resonance (FT-ICR) spectroscopy. *Journal of mass spectrometry : JMS*, 31: 581-585, 1996.
130. Michelini, E, Cevenini, L, Mezzanotte, L, Coppa, A, Roda, A: Cell-based assays: fuelling drug discovery. *Analytical and bioanalytical chemistry*, 398: 227-238, 2010.
131. Munteanu, B, Hopf, C: Emergence of whole-cell MALDI-MS biotyping for high-throughput bioanalysis of mammalian cells? *Bioanalysis*, 5: 885-893, 2013.
132. Anhalt, J, Fenselau, C: Identification of bacteria using mass spectrometry. *Analytical chemistry*, 47: 219-225, 1975.
133. Demirev, PA, Fenselau, C: Mass spectrometry for rapid characterization of microorganisms. *Annual review of analytical chemistry (Palo Alto, Calif)*, 1: 71-93, 2008.
134. Cain, TC, Lubman, DM, Weber, WJ, Vertes, A: Differentiation of bacteria using protein profiles from matrix-assisted laser desorption/ionization time-of-flight mass spectrometry. *Rapid communications in mass spectrometry : RCM*, 8: 1026-1030, 1994.
135. Seng, P, Rolain, JM, Fournier, PE, La Scola, B, Drancourt, M, Raoult, D: MALDI-TOF-mass spectrometry applications in clinical microbiology. *Future microbiology*, 5: 1733-1754, 2010.
136. Fenselau, C, Demirev, PA: Characterization of intact microorganisms by MALDI mass spectrometry. *Mass spectrometry reviews*, 20: 157-171, 2001.
137. Angeletti, S, Ciccozzi, M: Matrix-assisted laser desorption ionization time-of-flight mass spectrometry in clinical microbiology: An updating review. *Infection, genetics and evolution : journal of molecular epidemiology and evolutionary genetics in infectious diseases*, 76: 104063, 2019.
138. Zhang, X, Scalf, M, Berggren, TW, Westphall, MS, Smith, LM: Identification of mammalian cell lines using MALDI-TOF and LC-ESI-MS/MS mass spectrometry. *Journal of the American Society for Mass Spectrometry*, 17: 490-499, 2006.
139. Munteanu, B, von Reitzenstein, C, Hansch, GM, Meyer, B, Hopf, C: Sensitive, robust and automated protein analysis of cell differentiation and of primary human blood cells by intact cell MALDI mass spectrometry biotyping. *Analytical and bioanalytical chemistry*, 404: 2277-2286, 2012.
140. Hanrieder, J, Wicher, G, Bergquist, J, Andersson, M, Fex-Svenningsen, A: MALDI mass spectrometry based molecular phenotyping of CNS glial cells for prediction in mammalian brain tissue. *Analytical and bioanalytical chemistry*, 401: 135-147, 2011.
141. Ouedraogo, R, Flaudrops, C, Ben Amara, A, Capo, C, Raoult, D, Mege, JL: Global analysis of circulating immune cells by matrix-assisted laser desorption ionization time-of-flight mass spectrometry. *PloS one*, 5: e13691, 2010.
142. Petukhova, VZ, Young, AN, Wang, J, Wang, M, Ladanyi, A, Kothari, R, Burdette, JE, Sanchez, LM: Whole Cell MALDI Fingerprinting Is a Robust Tool for Differential Profiling of Two-Component Mammalian Cell Mixtures. *Journal of the American Society for Mass Spectrometry*, 30: 344-354, 2019.
143. Munteanu, B, Meyer, B, von Reitzenstein, C, Burgermeister, E, Bog, S, Pahl, A, Ebert, MP, Hopf, C: Label-free in situ monitoring of histone deacetylase drug target engagement by matrix-assisted laser desorption ionization-mass spectrometry biotyping and imaging. *Analytical chemistry*, 86: 4642-4647, 2014.

## References

---

144. Weigt, D, Sammour, DA, Ulrich, T, Munteanu, B, Hopf, C: Automated analysis of lipid drug-response markers by combined fast and high-resolution whole cell MALDI mass spectrometry biotyping. *Scientific reports*, 8: 11260, 2018.
145. Weigt, D, Parrish, CA, Krueger, JA, Oleykowski, CA, Rendina, AR, Hopf, C: Mechanistic MALDI-TOF Cell-Based Assay for the Discovery of Potent and Specific Fatty Acid Synthase Inhibitors. *Cell chemical biology*, 26: 1322-1331.e1324, 2019.
146. Gurard-Levin, ZA, Scholle, MD, Eisenberg, AH, Mrksich, M: High-throughput screening of small molecule libraries using SAMDI mass spectrometry. *ACS combinatorial science*, 13: 347-350, 2011.
147. Wigle, TJ, Swinger, KK, Campbell, JE, Scholle, MD, Sherrill, J, Admirand, EA, Boriack-Sjodin, PA, Kuntz, KW, Chesworth, R, Moyer, MP, Scott, MP, Copeland, RA: A High-Throughput Mass Spectrometry Assay Coupled with Redox Activity Testing Reduces Artifacts and False Positives in Lysine Demethylase Screening. *Journal of biomolecular screening*, 20: 810-820, 2015.
148. Ritorto, MS, Ewan, R, Perez-Oliva, AB, Knebel, A, Buhrlage, SJ, Wightman, M, Kelly, SM, Wood, NT, Virdee, S, Gray, NS, Morrice, NA, Alessi, DR, Trost, M: Screening of DUB activity and specificity by MALDI-TOF mass spectrometry. *Nature communications*, 5: 4763, 2014.
149. Heap, RE, Hope, AG, Pearson, LA, Reyskens, K, McElroy, SP, Hastie, CJ, Porter, DW, Arthur, JSC, Gray, DW, Trost, M: Identifying Inhibitors of Inflammation: A Novel High-Throughput MALDI-TOF Screening Assay for Salt-Inducible Kinases (SIKs). *SLAS discovery : advancing life sciences R & D*, 22: 1193-1202, 2017.
150. Beeman, K, Baumgartner, J, Laubenheimer, M, Hergesell, K, Hoffmann, M, Pehl, U, Fischer, F, Pieck, JC: Integration of an In Situ MALDI-Based High-Throughput Screening Process: A Case Study with Receptor Tyrosine Kinase c-MET. *SLAS discovery : advancing life sciences R & D*, 22: 1203-1210, 2017.
151. De Cesare, V, Johnson, C, Barlow, V, Hastie, J, Knebel, A, Trost, M: The MALDI-TOF E2/E3 Ligase Assay as Universal Tool for Drug Discovery in the Ubiquitin Pathway. *Cell chemical biology*, 25: 1117-1127.e1114, 2018.
152. Simon, RP, Winter, M, Kleiner, C, Ries, R, Schnapp, G, Heimann, A, Li, J, Zuvela-Jelaska, L, Bretschneider, T, Luippold, AH, Reindl, W, Bischoff, D, Buttner, FH: MALDI-TOF Mass Spectrometry-Based High-Throughput Screening for Inhibitors of the Cytosolic DNA Sensor cGAS. *SLAS discovery : advancing life sciences R & D*: 2472555219880185, 2019.
153. Haslam, C, Hellicar, J, Dunn, A, Fuetterer, A, Hardy, N, Marshall, P, Paape, R, Pemberton, M, Resemannand, A, Leveridge, M: The Evolution of MALDI-TOF Mass Spectrometry toward Ultra-High-Throughput Screening: 1536-Well Format and Beyond. *Journal of biomolecular screening*, 21: 176-186, 2016.
154. Burlina, F, Sagan, S, Bolbach, G, Chassaing, G: Quantification of the cellular uptake of cell-penetrating peptides by MALDI-TOF mass spectrometry. *Angewandte Chemie (International ed in English)*, 44: 4244-4247, 2005.
155. Aussedat, B, Sagan, S, Chassaing, G, Bolbach, G, Burlina, F: Quantification of the efficiency of cargo delivery by peptidic and pseudo-peptidic Trojan carriers using MALDI-TOF mass spectrometry. *Biochimica et biophysica acta*, 1758: 375-383, 2006.
156. Cheng, Z, Winant, RC, Gambhir, SS: A new strategy to screen molecular imaging probe uptake in cell culture without radiolabeling using matrix-assisted laser desorption/ionization time-of-flight mass spectrometry. *Journal of nuclear medicine : official publication, Society of Nuclear Medicine*, 46: 878-886, 2005.

## References

---

157. Arranz-Gibert, P, Guixer, B, Prades, R, Ciudad, S, Giralt, E, Teixidó, M: A MALDI-TOF-based Method for Studying the Transport of BBB Shuttles-Enhancing Sensitivity and Versatility of Cell-Based In Vitro Transport Models. *Scientific reports*, 9: 4875, 2019.
158. Strupat, K, Karas, M, Hillenkamp, F: 2,5-Dihydroxybenzoic acid: a new matrix for laser desorption-ionization mass spectrometry. *International Journal of Mass Spectrometry and Ion Processes*, 111: 89-102, 1991.
159. Karas, M, Ehring, M, Nordhoff, E, Stahl, B, Strupat, K, Hillenkamp, F, Grehl, M, Krebs, B: Matrix-assisted laser desorption/ionization mass spectrometry with additives to 2,5-dihydroxybenzoic acid. *Journal of Mass Spectrometry*, 28: 1476-1481, 1993.
160. Wenzel, T, Sparbier, K, Mieruch, T, Kostrzewa, M: 2,5-Dihydroxyacetophenone: a matrix for highly sensitive matrix-assisted laser desorption/ionization time-of-flight mass spectrometric analysis of proteins using manual and automated preparation techniques. *Rapid communications in mass spectrometry : RCM*, 20: 785-789, 2006.
161. Vermillion-Salsbury, RL, Hercules, DM: 9-Aminoacridine as a matrix for negative mode matrix-assisted laser desorption/ionization. *Rapid communications in mass spectrometry : RCM*, 16: 1575-1581, 2002.
162. Fulop, A, Porada, MB, Marsching, C, Blott, H, Meyer, B, Tambe, S, Sandhoff, R, Junker, HD, Hopf, C: 4-Phenyl-alpha-cyanocinnamic acid amide: screening for a negative ion matrix for MALDI-MS imaging of multiple lipid classes. *Analytical chemistry*, 85: 9156-9163, 2013.
163. Dai, Y, Whittall, RM, Li, L: Confocal Fluorescence Microscopic Imaging for Investigating the Analyte Distribution in MALDI Matrices. *Analytical chemistry*, 68: 2494-2500, 1996.
164. Wei, Y, Zhang, Y, Lin, Y, Li, L, Liu, J, Wang, Z, Xiong, S, Zhao, Z: A uniform 2,5-dihydroxybenzoic acid layer as a matrix for MALDI-FTICR MS-based lipidomics. *The Analyst*, 140: 1298-1305, 2015.
165. Nishikaze, T, Okumura, H, Jinmei, H, Amano, J: Correlation between Sweet Spots of Glycopeptides and Polymorphism of the Matrix Crystal in MALDI Samples. *Mass spectrometry (Tokyo, Japan)*, 1: A0006, 2012.
166. Sleno, L, Volmer, DA: Assessing the properties of internal standards for quantitative matrix-assisted laser desorption/ionization mass spectrometry of small molecules. *Rapid communications in mass spectrometry : RCM*, 20: 1517-1524, 2006.
167. Szájli, E, Fehér, T, Medzihradszky, KF: Investigating the quantitative nature of MALDI-TOF MS. *Molecular & cellular proteomics : MCP*, 7: 2410-2418, 2008.
168. Ruh, H, Sandhoff, R, Meyer, B, Gretz, N, Hopf, C: Quantitative characterization of tissue globotetraosylceramides in a rat model of polycystic kidney disease by PrimaDrop sample preparation and indirect high-performance thin layer chromatography-matrix-assisted laser desorption/ionization-time-of-flight-mass spectrometry with automated data acquisition. *Analytical chemistry*, 85: 6233-6240, 2013.
169. Schwamborn, K, Caprioli, RM: MALDI imaging mass spectrometry--painting molecular pictures. *Molecular oncology*, 4: 529-538, 2010.
170. Unger, MS, Mudunuru, J, Schwab, M, Hopf, C, Drewes, G, Nies, AT, Zamek-Gliszczyński, MJ, Reinhard, FBM: Clinically Relevant OATP2B1 Inhibitors in Marketed Drug Space. *Molecular pharmaceuticals*, 2020.
171. Karlgren, M, Vildhede, A, Norinder, U, Wisniewski, JR, Kimoto, E, Lai, Y, Haglund, U, Artursson, P: Classification of inhibitors of hepatic organic anion transporting polypeptides (OATPs): influence of protein expression on drug-drug interactions. *Journal of medicinal chemistry*, 55: 4740-4763, 2012.
172. Nies, AT, Niemi, M, Burk, O, Winter, S, Zanger, UM, Stieger, B, Schwab, M, Schaeffeler, E: Genetics is a major determinant of expression of the human hepatic uptake

## References

---

- transporter OATP1B1, but not of OATP1B3 and OATP2B1. *Genome medicine*, 5: 1, 2013.
173. Izumi, S, Nozaki, Y, Komori, T, Takenaka, O, Maeda, K, Kusuhara, H, Sugiyama, Y: Investigation of Fluorescein Derivatives as Substrates of Organic Anion Transporting Polypeptide (OATP) 1B1 To Develop Sensitive Fluorescence-Based OATP1B1 Inhibition Assays. *Molecular pharmaceuticals*, 13: 438-448, 2016.
174. Kane, SP: Introducing the ClinCalc Drug Stats Database and the 2017 Top 200 Drugs. 2017.
175. Khuri, N, Zur, AA, Wittwer, MB, Lin, L, Yee, SW, Sali, A, Giacomini, KM: Computational Discovery and Experimental Validation of Inhibitors of the Human Intestinal Transporter OATP2B1. *Journal of chemical information and modeling*, 57: 1402-1413, 2017.
176. Mak, L, Marcus, D, Howlett, A, Yarova, G, Duchateau, G, Klaffke, W, Bender, A, Glen, RC: Metrabase: a cheminformatics and bioinformatics database for small molecule transporter data analysis and (Q)SAR modeling. *Journal of cheminformatics*, 7: 31, 2015.
177. Weimer, M, Jiang, X, Ponta, O, Stanzel, S, Freyberger, A, Kopp-Schneider, A: The impact of data transformations on concentration-response modeling. *Toxicology letters*, 213: 292-298, 2012.
178. Team, RC: R: a language and environment for statistical computing. *R Foundation for Statistical Computing, Vienna, Austria*, 2018.
179. Cuisset, L, Tichonicky, L, Jaffray, P, Delpech, M: The effects of sodium butyrate on transcription are mediated through activation of a protein phosphatase. *The Journal of biological chemistry*, 272: 24148-24153, 1997.
180. Leuthold, S, Hagenbuch, B, Mohebbi, N, Wagner, CA, Meier, PJ, Stieger, B: Mechanisms of pH-gradient driven transport mediated by organic anion polypeptide transporters. *American journal of physiology Cell physiology*, 296: C570-582, 2009.
181. Bednarczyk, D: Fluorescence-based assays for the assessment of drug interaction with the human transporters OATP1B1 and OATP1B3. *Analytical biochemistry*, 405: 50-58, 2010.
182. Patik, I, Székely, V, Németh, O, Szepesi, Á, Kucsma, N, Várady, G, Szakács, G, Bakos, É, Özvegy-Laczka, C: Identification of novel cell-impermeant fluorescent substrates for testing the function and drug interaction of Organic Anion-Transporting Polypeptides, OATP1B1/1B3 and 2B1. *Scientific reports*, 8: 2630, 2018.
183. Brouwer, KL, Keppler, D, Hoffmaster, KA, Bow, DA, Cheng, Y, Lai, Y, Palm, JE, Stieger, B, Evers, R: In vitro methods to support transporter evaluation in drug discovery and development. *Clinical pharmacology and therapeutics*, 94: 95-112, 2013.
184. Ahlin, G, Hilgendorf, C, Karlsson, J, Szigyarto, CA, Uhlén, M, Artursson, P: Endogenous gene and protein expression of drug-transporting proteins in cell lines routinely used in drug discovery programs. *Drug metabolism and disposition: the biological fate of chemicals*, 37: 2275-2283, 2009.
185. Ogura, J, Yamaguchi, H, Mano, N: Stimulatory effect on the transport mediated by organic anion transporting polypeptide 2B1. *Asian J Pharm Sci*, 15: 181-191, 2020.
186. van de Steeg, E, Venhorst, J, Jansen, HT, Nooijen, IH, DeGroot, J, Wortelboer, HM, Vlaming, ML: Generation of Bayesian prediction models for OATP-mediated drug-drug interactions based on inhibition screen of OATP1B1, OATP1B1\*15 and OATP1B3. *European journal of pharmaceutical sciences : official journal of the European Federation for Pharmaceutical Sciences*, 70: 29-36, 2015.

## References

---

187. Grube, M, Köck, K, Oswald, S, Draber, K, Meissner, K, Eckel, L, Böhm, M, Felix, SB, Vogelgesang, S, Jedlitschky, G, Siegmund, W, Warzok, R, Kroemer, HK: Organic anion transporting polypeptide 2B1 is a high-affinity transporter for atorvastatin and is expressed in the human heart. *Clinical pharmacology and therapeutics*, 80: 607-620, 2006.
188. Letschert, K, Faulstich, H, Keller, D, Keppler, D: Molecular characterization and inhibition of amanitin uptake into human hepatocytes. *Toxicological sciences : an official journal of the Society of Toxicology*, 91: 140-149, 2006.
189. Kis, O, Zastre, JA, Ramaswamy, M, Bendayan, R: pH dependence of organic anion-transporting polypeptide 2B1 in Caco-2 cells: potential role in antiretroviral drug oral bioavailability and drug-drug interactions. *The Journal of pharmacology and experimental therapeutics*, 334: 1009-1022, 2010.
190. CER, F: In vitro metabolism and transporter-mediated drug-drug interaction studies *Office of Communications*: 45, 2017.
191. Riss, T, O'Brien, M, Moravec, R, Corporation, P: Choosing the right cell-based assay for your research. *Cell notes*, 2003.
192. Kruger, R, Pfenninger, A, Fournier, I, Gluckmann, M, Karas, M: Analyte incorporation and ionization in matrix-assisted laser desorption/ionization visualized by pH indicator molecular probes. *Analytical chemistry*, 73: 5812-5821, 2001.
193. Williams, TL, Andrzejewski, D, Lay, JO, Musser, SM: Experimental factors affecting the quality and reproducibility of MALDI TOF mass spectra obtained from whole bacteria cells. *Journal of the American Society for Mass Spectrometry*, 14: 342-351, 2003.
194. Liu, J, Ouyang, Z: Mass spectrometry imaging for biomedical applications. *Analytical and bioanalytical chemistry*, 405: 5645-5653, 2013.
195. Duncan, AJ, Heales, SJ, Mills, K, Eaton, S, Land, JM, Hargreaves, IP: Determination of coenzyme Q10 status in blood mononuclear cells, skeletal muscle, and plasma by HPLC with di-propoxy-coenzyme Q10 as an internal standard. *Clinical chemistry*, 51: 2380-2382, 2005.
196. Treiber, A, Schneider, R, Häusler, S, Stieger, B: Bosentan is a substrate of human OATP1B1 and OATP1B3: inhibition of hepatic uptake as the common mechanism of its interactions with cyclosporin A, rifampicin, and sildenafil. *Drug metabolism and disposition: the biological fate of chemicals*, 35: 1400-1407, 2007.
197. Tan, W, Mei, H, Chao, L, Liu, T, Pan, X, Shu, M, Yang, L: Combined QSAR and molecule docking studies on predicting P-glycoprotein inhibitors. *Journal of computer-aided molecular design*, 27: 1067-1073, 2013.
198. Le, MT, Phan, TV, Tran-Nguyen, VK, Tran, TD, Thai, KM: Prediction model of human ABCC2/MRP2 efflux pump inhibitors: a QSAR study. *Molecular diversity*, 2020.
199. Superti-Furga, G, Lackner, D, Wiedmer, T, Ingles-Prieto, A, Barbosa, B, Girardi, E, Goldmann, U, Gurtl, B, Klavins, K, Klimek, C, Lindinger, S, Lineiro-Retes, E, Muller, AC, Onstein, S, Redinger, G, Reil, D, Sedlyarov, V, Wolf, G, Crawford, M, Everley, R, Hepworth, D, Liu, S, Noell, S, Piotrowski, M, Stanton, R, Zhang, H, Corallino, S, Faedo, A, Insidioso, M, Maresca, G, Redaelli, L, Sassone, F, Scarabottolo, L, Stucchi, M, Tarroni, P, Tremolada, S, Batoulis, H, Becker, A, Bender, E, Chang, YN, Ehrmann, A, Muller-Fahrnow, A, Putter, V, Zindel, D, Hamilton, B, Lenter, M, Santacruz, D, Viollet, C, Whitehurst, C, Johnsson, K, Leippe, P, Baumgarten, B, Chang, L, Ibig, Y, Pfeifer, M, Reinhardt, J, Schonbett, J, Selzer, P, Seuwen, K, Bettembourg, C, Biton, B, Czech, J, de Foucauld, H, Didier, M, Licher, T, Mikol, V, Pommereau, A, Puech, F, Yaligara, V, Edwards, A, Bongers, BJ, Heitman, LH, AP, IJ, Sijben, HJ, van Westen, GJP, Grixti, J, Kell, DB, Mughal, F, Swainston, N, Wright-Muelas, M, Bohstedt, T, Burgess-Brown, N, Carpenter, L, Durr, K, Hansen, J, Scacioc, A, Banci, G, Colas, C,

## References

---

- Digles, D, Ecker, G, Fuzi, B, Gamsjager, V, Grandits, M, Martini, R, Troger, F, Altermatt, P, Doucerain, C, Durrenberger, F, Manolova, V, Steck, AL, Sundstrom, H, Wilhelm, M, Stepan, CM: The RESOLUTE consortium: unlocking SLC transporters for drug discovery. *Nature reviews Drug discovery*, 2020.
200. Kusahara, H, Furuie, H, Inano, A, Sunagawa, A, Yamada, S, Wu, C, Fukizawa, S, Morimoto, N, Ieiri, I, Morishita, M, Sumita, K, Mayahara, H, Fujita, T, Maeda, K, Sugiyama, Y: Pharmacokinetic interaction study of sulphasalazine in healthy subjects and the impact of curcumin as an in vivo inhibitor of BCRP. *British journal of pharmacology*, 166: 1793-1803, 2012.
201. Bunnage, ME, Chekler, EL, Jones, LH: Target validation using chemical probes. *Nature chemical biology*, 9: 195-199, 2013.
202. Drozdik, M, Groer, C, Penski, J, Lapczuk, J, Ostrowski, M, Lai, Y, Prasad, B, Unadkat, JD, Siegmund, W, Oswald, S: Protein abundance of clinically relevant multidrug transporters along the entire length of the human intestine. *Molecular pharmaceutics*, 11: 3547-3555, 2014.
203. Medwid, S, Li, MMJ, Knauer, MJ, Lin, K, Mansell, SE, Schmerk, CL, Zhu, C, Griffin, KE, Yousif, MD, Dresser, GK, Schwarz, UI, Kim, RB, Tirona, RG: Fexofenadine and Rosuvastatin Pharmacokinetics in Mice with Targeted Disruption of Organic Anion Transporting Polypeptide 2B1. *Drug metabolism and disposition: the biological fate of chemicals*, 47: 832-842, 2019.
204. Panfen, E, Chen, W, Zhang, Y, Sinz, M, Marathe, P, Gan, J, Shen, H: Enhanced and Persistent Inhibition of Organic Cation Transporter 1 Activity by Preincubation of Cyclosporine A. *Drug metabolism and disposition: the biological fate of chemicals*, 47: 1352-1360, 2019.
205. Bi, YA, Mathialagan, S, Tylaska, L, Fu, M, Keefer, J, Vildhede, A, Costales, C, Rodrigues, AD, Varma, MVS: Organic Anion Transporter 2 Mediates Hepatic Uptake of Tolbutamide, a CYP2C9 Probe Drug. *The Journal of pharmacology and experimental therapeutics*, 364: 390-398, 2018.
206. Watanabe, H, Sakaguchi, Y, Sugimoto, R, Kaneko, K, Iwata, H, Kotani, S, Nakajima, M, Ishima, Y, Otagiri, M, Maruyama, T: Human organic anion transporters function as a high-capacity transporter for p-cresyl sulfate, a uremic toxin. *Clinical and experimental nephrology*, 18: 814-820, 2014.
207. Shirasaka, Y, Mori, T, Murata, Y, Nakanishi, T, Tamai, I: Substrate- and dose-dependent drug interactions with grapefruit juice caused by multiple binding sites on OATP2B1. *Pharmaceutical research*, 31: 2035-2043, 2014.
208. Izumi, S, Nozaki, Y, Kusahara, H, Hotta, K, Mochizuki, T, Komori, T, Maeda, K, Sugiyama, Y: Relative Activity Factor (RAF)-Based Scaling of Uptake Clearance Mediated by Organic Anion Transporting Polypeptide (OATP) 1B1 and OATP1B3 in Human Hepatocytes. *Molecular pharmaceutics*, 15: 2277-2288, 2018.
209. Nozawa, T, Imai, K, Nezu, J, Tsuji, A, Tamai, I: Functional characterization of pH-sensitive organic anion transporting polypeptide OATP-B in human. *The Journal of pharmacology and experimental therapeutics*, 308: 438-445, 2004.
210. CDER, F: In Vitro Metabolism- and Transporter-Mediated Drug-Drug Interaction Studies. *Office of Communications*: 45, 2017.
211. Kaufman, DW, Kelly, JP, Rosenberg, L, Anderson, TE, Mitchell, AA: Recent patterns of medication use in the ambulatory adult population of the United States: the Slone survey. *Jama*, 287: 337-344, 2002.
212. Chen, M, Hu, S, Li, Y, Gibson, AA, Fu, Q, Baker, SD, Sparreboom, A: Role of OATP2B1 in drug absorption and drug-drug interactions. *Drug metabolism and disposition: the biological fate of chemicals*, 2020.



## References

---

213. Fisel, P, Nies, AT, Schaeffeler, E, Schwab, M: The importance of drug transporter characterization to precision medicine. *Expert opinion on drug metabolism & toxicology*, 13: 361-365, 2017.
214. Nies, AT, Koepsell, H, Winter, S, Burk, O, Klein, K, Kerb, R, Zanger, UM, Keppler, D, Schwab, M, Schaeffeler, E: Expression of organic cation transporters OCT1 (SLC22A1) and OCT3 (SLC22A3) is affected by genetic factors and cholestasis in human liver. *Hepatology (Baltimore, Md)*, 50: 1227-1240, 2009.
215. Shikata, E, Yamamoto, R, Takane, H, Shigemasa, C, Ikeda, T, Otsubo, K, Ieiri, I: Human organic cation transporter (OCT1 and OCT2) gene polymorphisms and therapeutic effects of metformin. *Journal of human genetics*, 52: 117-122, 2007.
216. Janzen, WP: Screening technologies for small molecule discovery: the state of the art. *Chemistry & biology*, 21: 1162-1170, 2014.
217. Martinez, NJ, Asawa, RR, Cyr, MG, Zakharov, A, Urban, DJ, Roth, JS, Wallgren, E, Klumpp-Thomas, C, Coussens, NP, Rai, G, Yang, SM, Hall, MD, Marugan, JJ, Simeonov, A, Henderson, MJ: A widely-applicable high-throughput cellular thermal shift assay (CETSA) using split Nano Luciferase. *Scientific reports*, 8: 9472, 2018.
218. Martinez Molina, D, Jafari, R, Ignatushchenko, M, Seki, T, Larsson, EA, Dan, C, Sreekumar, L, Cao, Y, Nordlund, P: Monitoring drug target engagement in cells and tissues using the cellular thermal shift assay. *Science (New York, NY)*, 341: 84-87, 2013.
219. Schürmann, M, Janning, P, Ziegler, S, Waldmann, H: Small-Molecule Target Engagement in Cells. *Cell chemical biology*, 23: 435-441, 2016.
220. Peters, WB, Frasca, V, Brown, RK: Recent developments in isothermal titration calorimetry label free screening. *Combinatorial chemistry & high throughput screening*, 12: 772-790, 2009.
221. Zhou, L, Zhang, J, DiGiammarino, E, Kavishwar, A, Yan, B, Chumsae, C, Ihnat, PM, Powers, D, Harlan, J, Stine, WB: PULSE SPR: A High Throughput Method to Evaluate the Domain Stability of Antibodies. *Analytical chemistry*, 90: 12221-12229, 2018.
222. Cooper, MA: Optical biosensors in drug discovery. *Nature reviews Drug discovery*, 1: 515-528, 2002.
223. Alterman, M, Sjöbom, H, Säfsten, P, Markgren, PO, Danielson, UH, Hämäläinen, M, Löfås, S, Hultén, J, Classon, B, Samuelsson, B, Hallberg, A: P1/P1' modified HIV protease inhibitors as tools in two new sensitive surface plasmon resonance biosensor screening assays. *European journal of pharmaceutical sciences : official journal of the European Federation for Pharmaceutical Sciences*, 13: 203-212, 2001.
224. Prideaux, B, Staab, D, Stoeckli, M: Applications of MALDI-MSI to pharmaceutical research. *Methods in molecular biology (Clifton, NJ)*, 656: 405-413, 2010.
225. Chandler, J, Haslam, C, Hardy, N, Leveridge, M, Marshall, P: A Systematic Investigation of the Best Buffers for Use in Screening by MALDI-Mass Spectrometry. *SLAS discovery : advancing life sciences R & D*, 22: 1262-1269, 2017.
226. Bornsen, KO: Influence of salts, buffers, detergents, solvents, and matrices on MALDI-MS protein analysis in complex mixtures. *Methods in molecular biology (Clifton, NJ)*, 146: 387-404, 2000.
227. Guo, Z, He, L: A binary matrix for background suppression in MALDI-MS of small molecules. *Analytical and bioanalytical chemistry*, 387: 1939-1944, 2007.
228. Mohr, MD, Bornsen, KO, Widmer, HM: Matrix-assisted laser desorption/ionization mass spectrometry: improved matrix for oligosaccharides. *Rapid communications in mass spectrometry : RCM*, 9: 809-814, 1995.
229. Gemperline, E, Rawson, S, Li, L: Optimization and comparison of multiple MALDI matrix application methods for small molecule mass spectrometric imaging. *Analytical chemistry*, 86: 10030-10035, 2014.

## References

---

230. Yao, J, Scott, JR, Young, MK, Wilkins, CL: Importance of matrix:analyte ratio for buffer tolerance using 2,5-dihydroxybenzoic acid as a matrix in matrix-assisted laser desorption/ionization-Fourier transform mass spectrometry and matrix-assisted laser desorption/ionization-time of flight. *Journal of the American Society for Mass Spectrometry*, 9: 805-813, 1998.
231. Smolira, A, Wessely-Szponder, J: Importance of the matrix and the matrix/sample ratio in MALDI-TOF-MS analysis of cathelicidins obtained from porcine neutrophils. *Applied biochemistry and biotechnology*, 175: 2050-2065, 2015.
232. Tamai, I, Nozawa, T, Koshida, M, Nezu, J, Sai, Y, Tsuji, A: Functional characterization of human organic anion transporting polypeptide B (OATP-B) in comparison with liver-specific OATP-C. *Pharmaceutical research*, 18: 1262-1269, 2001.
233. Hirano, M, Maeda, K, Shitara, Y, Sugiyama, Y: Contribution of OATP2 (OATP1B1) and OATP8 (OATP1B3) to the hepatic uptake of pitavastatin in humans. *The Journal of pharmacology and experimental therapeutics*, 311: 139-146, 2004.
234. Ugele, B, Bahn, A, Rex-Haffner, M: Functional differences in steroid sulfate uptake of organic anion transporter 4 (OAT4) and organic anion transporting polypeptide 2B1 (OATP2B1) in human placenta. *The Journal of steroid biochemistry and molecular biology*, 111: 1-6, 2008.
235. Zovo, K, Helk, E, Karafin, A, Tougu, V, Palumaa, P: Label-free high-throughput screening assay for inhibitors of Alzheimer's amyloid-beta peptide aggregation based on MALDI MS. *Analytical chemistry*, 82: 8558-8565, 2010.
236. Diao, L, Ekins, S, Polli, JE: Novel inhibitors of human organic cation/carnitine transporter (hOCTN2) via computational modeling and in vitro testing. *Pharmaceutical research*, 26: 1890-1900, 2009.
237. Saito, H, Hirano, H, Nakagawa, H, Fukami, T, Oosumi, K, Murakami, K, Kimura, H, Kouchi, T, Konomi, M, Tao, E, Tsujikawa, N, Tarui, S, Nagakura, M, Osumi, M, Ishikawa, T: A new strategy of high-speed screening and quantitative structure-activity relationship analysis to evaluate human ATP-binding cassette transporter ABCG2-drug interactions. *The Journal of pharmacology and experimental therapeutics*, 317: 1114-1124, 2006.
238. Badolo, L, Rasmussen, LM, Hansen, HR, Sveigaard, C: Screening of OATP1B1/3 and OCT1 inhibitors in cryopreserved hepatocytes in suspension. *European journal of pharmaceutical sciences : official journal of the European Federation for Pharmaceutical Sciences*, 40: 282-288, 2010.
239. Shah, P, Ding, Y, Niemczyk, M, Kudla, G, Plotkin, JB: Rate-limiting steps in yeast protein translation. *Cell*, 153: 1589-1601, 2013.
240. Bolognesi, B, Lehner, B: Reaching the limit. *eLife*, 7, 2018.
241. Hua, WJ, Hua, WX, Fang, HJ: The role of OATP1B1 and BCRP in pharmacokinetics and DDI of novel statins. *Cardiovascular therapeutics*, 30: e234-241, 2012.
242. Kellick, KA, Bottorff, M, Toth, PP, The National Lipid Association's Safety Task, F: A clinician's guide to statin drug-drug interactions. *Journal of clinical lipidology*, 8: S30-46, 2014.
243. Ravi, M, Paramesh, V, Kaviya, SR, Anuradha, E, Solomon, FD: 3D cell culture systems: advantages and applications. *Journal of cellular physiology*, 230: 16-26, 2015.
244. Liu, X, Weaver, EM, Hummon, AB: Evaluation of therapeutics in three-dimensional cell culture systems by MALDI imaging mass spectrometry. *Analytical chemistry*, 85: 6295-6302, 2013.
245. Huh, D, Kim, HJ, Fraser, JP, Shea, DE, Khan, M, Bahinski, A, Hamilton, GA, Ingber, DE: Microfabrication of human organs-on-chips. *Nature protocols*, 8: 2135-2157, 2013.

## References

---

246. Duenas, ME, Feenstra, AD, Korte, AR, Hinners, P, Lee, YJ: Cellular and Subcellular Level Localization of Maize Lipids and Metabolites Using High-Spatial Resolution MALDI Mass Spectrometry Imaging. *Methods in molecular biology (Clifton, NJ)*, 1676: 217-231, 2018.
247. Bowman, AP, Bogie, JFJ, Hendriks, JJA, Haidar, M, Belov, M, Heeren, RMA, Ellis, SR: Evaluation of lipid coverage and high spatial resolution MALDI-imaging capabilities of oversampling combined with laser post-ionisation. *Analytical and bioanalytical chemistry*, 412: 2277-2289, 2020.
248. Cui, Y, Konig, J, Leier, I, Buchholz, U, Keppler, D: Hepatic uptake of bilirubin and its conjugates by the human organic anion transporter SLC21A6. *The Journal of biological chemistry*, 276: 9626-9630, 2001.
249. Kullak-Ublick, GA, Ismail, MG, Stieger, B, Landmann, L, Huber, R, Pizzagalli, F, Fattinger, K, Meier, PJ, Hagenbuch, B: Organic anion-transporting polypeptide B (OATP-B) and its functional comparison with three other OATPs of human liver. *Gastroenterology*, 120: 525-533, 2001.
250. Konig, J, Cui, Y, Nies, AT, Keppler, D: Localization and genomic organization of a new hepatocellular organic anion transporting polypeptide. *The Journal of biological chemistry*, 275: 23161-23168, 2000.
251. Satoh, H, Yamashita, F, Tsujimoto, M, Murakami, H, Koyabu, N, Ohtani, H, Sawada, Y: Citrus juices inhibit the function of human organic anion-transporting polypeptide OATP-B. *Drug metabolism and disposition: the biological fate of chemicals*, 33: 518-523, 2005.
252. Bednarczyk, D, Sanghvi, MV: Organic anion transporting polypeptide 2B1 (OATP2B1), an expanded substrate profile, does it align with OATP2B1's hypothesized function? *Xenobiotica; the fate of foreign compounds in biological systems*: 1-10, 2020.
253. Kanai, N, Lu, R, Bao, Y, Wolkoff, AW, Schuster, VL: Transient expression of oatp organic anion transporter in mammalian cells: identification of candidate substrates. *The American journal of physiology*, 270: F319-325, 1996.
254. Bahn, A, Hagos, Y, Reuter, S, Balen, D, Brzica, H, Krick, W, Burckhardt, BC, Sabolic, I, Burckhardt, G: Identification of a new urate and high affinity nicotinate transporter, hOAT10 (SLC22A13). *The Journal of biological chemistry*, 283: 16332-16341, 2008.
255. Zhang, EY, Knipp, GT, Ekins, S, Swaan, PW: Structural biology and function of solute transporters: implications for identifying and designing substrates. *Drug metabolism reviews*, 34: 709-750, 2002.
256. Gui, C, Hagenbuch, B: Role of transmembrane domain 10 for the function of organic anion transporting polypeptide 1B1. *Protein science : a publication of the Protein Society*, 18: 2298-2306, 2009.
257. Noe, J, Portmann, R, Brun, ME, Funk, C: Substrate-dependent drug-drug interactions between gemfibrozil, fluvastatin and other organic anion-transporting peptide (OATP) substrates on OATP1B1, OATP2B1, and OATP1B3. *Drug metabolism and disposition: the biological fate of chemicals*, 35: 1308-1314, 2007.
258. Hacker, K, Maas, R, Kornhuber, J, Fromm, MF, Zolk, O: Substrate-Dependent Inhibition of the Human Organic Cation Transporter OCT2: A Comparison of Metformin with Experimental Substrates. *PloS one*, 10: e0136451, 2015.
259. Bentz, J, O'Connor, MP, Bednarczyk, D, Coleman, J, Lee, C, Palm, J, Pak, YA, Perloff, ES, Reyner, E, Balimane, P, Brannstrom, M, Chu, X, Funk, C, Guo, A, Hanna, I, Heredi-Szabo, K, Hillgren, K, Li, L, Hollnack-Pusch, E, Jamei, M, Lin, X, Mason, AK, Neuhoff, S, Patel, A, Podila, L, Plise, E, Rajaraman, G, Salphati, L, Sands, E, Taub, ME, Taur, JS, Weitz, D, Wortelboer, HM, Xia, CQ, Xiao, G, Yabut, J, Yamagata, T, Zhang, L, Ellens, H: Variability in P-glycoprotein inhibitory potency (IC<sub>50</sub>) using

## References

---

- various in vitro experimental systems: implications for universal digoxin drug-drug interaction risk assessment decision criteria. *Drug metabolism and disposition: the biological fate of chemicals*, 41: 1347-1366, 2013.
260. Volpe, DA: Variability in Caco-2 and MDCK cell-based intestinal permeability assays. *Journal of pharmaceutical sciences*, 97: 712-725, 2008.
261. Vildhede, A, Karlgren, M, Svedberg, EK, Wisniewski, JR, Lai, Y, Noren, A, Artursson, P: Hepatic uptake of atorvastatin: influence of variability in transporter expression on uptake clearance and drug-drug interactions. *Drug metabolism and disposition: the biological fate of chemicals*, 42: 1210-1218, 2014.
262. Kamo, S, Nakanishi, T, Aotani, R, Nakamura, Y, Gose, T, Tamai, I: Impact of FDA-Approved Drugs on the Prostaglandin Transporter OATP2A1/SLCO2A1. *Journal of pharmaceutical sciences*, 106: 2483-2490, 2017.

---

**Publications related to my PhD thesis:**

Unger, MS, Mudunuru, J, Schwab, M, Hopf, C, Drewes, G, Nies, AT, Zamek-Gliszczyński, MJ, Reinhard, FBM: Clinically Relevant OATP2B1 Inhibitors in Marketed Drug Space. *Molecular pharmaceutics*, 2020

Unger, MS, Schumacher, L, Enzlein, T, Weigt, D, Zamek-Gliszczyński, MJ, Schwab, M, Nies, A, Drewes, G, Schulz, S, Reinhard, FBM, Hopf, C, Direct Automated MALDI Mass Spectrometry Analysis of Cellular Transporter Function: Inhibition of OATP2B1 Uptake by 294 Drugs. *Analytical Chemistry*, 2020

## 8 CURRICULUM VITAE

### MELISSA UNGER

\*07.09.1993 in Kitzingen  
unverheiratet, keine Kinder

#### BERUFSERFAHRUNG

---

05/2017-heute                      Industrienähe Promotion an der Hochschule Mannheim in  
Kooperation mit der Firma Cellzome, a GSK company  
  
2020: Gewinn des SLAS Tony B Academic Travel Award

#### PRAKTISCHE ERFAHRUNG

---

04/2015-04/2017                      Hilfwissenschaftlerin im Lehrstuhl Pharmazeutische  
Biologie/Lehrstuhl Botanik  
  
08/2014 – 09/2014                      Praktikum in der Qualitätskontrolle und Qualitätssicherung  
bei Kneipp GmbH & Co. KG, Ochsenfurt

#### AUSBILDUNG

---

10/2015-04/2017                      Master Biologie an der Universität Würzburg mit den  
Schwerpunkten Humangenetik und Pharmazeutische  
Biologie, Abschlussnote 1,5  
  
10/2012-07/2015                      Bachelor Biologie an der Universität Würzburg mit der  
Abschlussnote 1,9  
  
09/2004-06/2012                      Gymnasium Marktbreit, Abitur mit der Gesamtnote 1,5

## 9 ACKNOWLEDGEMENT

Mit der folgenden Danksagung möchte ich gerne meinen herzlichen Dank an alle aussprechen, die einen Teil zur Ermöglichung dieser Doktorarbeit beigetragen haben.

Mein erster Dank geht an meinen Doktorvater Prof. Dr. Carsten Hopf. Von der Aufnahme in sein großartiges Team bis hin zur Abgabe der Arbeit hatte ich durchgehend seine Unterstützung. Trotz seiner Involvierung in viele Projekte, nahm er sich regelmäßig Zeit und scheute auch nicht davor auf vermeintlich kleine Probleme einzugehen. Nach jedem Gespräch hatte man wieder neue Motivation, dafür bin ich sehr dankbar. Auch Dr. Friedrich Reinhard, der meine Arbeit bei Cellzome, a GSK company vorrangig betreut hat, gilt ein besonderer Dank. Die Zusammenarbeit war stets locker und durch seine Erfahrung konnte er mir oft bei Problemen weiterhelfen. Für den besonderen Einblick in die industrielle Forschung bin ich besonders froh. Diesen möglich gemacht haben unter anderem auch Dr. Gitte Neubauer und Dr. Gerard Drewes, denen ich für die gute Zusammenarbeit danken möchte. Die Zusammenarbeit mit Cellzome war unter anderem auch geprägt von etlichen Skype Calls – hier möchte ich mich vor allem bei Dr. Maciej Zamek-Glisczynski und Dr. Jennypher Mudunuru bedanken. Mit Maciej einen der Transporter-Experten an seiner Seite zu haben ist eine Bereicherung für meine Arbeit gewesen und auch die Verfassung unserer gemeinsamen Veröffentlichungen gestaltete sich sehr angenehm. An der Hochschule Mannheim danke ich vor allem auch Prof. Dr. Thorsten Röder für die Organisation des M2Aind Projekts. Ich bin zudem sehr dankbar dafür, dass ich meine Arbeit beim Center for Mass Spectrometry and Optical Spectroscopy (CeMOS) durchführen konnte und dadurch hervorragende Instrumente zur Verfügung standen. Zu den hervorragenden Instrumenten möchte ich mich vor allem auch bei Swen Tyrasa von der Firma Analytik Jena, so wie Dr. Meike Hamester und Dr. Arndt Asperger von Bruker bedanken, die mir nicht nur bei gerätespezifischen Fragen weitergeholfen habe.

Auch Prof. Dr. Anne Nies und Prof. Dr. Matthias Schwab danke ich für die Bereitstellung der Zelllinien und vor allem für die Hilfestellung während des Fluoreszenzassays und die Diskussionen zu unseren Veröffentlichungen. Bei Cellzome wurde ich zudem sehr tatkräftig von Mitarbeitern unterstützt, hier möchte ich mich vor allem bei Ina Günthner bedanken, die mir durch die Programmierung des Pipettierroboters einige Zeit erspart hat. Auch Jana Krause, Sascha Knecht und

## Acknowledgement

---

Eugenia Stonehouse bin ich dankbar, dass sie immer wieder kleine Tätigkeiten für mich übernommen haben, sodass ich nicht dafür extra nach Heidelberg musste ☺. Den Angestellten in der Mensa vom EMBL bin ich sehr dankbar dafür, dass sie immer die besten vegetarischen und veganen Köstlichkeiten zubereitet haben. Das war eine wirkliche Bereicherung meiner Cellzome-Zeit!

Den Großteil der Zeit meiner Doktorarbeit durfte ich an der Hochschule Mannheim verbringen und dementsprechend gibt es hier die meisten Personen, denen ich sehr dankbar bin. Allen voran Dr. Sandra Schulz, für die Betreuung meines Projekts und die vielen Back- und Pizza- Abende bei ihr zuhause. Lena Schumacher gilt ein sehr großer Dank. Die Zusammenarbeit mit ihr während ihrer Bachelorarbeit war unkompliziert und extrem bereichernd. Ohne ihre Unterstützung würde ich vermutlich heute noch am Screen sitzen ;-). Eine große Unterstützung war auch Dr. David Weigt, der mir auch nach seinem Verlassen der Hochschule noch weitergeholfen hat, wenn es mal nicht voranging. Thomas Enzlein danke ich für die Analyse meiner Daten und dass wir uns immer wieder über die schlechten und guten Momente der Doktorarbeit austauschen konnten. Du warst eine ganz große Hilfe! Dr. Carina Ramallo Guevara und Rebecca Brendel danke ich von Herzen für die nötige Ablenkung und Unterstützung in allen freien Minuten und Pausen. Ihr seid während dieser drei Jahre zu echten Freunden geworden. Auch meinen anderen Kolleg\*innen möchte ich danken für die tolle Atmosphäre im Labor und die Hilfe bei vielen Kleinigkeiten. Joshua Jarzombek, James Cairns, Dr. Martina Blank, Ralf Müller, Denis Abu-Sammour, Matthias Schwartz, Alexander Geisel, Dr. Christian Marsching, Dr. Annabelle Fülöp, Dr. Qiuqin Zhou, Evelyn Jäger, Dr. Diego Yepes, Miriam Rittel und Tobias Bausbacher haben die drei Jahre wirklich zu einer tollen Erfahrung gemacht. Ich werde immer mit Freude an diese Zeit zurückdenken.

Der wohl wichtigste Dank gilt meinen Eltern. Die Unterstützung, die ich von euch bekomme ist beispiellos. Meiner Mutter möchte ich folgende Zeilen widmen: „Du bist mein Ursprung, mein Vertrauen, meine Insel und mein Schatz. Mein Mund der formt dein Lachen, mein Herz schlägt deinen Takt.“ Dein Einfluss macht mich zu einem besseren Menschen und dafür danke ich dir von Herzen. Meinem Vater danke ich vor allem für seine Stärke und seine Fähigkeit, mich immer wieder zu ermutigen. Ich weiß, dass du immer für mich da bist, dafür bin ich dir unendlich dankbar. Meine Brüder Oliver und Manuel spielen in meinem Leben schon immer eine große Rolle. Ihr seid



meine Vorbilder, nicht nur was den akademischen Abschluss angeht ☺ ich habe euch schon immer nachgeehrt, wen wundert es da, dass wir uns so ähnlich sind. Aber dennoch so verschieden. Ihr erdet mich. Ich bin so dankbar, dass es euch gibt! Und dass ihr zwei so tolle Frauen habt, Nicole und Siqi, ihr seid wie zwei Schwestern für mich. Ich kann mir gar nicht mehr vorstellen, wie es ohne euch ist. Auch Oma und Opa gebührt natürlich ein besonderer Dank. Leider kann ich nur noch Christa und Walter persönlich danken. Ich weiß aber, dass Franz und Gisela sich genauso darüber gefreut hätten. Ich vermisse euch. Oma und Opa, den unbändigen Stolz zu spüren, den ihr uns entgegenbringt ist etwas ganz Besonderes. Ihr seid unvergleichlich und ich liebe euch sehr. Auch meiner Patin möchte ich einen besonderen Dank aussprechen. Seit vielen Jahren ist sie eine meiner wichtigsten Ansprechpersonen und wird es immer bleiben. Danke, dass du immer für mich da bist.

Was wäre ein Leben ohne Freunde? Ich habe vielleicht nicht viele, aber ich habe sicherlich die besten ☺ Julia, seit 15 Jahren sind wir unzertrennlich, wir haben schon einige Höhen und Tiefen durchstanden, danke dass es dich gibt! Julian und Ariane sind zwar noch keine 15 Jahre dabei, aber immerhin schon seit der ersten Vorlesungsstunde ;- ) Ihr zwei seid meine liebste Erinnerung an Würzburger Studententage. Es freut mich, dass wir immer noch so gut in Kontakt sind und aufeinander vertrauen können. Vielen Dank auch fürs Korrigieren und Lesen der Doktorarbeit! Und wer natürlich nicht fehlen darf: Anne, Bodil, Denise, Sonny und Steffi. Ihr seid schon immer dabei und werdet es auch immer sein. Mit euch werde ich das hier ganz kräftig feiern und freue mich auf viele weitere Jahre.

Abschließend möchte ich einem ganz besonderen Menschen in meinem Leben danken, der alles mitgemacht hat, vom besten Gefühl, wenn die Veröffentlichung akzeptiert wurde, bis hin zu bitterster Enttäuschung und Erschöpfung, wenn etwas nicht so lief wie geplant. Es gibt niemanden, der mich besser aufmuntern könnte als du, Marko. Du zeigst mir mittlerweile seit einigen Jahren deine Welt und seit ich dich kenne ist meine Familie doppelt so groß wie vorher (Hiermit auch einen großen Dank an die Familien Jurjevic & Teubert!). Bei dir fühle ich mich zuhause und das soll immer so bleiben. Volim te, moja bubica.